

## **Distribution Agreement**

In presenting this thesis or dissertation as a partial fulfillment of the requirements for an advanced degree from Emory University, I hereby grant to Emory University and its agents the non-exclusive license to archive, make accessible, and display my thesis or dissertation in whole or in part in all forms of media, now or hereafter known, including display on the world wide web. I understand that I may select some access restrictions as part of the online submission of this thesis or dissertation. I retain all ownership rights to the copyright of the thesis or dissertation. I also retain the right to use in future works (such as articles or books) all or part of this thesis or dissertation.

Signature:

---

Charity G. Duran

---

Date

# **Functional Characterization of Anoctamins, a Novel Family of Transmembrane Proteins**

By

Charity G. Duran  
Doctor of Philosophy

Graduate Division of Biological and Biomedical Sciences  
Neuroscience

---

Criss Hartzell, Ph.D  
Advisor

---

Victor Faundez, M.D, Ph.D  
Committee Member

---

P. Michael Iuvone, Ph.D  
Committee Member

---

Richard A. Kahn, Ph.D  
Committee Member

---

Nael McCarty, Ph.D  
Committee Member

---

Stephen Traynelis, Ph.D  
Committee Member

Accepted:

---

Lisa A. Tedesco, Ph.D.  
2012

**Functional Characterization of Anoctamins, a Novel Family of  
Transmembrane Proteins**

By

Charity G. Duran  
B.S., Meredith College 2006

Advisor: Criss Hartzell, Ph.D

An abstract of  
A dissertation submitted to the Faculty of the  
James T. Laney School of Graduate Studies of Emory University  
in partial fulfillment of the requirements for the degree of  
Doctor of Philosophy  
Graduate Division of Biological and Biomedical Sciences  
Neuroscience  
2012

## **Abstract**

Characterization of Anoctamins, a Novel Family of Transmembrane Proteins

By Charity G. Duran

The vital roles of Ca<sup>2+</sup>-activated chloride channels (CaCCs) in various physiological processes are well documented, yet there has been considerable confusion regarding the molecular identity of “classical” outwardly rectifying CaCCs. When I began my thesis work, bestrophins represented the most promising molecular candidates for mediating these currents. However, the discovery of anoctamins (Anos) as CaCCs in 2008 necessitated reassessment of the relative contribution of bestrophins and anoctamins to native CaCC currents. The goal of this work was to examine the structure, function, and localization of anoctamins, and their relative contribution to endogenous CaCCs. Using a multi-disciplinary approach, this work shows that Ano1 and Ano2 function as plasma membrane CaCCs, while Anos 3-7 likely have intracellular roles. Although the channel function of intracellular anoctamins is unknown, the findings presented in this dissertation lay the groundwork for future studies examining the channel function of other anoctamins by identifying highly conserved residues within Ano1 critical for its channel function. Specifically, we have identified residues near the sixth transmembrane domain that are critical for Ca<sup>2+</sup> and voltage sensitivity of Ano1. This work also sheds light on the context dependent function of CaCCs and the discrete physiological roles of Ano1 and Best1 by examining endogenous CaCCs in *Drosophila* S2 cells and mouse retinal pigment epithelium. These findings reveal that S2 cell CaCCs are primarily mediated by Best1, and are activated via a Ca<sup>2+</sup>/calmodulin dependent kinase II dependent mechanism. In contrast, Ano1 represents the most likely candidate for CaCCs in mouse retinal pigment epithelium. In summation, the work presented here furthers our understanding of the functions of anoctamins and their roles in physiology and disease.

**Functional Characterization of Anoctamins, a Novel Family of  
Transmembrane Proteins**

By

Charity G. Duran  
B.S., Meredith College 2006

Advisor: Criss Hartzell, Ph.D

A dissertation submitted to the Faculty of the  
James T. Laney School of Graduate Studies of Emory University  
in partial fulfillment of the requirements for the degree of  
Doctor of Philosophy  
Graduate Division of Biological and Biomedical Sciences  
Neuroscience  
2012

## **Acknowledgements**

First and foremost I would like to thank my advisor, Criss Hartzell, for his guidance, enthusiasm, and support throughout my graduate career. His passion for learning is surpassed only by his insatiable curiosity. Thank you for mentoring me through uncharted scientific territory and for teaching me that sometimes the most interesting results are those that are contrary to what you expect. I would also like to thank my committee members: Victor Faundez, Mike Iuvone, Rick Kahn, Nael McCarty, and Steve Traynelis. Thank you all for your time and valuable input into my thesis work. A special thanks to Victor for always having an open door, and for his words of encouragement.

I am also very grateful to my friends and colleagues in the Hartzell Lab. My work would not have been possible without your help, and would not have been as fun. I am indebted to Li-Ting Chien for her help and generosity, to Kuai Yu for her advice and expertise on all things electrophysiology, and to Yuanyuan, who was patient enough to teach an electrophysiologist how to do molecular biology. I would also like to thank my Emory neuroscience classmates, especially Terrell Brotherton. Thank you for always having an open ear and keeping me grounded during the emotional rollercoaster that is graduate school.

Finally, I would like to thank my family for their support. A special thanks to my husband, David Brown, for tolerating me during “bad data” weeks, and helping me to put things into perspective. I am grateful for your patience and support, and am fortunate to have you, a fellow scientist, to talk science with at the end of the day.

## Table of Contents

---

### **CHAPTER 1: Introduction and Background**

Ion transport in biological membranes .....	2
Early advances in ion channel research	
Ion channels are selective and open in response to specific stimuli	
Chloride channel overview.....	4
Cl <sup>-</sup> channels have important physiological functions	
The molecular identity of some Cl <sup>-</sup> channels is uncertain	
Cl <sup>-</sup> channels exhibit low selectivity among anions	
Cl <sup>-</sup> channels exhibit a complex gating scheme	
The discovery of anoctamins provides new directions in Cl <sup>-</sup> channel research	
Ca <sup>2+</sup> -activate Cl <sup>-</sup> channels: channels with diverse properties.....	10
Bestrophins are bona fide CaCCs	
Regulation of Best1 by Ca <sup>2+</sup>	
Best1 functions as a CaCC in specific cell types	
Best vitelliform macular dystrophy	
BVMD: unanswered questions	
Anoctamins mediate “classical” CaCCs.....	20
Anoctamins 1 and 2 are CaCCs	
Anoctamin structure function	
Alternative splicing may contribute to heterogeneity of native CaCCs	
Gating mechanisms of Ano1	
Physiological roles and diseases of Anoctamins.....	26
Physiological functions of Ano1 and Ano2	
Some anoctamins may function as intracellular channels	
Diseases associated with anoctamin mutations	
The Cl <sup>-</sup> channel function of Anos 3-10 is unknown	
Rationale and Significance.....	35

### **CHAPTER 2: Anoctamins 3-7 are Intracellular Proteins**

Summary.....	43
Introduction.....	44
Results.....	45
Expression of Anos3-7 do not generate Ca <sup>2+</sup> -activated Cl <sup>-</sup> currents in HEK293 Cells	
Plasma membrane trafficking of Anos in various cell lines	
Subcellular localization of anoctamins	
Localization of endogenous Ano7 in prostate	
Sequence homology across Anos	

Chimeras between Ano1 and Ano5 or Ano7 do not generate Ca<sup>2+</sup>-activated Cl<sup>-</sup> currents

Discussion.....	51
Anoctamin family homology	
Ano5 and Ano7 may have significant structural and functional differences from Ano1	
Are Ano5 and Ano7 CaCCs?	
Materials and Methods.....	55

**CHAPTER 3: Epitope Accessibility and Mutagenesis Studies Implicate the Sixth Transmembrane Domain and Adjacent Residues in Regulation of Anoctamin 1 by Ca<sup>2+</sup> and Voltage**

Summary.....	75
Introduction.....	76
Results.....	77
Determinants of anion:cation permeability of Ano1	
E702 and E705 contribute to Ca <sup>2+</sup> gating	
Mutations within TM6 affect channel gating by voltage	
Discussion.....	82
Ca <sup>2+</sup> -dependent gating of Ano1	
E702 and E705 are critical for Ca <sup>2+</sup> -regulation of Ano1	
The role of TM6 in voltage sensitivity of Ano1	
Revised topology places Ca <sup>2+</sup> and voltage sensors near pore	
Ano1 may have a complex transmembrane topology	
Determinants of Ano1 Cl <sup>-</sup> selectivity are still unknown	
Materials and Methods.....	89

**CHAPTER 4: *Drosophila* Bestrophin-1 Currents are Regulated by Phosphorylation via a CaMKII Dependent Mechanism**

Summary.....	103
Introduction.....	104
Results.....	105
<i>Drosophila</i> anoctamin orthologs do not contribute to S2 cell CaCC current	
dBest1 currents are regulated by phosphorylation	
Regulation of dBest currents by phosphorylation is CaMKII-dependent	
Discussion.....	109
<i>Drosophila</i> anoctamins do not mediate S2 cell CaCCs	
dBest1 currents are regulated via a CaMKII dependent mechanism	

The mechanism of dBest regulation by CaMKII is unknown  
Studying Best1 in heterologous expression systems has limitations  
Future directions

Materials and Methods.....113

Acknowledgement.....116

## **CHAPTER 5: Anoctamin 1 May Mediate CaCCs in Mouse Retinal Pigment Epithelium**

Summary.....126

Introduction.....127

Results.....128

Model systems for studying RPE electrophysiology

Expression of anoctamins in mouse RPE

Generation of Ano1 inducible conditional knockout mouse

Expression of Best1 mutants does not affect Ano1 channel function

Discussion.....133

hiPS RPE are not amenable for whole-cell patch clamp electrophysiology

Whole cell recordings do not detect CaCCs in hRPE cells

Suitability of mouse models for studying BVMD

Does mBest1 regulate Ano1 channel function, and if so, how?

The mechanism of BVMD is still unknown

Materials and Methods.....140

## **CHAPTER 6: Conclusions and Implications**

Overview.....152

Summary and Significance.....153

What is the function and subcellular localization of Anos 3-10?

What are the determinants of anion/cation selectivity in anoctamins?

What are the mechanisms underlying Ca<sup>2+</sup> regulation of Ano1?

Best1 and Ano1: CaCCs with distinct roles in physiology

Concluding Remarks.....162

**REFERENCES**.....163

## Figure Index

---

Figure 1-1: Cl <sup>-</sup> channel genes and their relationship to biophysically identified Cl <sup>-</sup> currents.....	38
Figure 1-2: Phylogenetic tree of vertebrate Anoctamins.....	39
Figure 1-3: Anoctamin transmembrane topology.....	40
Figure 2-1: Anoctamin whole cell current response to intracellular [Ca <sup>2+</sup> ].....	61
Figure 2-2: Immunofluorescence confocal microscopy of various cell types expressing Anos 1, 3, 4, 5, 6, 7, and 10.....	62
Figure 2-3: Subcellular localization of An07.....	64
Figure 2-4: Characterization of An07 antibody specificity.....	65
Figure 2-5: Immunofluorescence confocal microscopy of human prostate expressing endogenous An07.....	67
Figure 2-6: Evolutionary divergence between An01 and 2 and An05 and 7.....	69
Figure 2-7: Trafficking and Cl <sup>-</sup> currents of chimeras between An01 and An07.....	71
Figure 2-8: Properties of An01-An05 chimeras.....	73
Figure 3-1: Effect of R621E mutation on anion:cation permeability of mAno1.....	92
Figure 3-2: Hydropathy analysis of An01 and An07.....	94
Figure 3-3: Immunofluorescent staining of mAno1 containing tandem hemagglutinin (HA) epitopes inserted at various locations.....	95
Figure 3-4: Sequence alignment of the sixth transmembrane domain.....	97
Figure 3-5: Representative whole-cell recordings of An01 constructs in transfected HEK293 cells at the indicated free [Ca <sup>2+</sup> ] <sub>i</sub> .....	98
Figure 3-6: Activation and deactivation kinetics of anoctamin-1 (Ano1) with rapid Ca <sup>2+</sup> perfusion in inside-out excised patches.....	99
Figure 3-7: Voltage sensitivity of mAno1 T714X mutants.....	100

Figure 3-8: Response of mAno1 T714X mutants to intracellular Ca <sup>2+</sup> .....	101
Figure 4-1: Contribution of <i>Drosophila</i> anoctamin orthologs to CaCC currents in S2 cells.....	117
Figure 4-2: Models of <i>Drosophila</i> Bestrophin mechanisms of activation/regulation.....	118
Figure 4-3: Time-dependent activation of S2 Cl <sup>-</sup> currents in response to high [Ca <sup>2+</sup> ] <sub>i</sub> .....	119
Figure 4-4: Nonselective kinase inhibitors inhibit <i>Drosophila</i> S2 Ca <sup>2+</sup> -activated currents.....	120
Figure 4-5: Reduction in bestrophin currents by kinase inhibitors occurs through inhibition of CaMKII.....	121
Figure 4-6: Dihydrochloride (H7) and KN-62 do not significantly reduce dBest currents.....	122
Figure 4-7: Comparison of the effects of various kinase inhibitors.....	123
Figure 4-8: Potential CaMKII phosphorylation sites in dBest1 identified by Phosphomotif finder and Scansite.....	124
Figure 5-1: Representative whole cell recordings from hiPS RPE cells.....	144
Figure 5-2: Representative whole cell patch clamp recordings of CaCCs in response to voltage steps from -100mV to +100mV.....	145
Figure 5-3: Expression of anoctamins in RPE.....	146
Figure 5-4: Tetracycline-inducible knockout of Ano1 in RPE.....	147
Figure 5-5: Ano1 expression in RPE from wild-type mice versus Ano1 conditional knockout mice.....	148
Figure 5-6: Co-expression of Ano1 with Best1 ΔI295.....	149

## Tables

---

Table 1-1: Disorders of Cl <sup>-</sup> channels/transporters.....	41
Table 5-2: RT-PCR primer pairs for mouse and human anoctamins.....	150

## **CHAPTER 1**

### **INTRODUCTION AND BACKGROUND**

## **Ion Transport in Biological Membranes**

All living cells possess a biological membrane, or phospholipid bilayer, that separates the internal cellular contents from the external environment. While this hydrophobic membrane provides a protective barrier, it is impermeable to charged molecules and ions. Therefore, specialized membrane proteins have evolved to allow for the control of ion transport. These specialized proteins, which include pumps, transporters, and channels, are integral membrane proteins and display specificity for the substrates they transport, but differ in their mechanisms of transport. Pumps use the energy from ATP-hydrolysis to transport small molecules or ions against their electrochemical gradient. Transporters also move molecules using active transport, but use the concentration gradient of one ion species to drive the uphill transport of another. In contrast, ion channels allow for the passive diffusion of ions across the plasma membrane by forming a hydrophilic pathway across the hydrophobic interior of the membrane. Transport of molecules by pumps and transporters is relatively slow compared to ion channels (approximately  $10^2 - 10^4$  molecules per second versus up to  $10^8$  per second respectively), because movement of each substrate requires a conformational change in the transporter. Ion channels are therefore critical for physiological processes that require the rapid flux of ions, such as the generation of action potentials, and muscle contraction. However, they also play crucial roles in maintaining long term ionic homeostasis.

### **Early advances in ion channel research**

The existence of ion channels was proposed in the early 1950's by Hodgkin and Huxley. Using the voltage-clamp technique developed by Cole and Marmont in 1949,

Hodgkin and Huxley clearly demonstrated that membrane excitability in the giant squid axon is determined by the passive flux of ions according to their electro-chemical gradients (Hodgkin and Huxley 1952a, 1952b). Their observations led them to conclude that ions “move in single file through narrow channels...which stretch through the membrane” (Hodgkin and Keynes 1955). Until the 1970’s, scientists had only been able to study ion channels collectively. The careful study of individual ion channel currents required the painstaking development of electrophysiological techniques which culminated in the development of patch-clamp in 1976 by Neher and Sakmann (Neher and Sakmann 1976). This powerful technique permitted scientists to record picoampere currents through isolated patches of membrane, thus allowing for the biophysical study of individual ion channels. With the discovery of the high resistance gigaohm seal, it became possible to manipulate the intra- and extracellular environment of the membrane (Hamill et al. 1981). The ability to study individual ion channels, coupled with increased control over experimental conditions, significantly advanced the understanding of ion channels. Scientists subsequently discovered that ion channels fall into several categories based on how they are opened, or gated, and their permeability to different ions.

### **Ion channels are selective and open in response to specific stimuli**

Ion channels are often categorized based on two properties: their selectivity for specific ions, and their mechanism of gating. These two important properties are what distinguish them from simple aqueous pores. Channels are selective for particular ions, allowing some to pass but not others. The selectivity filter of a channel confers physical and chemical constraints such that only ions of appropriate size and charge can pass. Furthermore, ion channels are not continuously open, but rather gated so that they can

be opened or closed depending on the presence of a stimulus. The main types of stimuli that gate ion channels are changes in the voltage across the membrane (voltage-gated channels), mechanical stress (volume-regulated channels and stretch-activated channels), or ligand binding (ligand-gated channels). In the case of ligand-gated channels, the ligand may be extracellular, such as a neurotransmitter, or intracellular, such as a nucleotide or ion. Ion channel gating can be further regulated by phosphorylation and dephosphorylation (for reviews see: (Jentsch et al. 2002; Nilius and Droogmans 2003; M. Suzuki et al. 2006)).

Ion channels can be divided into two major groups based on their ionic selectivity: cation channels and anion channels. These groups can be further subdivided based on gating mechanism. Anoctamins, one of the channel types I have explored in this thesis for example, are selective for  $\text{Cl}^-$  and open in response to increases in intracellular  $\text{Ca}^{2+}$ ; they are therefore categorized as  $\text{Ca}^{2+}$ -activated  $\text{Cl}^-$  channels. With advancements in molecular biology, biochemistry, and bioinformatics, the list of genes encoding for ion channels has grown exponentially. While cation channels have historically received more attention, studies on anion channels have greatly expanded over the past 20 years due to the association of  $\text{Cl}^-$  channel dysfunction with multiple diseases such as cystic fibrosis, and the identification of the genes encoding these channels (Duran et al. 2010).

### **Chloride Channel Overview**

In the scheme of ion channel research, chloride channels have not been as extensively studied as cation channels. Because it was thought that  $\text{Cl}^-$  was usually in electrochemical equilibrium across cell membranes,  $\text{Cl}^-$  channels did not initially attract

as much interest as their cation counterparts, which clearly exhibited the potential to do work. This misconception was due to the fact that many early studies on  $\text{Cl}^-$  were performed on skeletal muscle and erythrocytes, in which  $\text{Cl}^-$  is in electrochemical equilibrium because of the high resting permeability to  $\text{Cl}^-$ .

It is now evident that in most cells  $\text{Cl}^-$  is out of electrochemical equilibrium and actively transported, and is therefore capable of doing work. Because the expression of  $\text{Cl}^-$  transporters is regulated both temporally and spatially, resting intracellular  $\text{Cl}^-$  is dynamic. In neurons for example, the anion concentration gradient is the determinant of the excitatory (depolarizing) or inhibitory (hyperpolarizing) action of  $\text{GABA}_A$  receptors. In immature neurons, cation chloride cotransporters such as  $\text{Na}^+-\text{K}^+-2\text{Cl}^-$  (NKCC1) actively import  $\text{Cl}^-$ , resulting in accumulation of intracellular  $\text{Cl}^-$  concentration above electrochemical equilibrium. Under these conditions, activation of  $\text{GABA}_A$  results in a depolarizing current that may be important in stabilizing developing synapses (Ben-Ari et al. 2007). During development there is a functional shift in the response to GABA due to increased expression of chloride extruders such as KCC2. The resulting low intracellular  $\text{Cl}^-$  concentration renders  $\text{GABA}_A$  inhibitory. The importance of chloride transport in the adult brain is evidenced by the fact that disruption of chloride homeostasis is associated with neuropathologies including epilepsy and chronic pain (Planells-Cases and Jentsch 2009).

### **$\text{Cl}^-$ channels have important physiological functions**

$\text{Cl}^-$  channels are essential for the transport of electrolytes and water in various secretory epithelia. In salivary acinar cells, for example,  $\text{Cl}^-$  is the driving force for fluid secretion. The  $\text{Cl}^-$  concentration is maintained several-fold above its expected electrochemical gradient by  $\text{Na}^+-\text{K}^+-2\text{Cl}^-$  cotransporters located in the basolateral

membrane. An increase in intracellular  $\text{Ca}^{2+}$  activates  $\text{Cl}^-$  and  $\text{K}^+$  channels, resulting in the simultaneous efflux of  $\text{Cl}^-$  across the luminal membrane, and  $\text{K}^+$  into the interstitial fluid. The opposing movement of  $\text{Cl}^-$  and  $\text{K}^+$  creates a transepithelial potential difference that drives sodium ions across tight junctions into the lumen. In turn, the accumulation of  $\text{Na}^+$  and  $\text{Cl}^-$  in the lumen sets up a transepithelial osmotic gradient which drives the movement of water to generate saliva (Melvin 1999).  $\text{Cl}^-$  channels have a similar role in secretory epithelia in kidneys, airways, intestine, and pancreas (Barrett and Keely 2000; Devor et al. 1999; Quinton 1999).  $\text{Cl}^-$  channels also play important roles in regulating the electrical excitability of membranes. Mutations in  $\text{ClC-1}$ , for example, result in a skeletal muscle disorder called myotonia congenita. In myotonia congenita, efflux of  $\text{K}^+$  during muscle activity rapidly depolarizes the membrane due to impairment of  $\text{ClC-1}$  channels, resulting in prolonged muscle contraction (Pusch et al. 1995b).

### **The molecular identity of some chloride channels is uncertain**

The small number of known  $\text{Cl}^-$  channel genes does not reflect the large variety of biophysically identified  $\text{Cl}^-$  channels, suggesting that other gene families of anion channels have yet to be discovered. At the time I began this research, there were three well-established gene families of chloride channels. The cystic fibrosis transmembrane conductance regulator (CFTR), which is the only member in a large gene family of ABC transporters known to function as an ion channel, is controlled by intracellular ATP and through phosphorylation by cAMP or cGMP-dependent kinases.  $\text{ClC}$  channels, which are represented in mammals by 9 family members, function on both the plasma membrane and the membranes of intracellular organelles. However, only four members of the  $\text{ClC}$  family ( $\text{ClC 1, 2, Ka, Kb}$ ) are channels;  $\text{ClCs 3-7}$  are  $\text{Cl}^-/\text{H}^+$  antiporters. The ligand-gated

chloride channels, GABA- and glycine-receptors, represent the largest known family of Cl<sup>-</sup> channels (Jentsch et al. 2002) (Figure 1-1).

In addition to these extensively studied Cl<sup>-</sup> channel families, there are proteins whose status as Cl<sup>-</sup> channels is tentative or contentious, such as CLICs (Cl<sup>-</sup> intracellular channels). Some transporters, such as members of the SLC26 family and some glutamate transporters have also been shown to function as Cl<sup>-</sup> channels (Dorwart et al. 2008; Schenck et al. 2009; Vandenberg et al. 2008). Conversely, there are also chloride currents that have been biophysically identified, but whose molecular identities remain controversial. Identifying Cl<sup>-</sup> channels by sequence homology presents a unique challenge, because there are no known signature Cl<sup>-</sup> channel sequences that are conserved across the known Cl<sup>-</sup> channel families. Molecularly unidentified Cl<sup>-</sup> channels include volume-regulated anion channels (VRACs), which are expressed in nearly every vertebrate cell type and are critical for regulating cell volume. Until recently, the molecular identity of outwardly rectifying Ca<sup>2+</sup>-activated chloride channels (CaCCs) was also contentious. Several molecular candidates had been proposed for CaCCs, including members of the bestrophin family (C. Hartzell et al. 2005; H. C. Hartzell et al. 2008). While bestrophins can clearly function as CaCCs, they are unlikely to be responsible for the classical outwardly rectifying CaCC observed in various epithelia. Unlike endogenous CaCCs, bestrophins have a very limited expression profile and display biophysical properties that differ from native CaCCs (H. C. Hartzell et al. 2008). In 2008 it was discovered that members of the anoctamin family of transmembrane proteins mediate endogenous CaCCs (Caputo et al. 2008; Schroeder et al. 2008; Y. D. Yang et al. 2008). With the identification of anoctamins as a new family of Cl<sup>-</sup> channels, it is possible to perform structure function studies that may help uncover underlying principles regarding anion channel function. Studies on anoctamins will further our

understanding of the mechanisms underlying Cl<sup>-</sup> channel function, such as the determinants of anion selectivity and the molecular basis for channel gating.

### **Chloride channels exhibit low selectivity among anions**

Cl<sup>-</sup> channels allow the passive diffusion of negatively charged ions along their electrochemical gradient. Unlike most cation channels, which are relatively selective for specific cations, chloride channels exhibit very low selectivity among inorganic anions (Br<sup>-</sup>, I<sup>-</sup>, Cl<sup>-</sup>). Some are permeable to organic anions and HCO<sub>3</sub><sup>-</sup>, a less abundant but nevertheless important anion in physiology; thus, many “Cl<sup>-</sup> channels” should more accurately be called “anion channels” (C. Hartzell et al. 2005). The crystal structure of a bacterial ClC protein, despite it being a Cl<sup>-</sup>-H<sup>+</sup> antiporter and not a channel, identified the Cl<sup>-</sup> conduction pathway in ClCs. These results revealed that the principles underlying anion permeation and selectivity may be significantly different from those of cation channels (Dutzler et al. 2002). Many cation channels are oligomeric proteins in which the pore is comprised of homologous regions within each subunit. The tetrameric K<sup>+</sup> channel, for example, has four “P loops” within each subunit which contribute to the permeation pathway (Gajewski et al. 2011). In contrast, the pore of ClC channels is formed by a single subunit, with several non-homologous regions within the same protein contributing to the permeation pathway. Thus, identifying the pore using mutagenesis studies was difficult for ClCs, because mutations in several different regions of the protein affected pore properties.

### **Cl<sup>-</sup> channels exhibit a complex gating scheme**

Cl<sup>-</sup> channels can be functionally classified according to their gating mechanism. The gating mechanism of chloride channels can be dependent on a variety of factors

including membrane voltage, protein kinase activity, cell swelling, and intracellular  $\text{Ca}^{2+}$  (Jentsch et al. 2002). Research on cation channels has revealed certain common principles regarding channel gating, such as the positively charged S4 segment required for voltage-sensing (Papazian et al. 1991). In contrast, anion channel gating seems to differ in that anion permeation itself affects channel gating. Permeant anions may promote channel opening by binding to specific sites within the channel. Thus, the voltage sensitivity of some chloride channels is conferred not by voltage sensing regions, but by the voltage dependence of  $\text{Cl}^-$  binding to sites within the channel (Moroni et al. 2011) (Pusch et al. 1995a). In the case of  $\text{ClC}$  channels, gating is also strongly modulated by pH (Maduke et al. 1999). This feature may be a remnant of the evolution of  $\text{ClC}$  channels from ancestral transporters. CFTR, which in some respects behaves like a transporter, has an even more complex gating mechanism involving the phosphorylation of serine residues in the regulatory domain and ATP binding and hydrolysis (T. C. Hwang and Sheppard 2009). CaCCs also display unique gating properties from typical voltage- or ligand-gated channels, in that they exhibit strongly coupled voltage-dependence and ligand gating (Xiao et al. 2011). It is unknown how voltage-dependent and  $\text{Ca}^{2+}$ -dependent gating comes about at the molecular level. The discovery of anoctamins as the molecular correlate of CaCCs will allow for structure-function studies probing their channel function.

### **The discovery of anoctamins provides new directions in $\text{Cl}^-$ channel research**

For this dissertation, I focused on  $\text{Ca}^{2+}$ -activated  $\text{Cl}^-$  channels because it was known that they had important physiological functions, but their molecular identity and mechanisms of action were unknown. When I began these studies, bestrophins represented the best molecular candidate for CaCCs. Bestrophins were originally

identified because mutations in Bestrophin 1 (Best1) cause a form of macular degeneration called Best Vitelliform Macular Dystrophy (BVMD) (Marquardt et al. 1998; Petrukhin et al. 1998). The defining diagnostic feature of BVMD has been interpreted as a Cl<sup>-</sup> channel deficit in the retinal pigment epithelium (RPE); hence, it was originally hypothesized that Best1 was a Cl<sup>-</sup> channel and that mutations in Best1 resulted in Cl<sup>-</sup> channel dysfunction (Sun et al. 2002). As the field developed, however, it became clear that the story was more complicated. Foremost, Best1 knockout mice did not display deficits in CaCC currents, and the biophysical properties of bestrophins were not identical to those of endogenous CaCCs (H. C. Hartzell et al. 2008; L. Y. Marmorstein et al. 2006; A. D. Marmorstein et al. 2009). At the same time, new molecular candidates for CaCCs were discovered: anoctamins. We therefore hypothesized that anoctamins mediated CaCC currents in RPE. The anoctamin family consists of ten members, raising the question of which anoctamins potentially mediate CaCC currents in RPE, and whether all anoctamins function as CaCCs. In the following passages I will describe in detail the studies that led to the hypothesis that Best1 mediated the classical CaCC current observed in epithelia, and the downfall of this idea.

### **Ca<sup>2+</sup>-activated Cl<sup>-</sup> channels: channels with diverse properties**

The molecular identity of CaCCs had been controversial prior to the discovery of anoctamins, in part due to the diversity of CaCC currents. At the macroscopic level, CaCCs share similar features in whole -cell recordings from a variety of cell types. They are Ca<sup>2+</sup> sensitive, activate slowly upon depolarization, and display an outwardly rectifying I-V curve at steady state. In addition, CaCCs appear to be more sensitive to Ca<sup>2+</sup> at positive voltages than at negative voltages. While CaCCs across various cell types

display some similarities, understanding CaCC physiology has been confounded by the fact that they display heterogeneity in their biophysical properties and regulatory mechanisms.

At the single channel level there is significant diversity in CaCCs. Three different groups of CaCCs have been identified based on their conductance. Small conductance (1-3pS) CaCCs have been observed in *Xenopus* oocytes (Takahashi et al. 1987), cardiac myocytes (Collier et al. 1996), arterial smooth muscle (Klockner 1993), A6 kidney cells (Nakahari and Marunaka 1995), and endocrine cells (Taleb et al. 1988). They have varying biophysical properties depending on the conditions. A mid-conductance CaCC (8-15pS) with a linear I-V curve has been described in endothelial cells (Nilius et al. 1997c), hepatocytes (Koumi et al. 1994), and colon. Finally, an outwardly rectifying big-conductance CaCC (40-50pS) has been described in Jurkat T cells (Nishimoto et al. 1991), *Xenopus* spinal neurons (Hussy 1992), vascular smooth muscle cells (Piper and Large 2003), and airway epithelial cells (Frizzell et al. 1986). While this variety suggests an underlying molecular diversity for CaCCs, it is uncertain how single-channel recordings correlate with observed macroscopic currents.

CaCCs can be further subdivided into two groups based on their mechanism of activation, which varies across cell types. CaCCs can either be activated by  $\text{Ca}^{2+}$  binding directly to the channel, or indirectly via  $\text{Ca}^{2+}$  binding proteins or  $\text{Ca}^{2+}$  dependent enzymes such as calmodulin (CaM) and  $\text{Ca}^{2+}$ /calmodulin-dependent protein kinase II (CaMKII). Differences in the mechanisms of CaCC activation appear to be dependent on the cell type in which they are expressed. In salivary gland acinar cells (Martin 1993), ventricular myocytes (Collier et al. 1996), *Xenopus* oocytes (GomezHernandez et al. 1997), hepatocytes (Koumi et al. 1994), and glomerular mesangial cells (Ling et al. 1993), CaCCs appear to be directly activated by  $\text{Ca}^{2+}$ , as they do not show a rundown of channel

activity in excised patches. Furthermore, excised patches from *Xenopus* oocytes are activated quickly via rapid  $\text{Ca}^{2+}$  perfusion and do not require the presence of ATP, suggesting that phosphorylation is not involved (Kuruma and Hartzell 2000).

In contrast, other studies demonstrate that CaCCs exhibit rundown after excision (Klockner 1993; Morris and Frizzell 1993; Nilius et al. 1997c; Reisert et al. 2003). There may be other components in addition to  $\text{Ca}^{2+}$ , such as CaM, required for activation that are lost upon patch excision (Watanabe et al. 1994). Treatment of T84 cells (a human colonic tumor cell line) with selective inhibitors of CaM and CaMKII reveal that currents in these cells are activated via a CaM/CaMKII dependent mechanism (Arreola et al. 1997). In the *Odora* olfactory cell line, CaM appears to be a critical component for CaCC gating (Kaneko et al. 2006). Transfection of dysfunctional mutant CaM inhibits CaCC activation. Because channel activation with  $\text{Ca}^{2+}$  is too fast to be consistent with phosphorylation, and because this current in rat olfactory receptor neurons is not dependent on ATP (Reisert et al. 2003), it is proposed that CaM likely interacts directly with the olfactory CaCC.

CaCCs also vary in their responsiveness to different sources of intracellular  $\text{Ca}^{2+}$ ; some endogenous CaCCs can be activated in response to  $\text{Ca}^{2+}$  influx through  $\text{Ca}^{2+}$  channels, while others require a rise in intracellular calcium via release from intracellular stores. In medium and large DRG neurons for example, activation of voltage-gated calcium channels results in CaCC activation (Andre et al. 2003); in contrast, this coupling between voltage-gated  $\text{Ca}^{2+}$  channels and CaCCs is absent in the majority of small DRG neurons (Liu et al. 2010). Because the molecular identity of CaCCs had been controversial, it was difficult to explain the diversity in their regulatory mechanisms. CaCCs may be differentially regulated due to differences in regulatory mechanisms across various cell types. It is also likely that the heterogeneity is partly due

to the fact that several different proteins, including members of both the bestrophin and anoctamin families, can function as CaCCs.

### **Bestrophins are bona fide CaCCs**

Studies in the 1970's examining the inheritance pattern of Best Vitelliform Macular Dystrophy (BVMD) (Nordstrom and Barkman 1977) led to the discovery of the gene encoding Bestrophin 1 (Best1) (Cooper et al. 1997; Marquardt et al. 1998; Petrukhin et al. 1998; Stohr et al. 1998; Weber et al. 1994). When the Best1 gene was identified, it was originally designated *VMD2*; subsequently, three human bestrophin paralogs were identified by Stohr et al, originally called *VMD2L1*, *VMD2L2*, and *VMD2L3*. The nomenclature for Best1 genes was later revised, resulting in the genes *VMD2*, *VMD2L1*, and *VMD2L3* being renamed *BEST1*, *BEST2*, *BEST3*, and *BEST4*. All mammals have either three or four bestrophins paralogs. The mouse genome, for example, contains three paralogs and one pseudogene (F. Kramer et al. 2004). There is substantial evidence that bestrophins are CaCCs. First, expression of hBest1 and other bestrophins in HEK cells induce Ca<sup>2+</sup>-dependent Cl<sup>-</sup> currents (Chien et al. 2006; Qu et al. 2003; Qu et al. 2004; Sun et al. 2002). hBest1 currents are slightly outwardly rectifying, while other bestrophins display pronounced rectification. This heterogeneity in the biophysical properties of bestrophins suggests that they are pore forming subunits of a channel rather than channel regulators. In addition, mutagenesis studies provide strong evidence that Best1 is a pore forming subunit.

Disease causing mutations in hBest1 have provided significant insight into the channel function of bestrophins. Several disease causing mutations are clustered within the second transmembrane domain. This region has now been identified as forming, at least in part, the Cl<sup>-</sup> conduction pathway of the channel. Studies on hBest1 show that

currents from several cysteine-substituted mutants within the second transmembrane domain (amino acids 75-95) are modified by extracellularly applied MTSET<sup>+</sup>, indicating that this region is involved in the conduction pathway of the channel (Tsunenari et al. 2003). The most extensive work on the role of the second transmembrane domain in bestrophin function has been performed on mBest2, which is ~90% identical to hBest1 within this region. In mBest2, mutation of tryptophan at position 93 to histidine dramatically alters the nearly linear current-voltage (I-V) curve such that it is inwardly rectifying (Qu et al. 2006). Similarly, another cysteine mutant, F80C, displays altered rectification upon modification with either positively or negatively charged sulfhydryl reagents. Residues within the second transmembrane domain that are closer to the C-terminal end are more slowly modified by sulfhydryl reagents, consistent with a deeper localization within the pore. Together, these molecular manipulations of bestrophins indicate that they form an integral part of the Cl<sup>-</sup> conduction pathway of CaCCs. Because the second transmembrane is one of the most highly conserved regions across the bestrophin family, it is likely that this region plays a similar role in the function of other bestrophin members.

### **Regulation of Best1 by Ca<sup>2+</sup>**

As with endogenous CaCCs, there appear to be different mechanisms for bestrophin activation; some bestrophins are directly by Ca<sup>2+</sup>, while others are activated via indirect mechanisms involving phosphorylation (Chien et al. 2006; Xiao et al. 2008). Understanding the mechanisms of Ca<sup>2+</sup> activation of bestrophins, as well as anoctamins, will be instrumental to understanding their physiological roles in specific tissues where CaCC currents have been observed. Ca<sup>2+</sup>-activation of bestrophins has been most closely examined for hBest1, which is activated directly by Ca<sup>2+</sup> binding (Xiao et al. 2008).

While hBest1 does not contain any canonical  $\text{Ca}^{2+}$  binding motifs, it does contain a C-terminal region reminiscent of the “calcium bowl” of the BK channel, followed by a potential EF hand-like structure. Like the BK calcium bowl, hBest1 possesses a region rich in negatively charged amino acids, specifically aspartic acid, which may serve to coordinate  $\text{Ca}^{2+}$ . Residues with negatively charged side chains are critical for BK channel  $\text{Ca}^{2+}$  sensitivity, as neutralization of aspartic acid residues within the  $\text{Ca}^{2+}$  bowl affects  $\text{Ca}^{2+}$  binding (Bao et al. 2002; Bao et al. 2004; Bian et al. 2001; M. Schreiber and Salkoff 1997). Mutagenesis studies reveal that both this region and the EF hand-like structure are critical for  $\text{Ca}^{2+}$  sensitivity of hBest1 (Xiao et al. 2008). Furthermore,  $\text{Ca}^{2+}$  overlay experiments show that  $\text{Ca}^{2+}$  directly binds the C-terminus of hBest1. Studies on the aspartate rich domain of mBest2 yielded results similar to those for hBest1 (Kranjc et al. 2009).

In contrast to hBest1, the *Drosophila* Best1 ortholog, dBest1, is indirectly regulated by  $\text{Ca}^{2+}$ . Endogenous dBest1 currents recorded from S2 cells activate slowly over a time course of ~4 minutes (Chien et al. 2006). One possible explanation is that the channel is regulated by phosphorylation. When ATP is excluded from the intracellular recording solution, the time course of activation for dBest1 is significantly decreased. dBest1 currents can also be activated by osmotic pressure differences between the intracellular and extracellular solutions (Chien and Hartzell 2007). In the presence of a hypotonic external solution, endogenous dBest1 currents activate in a  $\text{Ca}^{2+}$ -independent manner. Although  $\text{Ca}^{2+}$  is not required for activation by osmotic pressure, it is facilitative; in the presence of intracellular  $\text{Ca}^{2+}$ , the amplitude of osmotically activated currents is significantly larger. A variety of regulatory mechanisms, in addition to an underlying molecular heterogeneity, may contribute to the apparent differences in CaCC currents across tissues.

### **Best1 functions as a CaCC in specific cell types**

We now know that Best1 does not mediate the classical outwardly rectifying CaCC observed in various epithelia, but it is nonetheless important in the limited tissues in which it is expressed. For example, Best 1 may have important functions in specific neuronal populations. Following peripheral nerve injury, sensory neurons enter a regrowth mode in which they express an array of injury-related genes; among these are CaCCs. The growth competency of sensory neurons is closely correlated with CaCC expression (Andre et al. 2003). Functional gene screening with siRNA demonstrates that Best1 is involved in injury induced CaCC expression. In addition, CaCC currents recorded from axotomized sensory neurons have biophysical properties similar to those of Best1 currents (Boudes et al. 2009). The role that Best1 plays in neuronal regeneration is uncertain, but it is postulated that CaCCs may contribute to either electrical silencing necessary for growth competence, or regulation of osmotic tension important for neurite growth (Boudes and Scamps 2012). Best1 may also be the molecular correlate of the CaCC expressed in hippocampal astrocytes (Park et al. 2009). The function of Best1 in hippocampal astrocytes is uncertain, but it could possibly play a role in tonic inhibition; in cerebellar glial cells, for example, Best1 mediates tonic inhibition via its permeability to GABA (Lee et al. 2010). In the aforementioned neuronal cell-types, Best1 likely mediates a plasma membrane CaCC. However, its function in other types of epithelia, notably RPE, is controversial.

The physiological importance of Best1 has been most appreciated in the retinal pigment epithelium. Mutations in Best1 cause four clinically distinct diseases: autosomal dominant vitreoretinopathopathy (ADVIRC), autosomal recessive bestrophinopathy (ARB), adult vitelliform macular dystrophy (AVMD), and best vitelliform macular dystrophy (BVMD). Of these, BVMD has been the most extensively

studied. The major functional impairment for BVMD is a decrease in visual acuity, although this deficit is highly variable across BVMD patients. Although there is some heterogeneity in the clinical presentation of bestrophinopathies, one consistent feature is a deficit in the light peak (LP) of the EOG. Because the LP is likely mediated by a CaCC expressed in RPE, it was originally hypothesized that Best1 mediated the LP, and that mutations resulted in Best1 channel dysfunction. Bestrophins are indeed CaCCs, but there is evidence that is incongruous with the idea that Best1 mediates RPE CaCC currents. The caveats to this hypothesis and the potential role of anoctamins in BVMD will be discussed further below.

### **Best Vitelliform Macular Dystrophy**

BVMD, which is caused by mutations in the Best1 gene, is an autosomal-dominant, progressive juvenile-onset macular dystrophy. While there is some heterogeneity in BVMD symptoms, patients commonly present with a vitelliform (egg-yolk-like) lesion, caused by large deposits of a yellow pigmented material, lipofuscin, in and around the retinal pigment epithelium (RPE). The characteristic feature of BVMD that differentiates it from other forms of macular dystrophy is a deficit in the LP of the electrooculogram (Blodi and Stone 1990; Cross and Bard 1974; Mohler and Fine 1981; Thorburn and Nordstrom 1978; Wajima et al. 1993). The LP is thought to be mediated by a CaCC expressed in the basolateral membrane of the RPE (Gallemore and Steinberg 1993; Griff and Steinberg 1982). Because Best1 is expressed on the basolateral membrane in RPE, it was originally hypothesized that mutations in Best1 impair its Cl<sup>-</sup> channel function, consequently resulting in the pathology of BVMD (Sun et al. 2002). In agreement with the dominant-negative inheritance pattern of BVMD, expression of Best1 mutants have a dominant negative effect on wild-type Best1 (Yu et al. 2007). In

addition, disease causing mutations cluster in regions of Best1 that are known to be critical for channel function (H. C. Hartzell et al. 2008; Yu et al. 2006; Yu et al. 2007). It is important to note, however, that the majority of studies on Best1 channel function have been conducted in heterologous over-expression systems, an approach which presents major limitations. Heterologous systems may not express accessory/regulatory subunits endogenously associated with Best1, such that Best1 functions differently depending on the system. Differences in Best1 function have been observed between *Xenopus oocytes* and HEK293 cells, in that Best1 only produces current when expressed in HEK293 cells (Tsunenari et al. 2003). Best1 itself has a very restricted expression profile and is primarily expressed in RPE cells, which are very specialized and have a unique expression profile.

Although the idea that Best1 mediates the LP is appealing, there is compelling evidence against this hypothesis. The most challenging data are that RPE cells from Best1 knockout mice have normal CaCC currents and do not display any disease phenotype (L. Y. Marmorstein et al. 2006). Similarly, CaCC currents from a Best1 mutant (W93C) knock-in mouse model are normal (Zhang et al. 2010). While it is clear that Best1 is not required for CaCCs in mouse RPE, knock-in mice do exhibit a phenotype reminiscent of BVMD. W93C knockin mice present with an accumulation of lipofuscin in and around the RPE, and fluid and debris filled retinal detachments. In addition, knock-in mice had altered LP luminance responses with an otherwise normal ERG, as is observed in BVMD patients. These studies demonstrate that while Best1 may not directly mediate the LP in mice, it is a modulator of the LP response.

Best1 could modulate the LP response in several ways. One alternative hypothesis for how Best1 mutations affect the LP is that hBest1 functions intracellularly to modulate intracellular Ca<sup>2+</sup> signaling. RPE cells of Best1-deficient mice have higher

levels of resting intracellular  $\text{Ca}^{2+}$  than wild-type mice; furthermore, the time course of ATP-stimulated changes in  $[\text{Ca}^{2+}]_i$  is altered (L. Y. Marmorstein et al. 2006). Most studies examining Best1 function have been performed in overexpression experiments, where it functions as a plasma membrane CaCC. Studies in primary mouse RPE cell cultures show that the majority of endogenous Best1 co-fractionates with intracellular membrane proteins (Neussert et al. 2010; Strauss et al. 2012). Immunofluorescence confocal microscopy of porcine retina also supports the intracellular localization of Best1. While some Best1 is expressed on the membrane, a significant portion of Best1 is near the basolateral membrane where it does not co-localize with the membrane proteins cadherin and beta-catenin. Another study examining overexpressed Best1 shows that a large proportion of Best1 is found in the cytoplasm (Milenkovic et al. 2009).

There is also substantial evidence that Best1 can act as a channel regulator. The multi-functionality of Best1 may help to explain the confusion surrounding its role in RPE physiology, as well as other cell types. For example, hBest1 can regulate the kinetics and voltage dependence of voltage-gated  $\text{Ca}^{2+}$  channels (Rosenthal et al. 2006; Yu et al. 2008). More recently it was determined that Best1 is expressed in the ER of airway epithelia where it plays an important role in  $\text{Ca}^{2+}$  handling (Barro-Soria et al. 2010). As an ER protein, Best1 may serve as a counterion channel for  $\text{Ca}^{2+}$  release and reuptake. By affecting  $\text{Ca}^{2+}$  signaling, Best1 could affect the activation of plasma membrane  $\text{Ca}^{2+}$ -activated channels, including anoctamins. Further supporting a role for Best1 in ER  $\text{Ca}^{2+}$  homeostasis is that airway epithelia from Best1 deficient mice display bloated ER cisterns and  $\text{Ca}^{2+}$  deposits, and also have attenuated  $\text{Ca}^{2+}$ -activated  $\text{Cl}^-$  currents. Best1 may function similarly in other epithelial cells to modulate the activity of plasma membrane CaCCs.

### **BVMD: Unanswered Questions**

Mutations in Best1 reproduce some phenotypic features of BVMD in mice, but it is unknown how Best1 mutations result in a decrease in the LP in humans, and if this reduction is critical for the development of BVMD pathology. A reduction in the LP is a consistent feature of BVMD, yet the EOG deficit in the LP is not necessarily correlated with the severity of the disease. Patients harboring the same BVMD mutations have varying degrees of degeneration, suggesting that other genetic or environmental factors are involved with the progression of the disease. Nonetheless, it is clear that Best1 mutations cause BVMD. Mutant Best1 may regulate the activity of an unknown Cl<sup>-</sup> channel in the basolateral membrane of RPE to produce LP deficits. Identifying the molecular correlate of the CaCC in RPE will be instrumental to our understanding of the mechanisms underlying BVMD. In this thesis, I propose that anoctamins mediate CaCC currents in RPE. Given the physiological importance of anoctamins in several epithelial tissues, anoctamins may be implicated in the pathology of BVMD.

### **Anoctamins mediate classical CaCCs<sup>1</sup>**

The discovery of anoctamins provides new avenues to explore and an exciting new hypothesis regarding BVMD, but the Anos themselves are somewhat peculiar. Although the chloride channel functions of Ano1 and Ano2 have been determined, the function of the remaining 8 mammalian anoctamins is unknown. Furthermore, little is known regarding the mechanisms underlying Ca<sup>2+</sup> activation, chloride permeation, and

---

<sup>1</sup> Section contains select material from the previously published article: Duran, C., et al. (2010) 'Chloride channels: often enigmatic, rarely predictable', *Annu Rev Physiol*, 72, 95-121. Substantial changes have been made to the text.

regulation of Ano1. CaCCs were first described in *Xenopus* oocytes (Barish 1983; Miledi 1982) and salamander rods (Bader et al. 1982) in the early 1980's, but it was not until 2008 that anoctamins were identified. In 2008, members of three labs independently cloned genes that encode classical CaCCs (C. Hartzell et al. 2005; T. C. Hwang and Sheppard 2009; Schroeder et al. 2008). The two genes that have been definitively shown to encode CaCCs are called Ano1 and Ano2 (previously named *Tmem16A* and *Tmem16B*). These are two members of a family that consists of 10 genes in mammals (Milenkovic et al. 2010) (Figure 1-2). Yang *et al* (Y. D. Yang et al. 2008) proposed the new name “anoctamin” or Ano (anion+octa=8) and this name is now the official HUGO nomenclature and has replaced *Tmem16* in Genbank. *Tmem16A* is now Ano1, *Tmem16B* is Ano2, and so-on except that the letter I is skipped in the *Tmem16* nomenclature so that *Tmem16J* is Ano 9 and *Tmem16K* is Ano10.

### **Anoctamins 1 and 2 are CaCCs**

Expression of Ano1 and Ano2 in various cell types induces Cl<sup>-</sup> currents with biophysical properties similar to native CaCCs. The Ca<sup>2+</sup> sensitivity and voltage dependence of Ano1 are similar to those of endogenous CaCCs, with an EC<sub>50</sub> of 2.6 μM at -60 mV (Y. D. Yang et al. 2008). The Ca<sup>2+</sup> sensitivity increases with depolarization, much like endogenous CaCC currents in *Xenopus* oocytes (Kuruma and Hartzell 2000). Furthermore, the current is strongly outwardly rectifying at Ca<sup>2+</sup> concentrations <1μM (Schroeder et al. 2008; Y. D. Yang et al. 2008). At Ca<sup>2+</sup> concentrations >10 μM Ano1 current is activated less, which is also consistent with native CaCCs (Fuller et al. 1994; Y. D. Yang et al. 2008). *Xenopus* Ano1 is similar to native *Xenopus* oocyte CaCCs, as it exhibits an outwardly rectifying current at low intracellular Ca<sup>2+</sup> but displays a linear current-voltage relationship at higher intracellular Ca<sup>2+</sup> (Schroeder et al. 2008). Ano2 is

also outwardly rectifying but activates more quickly with depolarization than Ano1, and has a significantly lower apparent  $\text{Ca}^{2+}$  affinity (Pifferi et al. 2009a; Stohr et al. 2009). The anion selectivity sequence of Ano1 and Ano2, ( $\text{NO}_3^- > \text{I}^- > \text{Br}^- > \text{Cl}^- > \text{F}^-$ ), is the same as those of native CaCCs (Caputo et al. 2008; Gajewski et al. 2011; Takahashi et al. 1987; Y. D. Yang et al. 2008), as is the pharmacology. Ano1 and 2 are blocked by traditional  $\text{Cl}^-$  channel blockers, including DIDS (4,4'-diisothiocyanatostilbene-2,2'-disulfonic acid), NPPB [5-nitro-2-(3-phenylpropylamino)benzoic acid], tamoxifen, and NFA (niflumic acid) (Pifferi et al. 2009a; Y. D. Yang et al. 2008). Although Pifferi et al. (Pifferi et al. 2009a) showed that Ano2 is blocked by DIDS, Stohr and colleagues (Stohr et al. 2009) found that it was not blocked by DIDS.

Ano1 and Ano2 are the first CaCC candidates shown to be activated by physiological  $\text{Ca}^{2+}$  signals provided by G protein-coupled receptor (GPCR) stimulation. When mAno1 or mAno2 are cotransfected with GPCRs that raise intracellular  $\text{Ca}^{2+}$ , including endothelin, angiotensin II, muscarinic, histamine, and purinergic receptors, GPCR activation induces Ano1 currents (Pifferi et al. 2009a; Y. D. Yang et al. 2008). GPCR activation of a CaCC resembling Ano1 is observed in the pancreatic cell line CFPAC-1 in response to purinergic receptor activation. This current is abolished in cells transfected with Ano1 siRNA (Caputo et al. 2008). Similarly, coexpression of *Xenopus* Ano1 with the M1 muscarinic acetylcholine receptor induces  $\text{Cl}^-$  currents in response to carbachol (Schroeder et al. 2008).

### **Anoctamin Structure Function**

The anoctamins do not share significant sequence homology with other known ion channel families. However, they do share distant primary sequence homology with a family of transmembrane proteins of unknown function, the transmembrane channel

like (TMC) family (Hahn et al. 2009). Although anoctamins are found in all eukaryotic kingdoms, they are best represented in higher vertebrates. Mammalian anoctamins have 10 gene members that are well conserved across species and are predicted to have similar topologies. Hydropathy analysis shows that all anoctamins have eight hydrophobic helices that are likely to be transmembrane domains with cytosolic N- and C-termini. This predicted topology has been confirmed experimentally for Ano7, whose topology has been determined using inserted HA epitope tag accessibility and endogenous N-glycosylation (Das et al. 2008) (Figure 1-3). Although this topology is appealing, the epitope tag accessibility methodology used to identify intracellular domains of Ano7 does not clearly distinguish between intracellular domains and protein that is not efficiently trafficked to the plasma membrane. Because of this technical limitation and the fact that the topology of other Anos has not been experimentally determined, more investigation is required to establish the topology of these proteins.

Identifying residues indispensable for Ano1 channel function will be crucial for examining functional differences across anoctamins. Thus far, few structure-function studies have been done to identify regions important for Ano1 channel function. Mutational analysis of Ano1 places the putative pore region in a highly conserved region between transmembrane domains 5 and 6 (TM5 and TM6) (Y. D. Yang et al. 2008). This region is predicted to form a reentrant loop and contains two positively charged residues that are conserved in most isoforms (R621, and K645). When these residues are mutated to a negatively charged residue, glutamate, Ano1 shows a marked increase in cation permeability relative to anion permeability. Mutation of K668 to glutamate also alters the relative cation-anion permeability, but this residue is predicted to lie within the extracellular loop between TM5 and TM6. To further examine the importance of this region in the ion conduction pathway, Yang et al. determined the accessibility of

cysteines in this region to membrane-impermeant thiol reagents (Y. D. Yang et al. 2008). MTSET completely blocks the wild-type Ano1 current but has no effect on mutants in which the three cysteines in the reentrant loop are replaced with alanines (C625A, C630A, C635A). These data suggest that the region encompassing TM5 and TM6 is a pore-forming region and is an important determinant of the ion permeation pathway in Ano1.

### **Alternative splicing may contribute to heterogeneity of native CaCCs**

At least 4 splice variants have been identified for Ano1 (Ferrera et al. 2009) and two splice variants have been found for Ano7 (Bera et al. 2004). Human Ano1 has 4 different alternatively-spliced segments, *a*, *b*, *c*, and *d* corresponding, respectively, to an alternative initiation site, exon-6b, exon-13, and exon-15 (Ferrera et al. 2009). Segments *a* and *b* are located in the N-terminus and *c* and *d* are in the first intracellular loop. The variant with all 4 segments is designated as *Ano1abcd*; the variant lacking segments *b* and *d*, for example, is *Ano1ac*. Analysis of ESTs in Genbank predicts that several of the other Anos also have multiple splice variants. Some of these variants may not have channel functions because they are predicted to lack some or all of the transmembrane domains. For example, a splice variant of Ano7 that lacks several exons encodes for a 179 amino acid soluble protein with a distinct C-terminus compared to the long isoform (Bera et al. 2004). The four splice variants of Ano1 exhibit different voltage-dependent and Ca<sup>2+</sup>-dependent gating properties (Ferrera et al. 2009; Xiao et al. 2011). Thus, alternative splicing is likely to contribute to the heterogeneity of CaCC currents observed in native tissues.

### Gating mechanisms of Ano1

Ano1 is gated by both voltage and  $\text{Ca}^{2+}$ , but examination of the sequence of Ano1 gives few clues about the sites that sense voltage or bind to  $\text{Ca}^{2+}$ . Unlike voltage-gated channels that have amphipathic transmembrane helices with charged amino acids that serve to sense voltage, Ano1 has no such sequences. Similar to bestrophins, there are no obvious canonical  $\text{Ca}^{2+}$  binding sites. Reminiscent of the  $\text{Ca}^{2+}$  sensor of hBest1, the first intracellular loop of Ano1 between TMD2 and TMD3 has a large number of acidic amino acids including a stretch of 5 consecutive glutamates ( $_{444}\text{EEEEEE}_{448}$ ) that have attracted attention as a possible  $\text{Ca}^{2+}$  sensor (Xiao et al. 2011). The last glutamate in this sequence is the first residue of a 4-amino acid alternatively-spliced segment ( $_{448}\text{EAVK}_{451}$ ). Neutralization of the glutamates has little effect on  $\text{Ca}^{2+}$  sensitivity, although deletion of the alternatively-spliced segment ( $\Delta\text{EAVK}$ ) alters both voltage-dependent gating and  $\text{Ca}^{2+}$  sensitivity (Ferrera et al. 2009; Xiao et al. 2011). Similar studies in Ano2 where  $_{444}\text{EEEEEE}_{448}$  was deleted show that this region has little effect on  $\text{Ca}^{2+}$  sensitivity, but does affect voltage-dependent gating (Cenedese et al. 2012). Thus, although the first intracellular loop plays an important role in coupling both voltage and  $\text{Ca}^{2+}$  binding to channel opening, it is unlikely to be the binding site for  $\text{Ca}^{2+}$ .

It is unknown whether  $\text{Ca}^{2+}$  activates Ano1 via an accessory subunit such as calmodulin (CaM), or binds directly to the channel. CaM reportedly binds to a 22-amino acid region that overlaps with the *b* segment in the N-terminus called CaM-BD1 and is essential for gating Ano1 (Tian et al. 2011). This putative CaM binding site is not canonical, but resembles some other CaM binding sites. However, only the Ano1 splice variants containing the *b* segment (*e.g.*; Ano1*abc*) seem to require CaM. Ano1*ac*, which lacks the CaM-BD1, does not require CaM and is activated directly by  $\text{Ca}^{2+}$ . Additional work is required to clarify the role of CaM in regulation of Ano1. Some endogenous

CaCCs are regulated directly by  $\text{Ca}^{2+}$  and others by CaM-dependent pathways (Arreola et al. 1998; C. Hartzell et al. 2005; Kaneko et al. 2006). This may be explained by expression of different splice variants, isoforms, or even different channel subunits. For example, the  $\text{Ca}^{2+}$  sensitivity of the CaCC in olfactory receptor neurons, which is now thought to be Ano2, is decreased by a factor of  $\sim 2$  by over-expression of dominant-negative inactive CaMs; unlike the Ano1*abc* isoform however, CaM is not essential for activation (Kaneko et al. 2006). Understanding how anoctamins are regulated by  $\text{Ca}^{2+}$  is essential to determine how they are incorporated into various signaling pathways.

### **Physiological roles and diseases of anoctamins<sup>2</sup>**

Anoctamins display differential temporal and spatial expression in a variety of tissues during development, suggesting they may have numerous physiological functions (Duran and Hartzell 2011; Gritli-Linde et al. 2009; Rock and Harfe 2008; Rock et al. 2008). In murine tissues, Anos 1, 6, 7, 8, 9, and 10 are expressed in a variety of epithelia, while Anos 2, 3, 4, and 5 are more restricted to neuronal and musculoskeletal tissues (R. Schreiber et al. 2010). Mutations in anoctamins are associated with several disease states, but the mechanisms underlying these pathologies are unknown (Figure 1-2). In order to understand the physiological significance of anoctamins, it will be necessary to determine their subcellular localization and if they function as chloride channels, which is currently unknown for Anos 3-10. Thus far, Ano1 and Ano2 are the only two members of the family that have been shown conclusively to mediate

---

<sup>2</sup>Section contains material from the previously published article: Duran, C. and Hartzell, H. C. (2011), 'Physiological roles and diseases of Tmem16/Anoctamin proteins: are they all chloride channels?', *Acta Pharmacol Sin*, 32 (6), 685-92. Changes have been made to the text.

endogenous plasma membrane CaCC currents.

### **Physiological functions of Ano1 and Ano2**

Ano1 is expressed in virtually every kind of secretory epithelium, for example, salivary gland, pancreas, gut, mammary gland, and airway epithelium (Caputo et al. 2008; F. Huang et al. 2009; Ousingsawat et al. 2009; Rock et al. 2009; Romanenko et al. 2010; Y. D. Yang et al. 2008). Ano1 knockout mice display defective Ca<sup>2+</sup>-dependent Cl<sup>-</sup> secretion in a variety of epithelia (Ousingsawat et al. 2009; Rock et al. 2008; Romanenko et al. 2010) and Ano1 has been implicated in rotovirus-induced diarrhea (Ousingsawat et al. 2011). In addition, Ano1 is expressed in a variety of other cell types including certain smooth muscle and sensory neurons. In addition to epithelia, Ano1 is robustly expressed in interstitial cells of Cajal, which are responsible for generating pacemaker activity in smooth muscle of the gut (F. Huang et al. 2009; S. J. Hwang et al. 2009; Zhu et al. 2009). Mice homozygous for a null allele of Ano1 fail to develop slow wave activity in gastrointestinal smooth muscle. The resulting loss of gastrointestinal motility may be an important contributor to the early death of Ano1 knockout mice (F. Huang et al. 2009), and decreased expression of Ano1 in interstitial cells of Cajal may contribute to gastroparesis common in diabetic patients (Mazzone et al. 2011). Ano1 is also expressed robustly in various kinds of smooth muscle including vascular smooth muscle cells (Davis et al. 2010; F. Huang et al. 2009; Manoury et al. 2010). Treatment of rat pulmonary aortic smooth muscle cells with siRNA against Ano1 results in a reduction of CaCCs (Manoury et al. 2010). Ano1 is also strongly expressed in airway smooth muscle cells and airway epithelia, where it is involved in mucus hypersecretion and airway smooth muscle hyperresponsiveness in asthmatics (F. Huang et al. 2009; F. Huang et al. 2012a).

Ano1 is also expressed in small dorsal root ganglion neurons and is implicated in mediating nociceptive signals triggered by bradykinin (Liu et al. 2010). Bradykinin is a very potent inflammatory and pain-inducing substance that is released at sites of tissue damage or inflammation. Bradykinin acts on G<sub>q</sub>-coupled B2 receptors to stimulate phospholipase-C, IP<sub>3</sub> production, and release of Ca<sup>2+</sup> from intracellular stores. The elevation of intracellular Ca<sup>2+</sup> opens CaCCs apparently encoded by Ano1. CaCC current, along with KCNQ channel activation, depolarizes and increases AP firing. Local injection of CaCC inhibitors attenuates the nociceptive effect of local injections of BK. Recently it was discovered that Ano1 can be activated by noxious thermal stimuli, and that knockdown of Ano1 in DRG neurons impairs nociceptive behavior in thermal pain models (Cho et al. 2012).

Before Ano1 was identified as a CaCC, it had originally attracted the interest of cancer biologists because it is upregulated in several cancers (Carles et al. 2006; X. Huang et al. 2002; West et al. 2004). Oncologists have recognized Ano1 by several other names including DOG1 (Discovered On GIST-1 tumor), ORAOV2 (Oral cancer Overexpressed), and TAOS-2 (Tumor Amplified and Overexpressed). Ano1 may prove a useful tool for the diagnosis of certain cancers. Gene expression profiling identified *Ano1* as being highly expressed in gastrointestinal stromal tumors (GISTs). In both oral and head and neck squamous cell carcinomas, amplification of the Ano1 locus is correlated with a poor outcome (Carles et al. 2006; X. Huang et al. 2006). Ano1 expression is significantly increased in patients with a propensity to develop metastases. Given the role that Cl<sup>-</sup> channels play in cell proliferation and migration, it is possible that Ano1 overexpression provides a growth or metastatic advantage to cancer cells (Kunzelmann 2005). Supporting the role of Ano1 in metastasis is that overexpression of Ano1 stimulates cell movement (Ayoub et al. 2010). In contrast, silencing of Ano1 decreases

cell migration; treatment of cells with CaCC blockers has a similar effect. Another study shows that overexpression of Ano1 induces cancer cell proliferation and tumor growth via induction of MAPK (Duvvuri et al. 2012). Identifying the protein networks with which Ano1 is associated will be critical for understanding how Ano1 signaling mediates cell proliferation and migration in cancer.

Ano2 may play a role in olfactory sensory neurons, although its precise role is unclear. In olfactory sensory neurons, odorants open cyclic nucleotide gated channels by binding to G-protein coupled olfactory receptors that elevate cAMP (Hengl et al. 2010). In the canonical signal transduction pathway, Ca<sup>2+</sup> influx through the cyclic nucleotide gated channels activates CaCCs that amplify the receptor potential. From immunostaining studies, it was first suggested that Best2 might be the olfactory CaCC (Pifferi et al. 2006), but electrophysiological recordings from Best2 knockout mice failed to confirm a role for Best2 in mediating the olfactory receptor potential (Pifferi et al. 2009b). It seems Ano2 is now the best candidate for the pore-forming subunit of CaCCs in olfactory sensory neurons (Hengl et al. 2010; Rasche et al. 2010; Sagheddu et al. 2010; Stephan et al. 2009). Ano2 generates Ca<sup>2+</sup> activated chloride currents when expressed in heterologous systems, (Pifferi et al. 2009a; Schroeder et al. 2008) and Ano2 knockout mice lack CaCC currents. However, it is now apparent that Ano2 currents are unnecessary for olfaction, calling into question the view that CaCCs are critical for mammalian olfaction (Billig et al. 2011). The precise function of CaCCs in olfactory sensory neurons is unclear, but the importance of CaCCs in mammalian olfactory signal transduction may have been overestimated in previous studies. First, many studies examining the role of CaCCs in olfaction use niflumic acid as a CaCC inhibitor, which can also modulate other ion channels and targets in the main olfactory epithelium (Gribkoff et al. 1996; Vogalis et al. 2005). That niflumic acid attenuates olfactory responses in

Ano2 knockout mice demonstrates that it affects other targets besides CaCCs (Billig et al. 2011). Another important consideration is that electrophysiological studies of olfactory sensory neurons are often performed in dissociated neurons that are patch clamped at the cell body. Therefore, channels in the cell body would be more electrically accessible, while the electrical contribution of channels located in the distal part of cilia would be underestimated (Lindemann 2001). It has been suggested that Ano2 may redistribute to the cell body following disruption of tight junctions during the neuronal isolation procedure, thus increasing its electrical accessibility (Billig et al. 2011).

Ano2 may also have important roles in photoreceptors. Release of the neurotransmitter glutamate at photoreceptor synapses is controlled by intracellular  $\text{Ca}^{2+}$ .  $\text{Ca}^{2+}$ -activated  $\text{Cl}^-$  channels located in photoreceptor nerve terminals (Bader et al. 1982; MacLeish and Nurse 2007) have been shown to provide a feedback control on transmitter release (Mercer et al. 2011). Ano2 is highly expressed in photoreceptor synaptic terminals (Stohr et al. 2009). Ano2 is localized to presynaptic membranes in ribbon synapses, where it co-localizes with the adapter proteins PSD95, MPP4, and VGLL3. Ano2 contains a consensus C-terminal PDZ class I binding motif that interacts with the PDZ domains of PSD95. Through this interaction, Ano2 is tethered to membrane domains along photoreceptor terminals, and may serve to regulate synaptic output in these cells. Ano1 has also been shown to be expressed in photoreceptor terminals, suggesting there may be a contribution by both proteins to CaCCs in photoreceptors (Mercer et al. 2011).

### **Some anoctamins may function as intracellular $\text{Cl}^-$ channels**

While Ano1 and Ano2 clearly function as plasma membrane CaCCs, the subcellular localization of several anoctamins is unknown. Ano5 is predominantly

localized intracellularly (Mizuta et al. 2007), suggesting that other anoctamin members may have intracellular roles. The roles of Cl<sup>-</sup> channels localized to intracellular organelles have not been as extensively studied as those of plasma membrane channels. Cl<sup>-</sup> homeostasis in intracellular organelles must be important, because different subcellular compartments have distinctive [Cl<sup>-</sup>] (Faundez and Hartzell 2004). The roles of intracellular ClCs in physiology have recently begun to be elucidated. The physiological functions of intracellular ClCs may give clues to the function of intracellular anocatmins, but it is important to note that intracellular ClCs are H:Cl antiporters rather than channels (Picollo and Pusch 2005). These proteins mediate the exchange of two Cl<sup>-</sup> ions for one proton. Several studies employed knockout mice to demonstrate that intracellular ClC's are important for the maintenance of organelle pH and endosomal/lysosomal acidification. Both ClC-3 and ClC-4 knockout mice display impairments in the regulation of endosomal pH (Mohammad-Panah et al. 2009; Stobrawa et al. 2001; Yoshikawa et al. 2002). Similarly, endosomes from ClC-5 knockout mice are acidified at a significantly slower rate than wild type (Piwon et al. 2000; S. S. Wang et al. 2000). Impairment of endosomal acidification may underlie Dent's disease, a syndrome caused by mutations in ClC-5 which is characterized by kidney stones, proteinuria, and hypercalciuria. Impairment of vesicular acidification has severe physiological effects because it is crucial for several cellular processes including the modulation of enzymatic activity, sorting, endocytosis, vesicle trafficking, and the transport of other substances across the vesicle membrane (Thevenod 2002). ClC antiporters are typically present in the membranes of intracellular organelles and vesicles, but some can reach the plasma membrane upon overexpression, thus allowing for characterization of their transporter function. It is unknown if intracellular anocatmins function as channels because a similar approach has thus far been

unsuccessful. An alternative approach may be to express anoctamins in yeast, as their insertion into vacuoles allows for use in electrophysiological techniques (Costa et al. 2012).

### **Diseases associated with anoctamin mutations**

Mutations in *Ano5* result in a spectrum of musculoskeletal disorders. *Ano5* was originally identified as *GDD1*, the gene product mutated in a rare autosomal dominant skeletal syndrome called gnathodiaphyseal dysplasia (GDD) (Tsutsumi et al. 2004). Mutations in cysteine-356, a highly conserved cysteine in the first extracellular loop of *Ano5*, results in abnormal bone mineralization and bone fragility. *Ano5* primarily resides in intracellular membrane vesicles, but the nature of these compartments is still unknown (Mizuta et al. 2007). *Ano5* clearly plays important roles in musculoskeletal development. *Ano5* is expressed in growth-plate chondrocytes and osteoblasts at sites of active bone turnover, indicating an important role in bone formation. *Ano5* is also expressed in somites and in developing skeletal muscle, and is upregulated during the myogenic differentiation of the skeletal muscle cell line C2Cl2 (Mizuta et al. 2007).

The importance of *Ano5* in skeletal muscle physiology is further highlighted by the recent finding that mutations in *Ano5* produce several recessive muscular dystrophies (Bolduc et al. 2010; Hicks et al. 2011; Mahjneh et al. 2010). Patients with a proximal limb-girdle muscular dystrophy (LGMD2L) and distal non-dysferlin Miyoshi myopathy (MMD3) carry mutations in *Ano5*. These mutations include a splice site and base pair duplication that result in premature stop codons, and two missense mutations, R758C and G231V. The phenotypes resulting from these mutations are reminiscent of dysferlinopathies, in which a deficiency in dysferlin causes defective skeletal muscle membrane repair. It has been suggested that chloride currents are important in

membrane repair (Fein and Terasaki 2005) and Ano5 may be one of the channels involved in this process. Additional evidence implicating Ano5 in the maintenance of skeletal muscle is that Ano5 expression is increased in dystrophin-deficient mdx mice, a mouse model of Duchenne muscular dystrophy. In contrast to the Duchenne muscular dystrophy phenotype, dystrophin-deficient mdx mice maintain their ability to regenerate muscle fibers and have reduced endomysial fibrosis (Sicinski et al. 1989). The role of Ano5 in muscle membrane repair is still speculative, but determining if Ano5 functions as a Cl<sup>-</sup> channel will be critical for elucidating its role in musculoskeletal pathologies.

Mutations in Ano6 have recently been implicated in Scott syndrome, a rare congenital bleeding disorder caused by a defect in blood coagulation (J. Suzuki et al. 2010). In platelets, like other cell types, phosphatidylserine is located on the inner leaflet of the plasma membrane. When platelets are activated they expose phosphatidylserine on the outer leaflet of the plasma membrane to promote clotting. This redistribution of phosphatidylserine is mediated by phospholipid scramblases that transport phospholipids bidirectionally from one leaflet to the other. In patients with Scott syndrome this mechanism is defective, resulting in impaired blood clotting. Ano6 was found to be critical for Ca<sup>2+</sup>-dependent exposure of phosphatidylserine on the cell surface in Ba/F3 platelet cells. Furthermore, a patient with Scott syndrome harbored a mutation at a splice-acceptor site of Ano6, resulting in premature termination of the protein. Cells derived from this patient did not expose phosphatidylserine in response to a Ca<sup>2+</sup> ionophore, unlike cells derived from the patient's unaffected parents. These data imply that Ano6 is required for scramblase activity. However, there is conflicting evidence regarding the function of Ano6. Ano6 has also been reported to be both a Ca<sup>2+</sup>-activated non-selective cation channel (H. Yang et al. 2011), and a Cl<sup>-</sup> channel of intermediate conductance that is not dependent on Ca<sup>2+</sup> (Martins et al. 2011). These

reports are difficult to reconcile, and more work regarding the channel function of Ano6 is needed.

Ano7, which is highly expressed in prostate, was discovered in a search for genes whose expression patterns mimicked those of known prostate cancer genes (Bera et al. 2004; Das et al. 2007). Of 40,000 human genes examined, 8 novel genes, including Ano7, were identified as being the most closely linked to known prostate cancer genes. Ano7 is expressed on the apical and lateral membranes of normal prostate. In the prostate LNCaP cell line stably transfected with Ano7, the protein localizes to cell-cell contact regions. It has been suggested that Ano7 promotes cell association because cell association can be reduced with RNAi targeted to Ano7 (Das et al. 2007). The predominant expression of Ano7 in prostate and prostate cancers poise Ano7 as an attractive candidate for immunotherapy (Cereda et al. 2010; Williams and Naz 2010), although the role of Ano7 in the development of prostate cancer is uncertain.

Mutations in Ano10 have been linked to autosomal-recessive cerebellar ataxias associated with moderate gait ataxia, downbeat nystagmus, and dysarthric speech (Vermeer et al. 2010). Affected individuals display severe cerebellar atrophy. Two of the mutations introduce premature stop codons, probably leading to null protein expression. The other mutation is a missense mutation, L510R, a highly conserved residue among the Anos that lies within the sixth transmembrane domain and the highly conserved anoctamin domain (pfam04547). It remains uncertain whether Ano10 is an ion channel, because Ano10 and Ano8 constitute the most divergent branch of the anoctamin family. While there is little functional data for Ano10, a *Drosophila* ortholog of Ano8/10, called Axs, is necessary for normal spindle formation and cell cycle progression (J. Kramer and Hawley 2003). Axs co-localizes with ER components, and is recruited to microtubules of assembling spindles during mitosis and meiosis. A dominant mutation in Axs causes

abnormal segregation of homologous achiasmate chromosomes due to defects in spindle formation, and disrupts cell cycle progression. It remains to be seen if Ano10 plays a similar role in mammalian systems.

### **The Cl<sup>-</sup> channel function of Anos 3-10 is unknown**

With the exception of Ano1 and Ano2, the status of other anoctamin family members as channels is unclear. In a study by Schreiber *et al* (R. Schreiber et al. 2010), it was concluded that in addition to Ano1 and Ano2, Anos 6, 7, and 10 were Cl<sup>-</sup> channels. However, in iodide flux assays, the ATP- or ionomycin-stimulated flux reported for Anos 6, 7, and 10 were <10% of those for Ano1. Furthermore, the short form of Ano7 (Ano7S), which is a 179 amino acid protein with no predicted transmembrane domains and very unlikely to be an ion channel, produced approximately the same flux as the long form of Ano7. No patch clamp data were reported for Ano7. Over-expression of Ano10 produced a Cl<sup>-</sup> current that was activated slowly over a time frame of 10 min. However, expression of Ano10 also suppressed maximal currents produced by Ano1. To date, no functional data have been published for Anos 3 and 4. Ano 6 has been reported to be a non-selective cation channel that is more permeable to Ca<sup>2+</sup> than Na<sup>2+</sup> (Yang 2011), but has also been reported to be a Cl<sup>-</sup> channel not dependent on Ca<sup>2+</sup> by another group (Martins et al. 2011). As these are relatively newly discovered proteins, little functional data is available for many of the Ano family members.

### **Rationale and Significance**

The greatest challenge in studying CaCCs has certainly been the controversy surrounding their molecular identity. Endogenous CaCC currents are heterogeneous in

terms of their biophysical properties and mechanisms of regulation; it is likely that this variety reflects an underlying diversity in their molecular identities. The discovery that Ano1 mediates CaCCs in several tissues opens many new avenues of research. Only two of ten anoctamins have been definitively shown to be CaCCs, and there is little information on the mechanisms underlying channel function. In this dissertation, I focus on the functional characterization of members of the Anoctamin family, with a special emphasis on Ano1. Specifically, I will address questions regarding the following:

- 1) channel function and plasma membrane trafficking of anoctamin family members
- 2) mechanisms underlying  $\text{Ca}^{2+}$  and voltage regulation of Ano1
- 3) regulation of endogenous CaCCs in *Drosophila* S2 cells and the contribution of anoctamin orthologs
- 4) the role of Ano1 in RPE as a potential mediator of the light peak

Despite the fact that anoctamins were only recently discovered, they have already been implicated in several diseases. Ascertaining which anoctamins function as  $\text{Cl}^-$  channels and determining their subcellular localization will be key to understanding how they are involved in various disease states, as well as normal physiological functions.

Understanding the mechanisms underlying  $\text{Ca}^{2+}$  and voltage regulation of Ano1 will lay the groundwork for future studies examining differences/similarities in the function of other anoctamins and how they are involved in various signaling pathways. Because bestrophins also function as CaCCs, it is important to examine the relative contribution of anoctamins and bestrophins to endogenous CaCCs. It is also critical to examine the regulation and function of endogenous CaCCs because the regulatory mechanisms governing CaCC function varies depending on the system. In this dissertation I will explore the contribution of anoctamins to endogenous CaCCs in S2 cells and mouse RPE.

Taken together, these studies may lend insight into the mechanisms underlying BVMD pathology. The physiological importance of anoctamins will undoubtedly become more evident as future studies advance our understanding of anoctamin function.

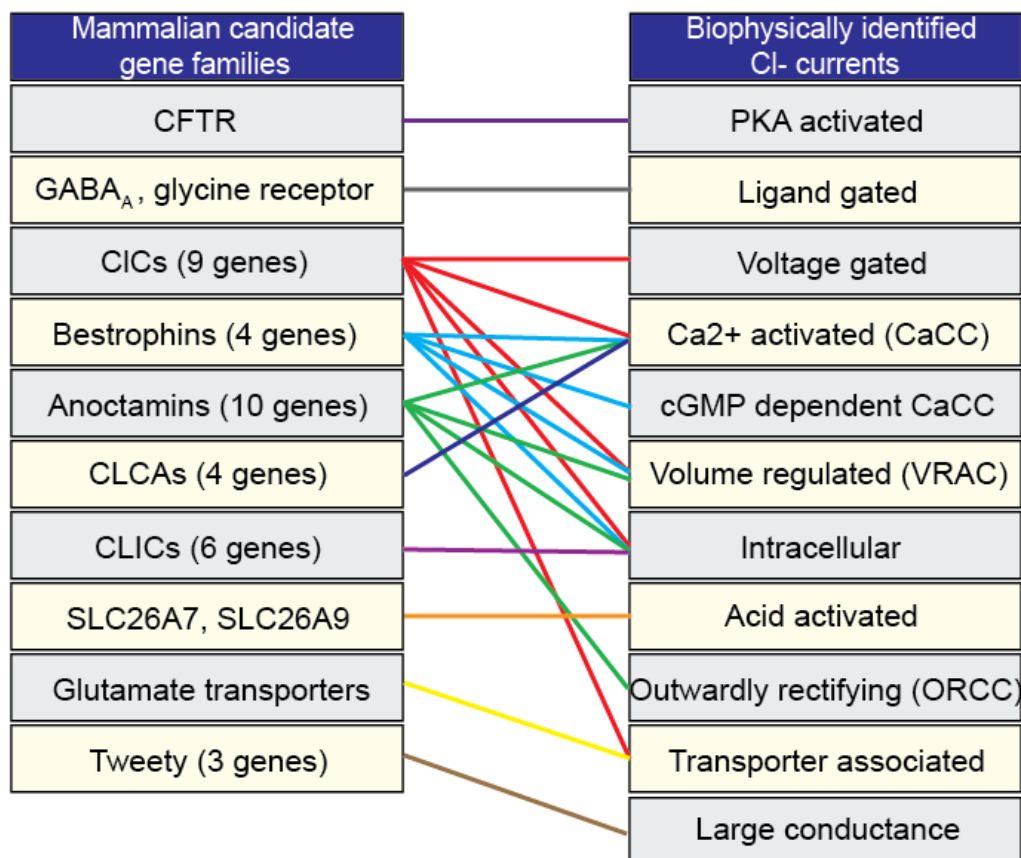


**Figure 1-1.** Cl<sup>-</sup> channel genes and their relationship to biophysically identified Cl<sup>-</sup> currents. Various candidate Cl<sup>-</sup> channel genes are shown on the left, and currents that have been electrophysiologically identified in native cells is shown on the right. Lines show proposed relationships between candidate genes and native channels. In many cases, a biophysically identified channel has been linked to multiple genes.

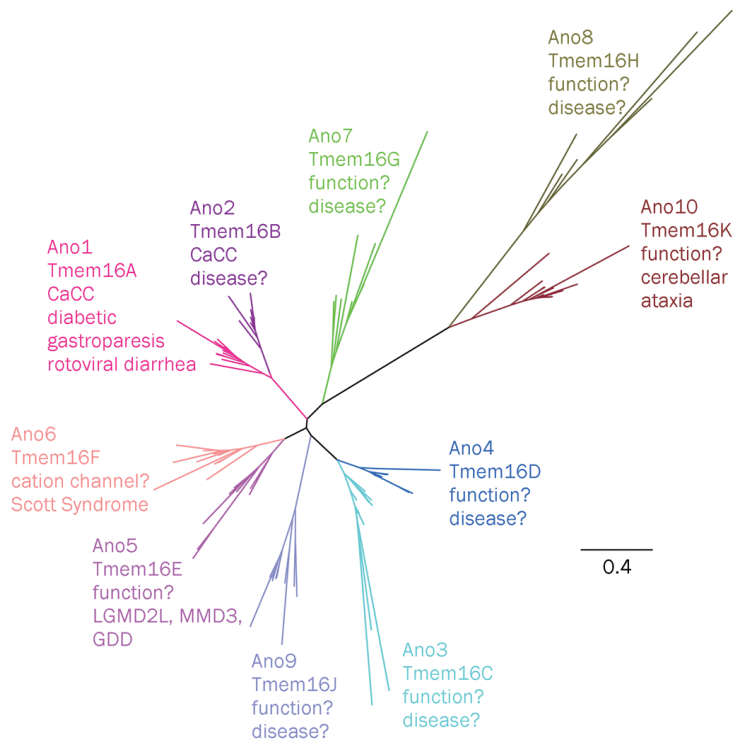


**Figure 1-2.** Phylogenetic tree of vertebrate Anoctamins. Each branch is labeled with the Ano and Tmem16 nomenclature, followed by the known or suspected physiological function, and any diseases that have been associated with this protein. GDD: gnathodiaphyseal dysplasia; LGMD2L: proximal limb girdle muscular dystrophy; MMD3: distal Miyoshi muscular dystrophy. The tree was computed using 103 vertebrate Anoctamins found in Genbank and Ensembl using nearest neighbor statistics. Reprinted from *Acta Pharmacologica Sinica* 32: 685-692, Duran C., and Hartzell, H.C., Physiological Roles and Diseases of Tmem16/Ano proteins: are they all chloride channels?, Copyright (2011).

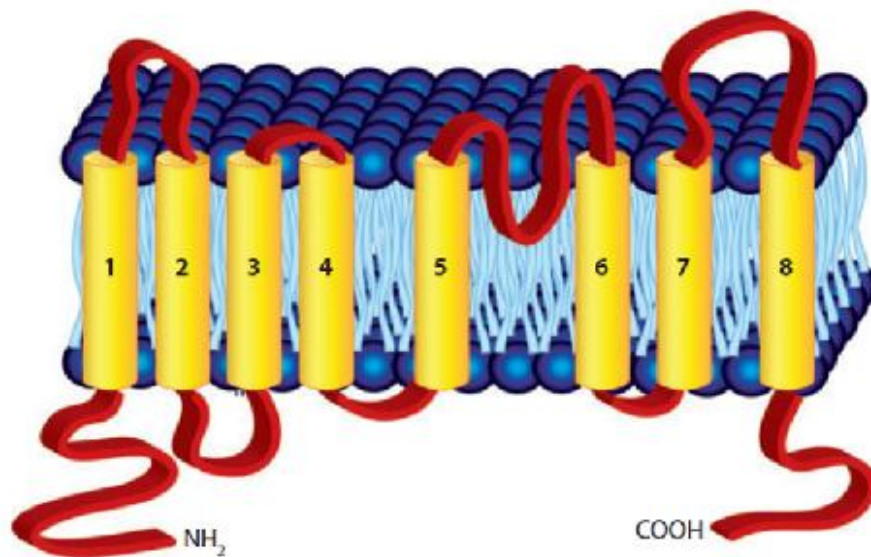


**Figure 1-3:** Anoctamin transmembrane topology. Anoctamins are thought to have 8 transmembrane domains and a reentrant loop between transmembrane domains 5 and 6 with cytoplasmic N and C termini. The structure is based on experimental studies on Ano7 (Das 2008). The pore of the channel is thought to be located between TM5 and TM6. Reprinted from Annual Review of Physiology 72: 95-121, Duran, C., et al, Chloride Channels: Often Enigmatic, Rarely Predictable, Copyright (2012).

Protein Name	Localization	Human Disease	Defective Function
CFTR	Plasma membrane	Cystic fibrosis	Airway epithelial transport
CIC-1	Plasma membrane	Myotonia congenita	Membrane potential
CIC-Kb	Plasma membrane	Bartter III	Renal salt balance
CIC-5	Endosomes	Dent's disease	Endosomal acidification
CIC-7	Late endosomes, lysosomes	Osteopetrosis Neuronal ceroid lipofuscinosis	Osteoclast acid secretion Lysosomal dysfunction
GABAA receptor $\gamma 2$	Plasma membrane	Epilepsy	Synaptic inhibition
GABAA receptor $\alpha 1$	Plasma membrane	Juvenile myoclonus epilepsy	Synaptic inhibition
Glycine receptor	Plasma membrane	Hyperplexia	Synaptic inhibition
Bestrophin 1	Plasma membrane / ER?	Vitelliform macular dystrophy	RPE Cl <sup>-</sup> transport?
Anoctamin 5	Intracellular vesicles?	Gnathodiaphyseal dysplasia GDD1 Limb girdle muscular dystrophy (LGMD2L) Miyoshi muscular dystrophy.	? ? ?
Anoctamin 6	Plasma membrane?	Scott syndrome	Phospholipid scrambling
Anoctamin 10	?	Autosomal-recessive cerebellar ataxia	?

**Table 1-1.** Disorders of Cl<sup>-</sup> channels/transporters

## CHAPTER 2

### ANOCTAMINS 3-7 ARE INTRACELLULAR PROTEINS<sup>3</sup>

---

<sup>3</sup> Reproduced with minor edits from original publication: Duran, C., et al. (2012) 'ANOs 3-7 in the anoctamin/Tmem16Cl<sup>-</sup> channel family are intracellular proteins', *Am J Physiol Cell Physiol*, 302 (3), C482-93

## Summary

Ca<sup>2+</sup>-activated Cl<sup>-</sup> channels (CaCCs) participate in numerous physiological functions such as neuronal excitability, sensory transduction, and transepithelial fluid transport. Recently, it was shown that heterologously expressed anoctamins Ano1 and Ano2 generate currents that resemble native CaCCs. The anoctamin family (also called Tmem16) consists of 10 members, but it is not known whether all members of the family are CaCCs. Expression of Anos 3–7 in HEK293 cells did not generate Cl<sup>-</sup> currents activated by intracellular Ca<sup>2+</sup>, as determined by whole cell patch clamp electrophysiology. With the use of confocal imaging, only Ano1 and Ano2 traffic to the plasma membrane when expressed heterologously. Furthermore, endogenously expressed Ano7 in the human prostate is predominantly intracellular. We took a chimeric approach to identify regions critical for channel trafficking and function. However, none of the chimeras of Ano1 and Ano5/7 that we made trafficked to the plasma membrane. Our results suggest that intracellular anoctamins may be endoplasmic reticulum proteins, although it remains unknown whether these family members are CaCCs. Determining the role of anoctamin family members in ion transport will be critical to understanding their functions in physiology and disease.

## Introduction

Ca<sup>2+</sup>-activated Cl<sup>-</sup> channels (CaCCs) play important roles in physiological processes including sensory transduction, epithelial secretion, and smooth muscle contraction (Eggermont 2004). Recently, three groups independently identified a gene encoding for a transmembrane protein (Anoctamin 1, Ano1, TMEM16A) that closely recapitulates the properties of endogenous CaCCs (Caputo et al. 2008; Schroeder et al. 2008; Y. D. Yang et al. 2008). Ano1 is highly expressed in epithelial tissues, where it plays an important role in Ca<sup>2+</sup>-dependent Cl<sup>-</sup> secretion (Dutta et al. 2011; F. Huang et al. 2009; Manoury et al. 2010; Namkung et al. 2011; Ousingsawat et al. 2009; Romanenko et al. 2010). Ano1 can be activated both by intracellular Ca<sup>2+</sup> and by activation of GPCRs that raise intracellular Ca<sup>2+</sup> (35, 42). Ano2 has also been shown to be a CaCC and mediates Ca<sup>2+</sup>-activated Cl<sup>-</sup> currents in olfactory sensory neurons and photoreceptor synapses (Pifferi et al. 2009a; Rasche et al. 2010; Sagheddu et al. 2010; Stephan et al. 2009; Stohr et al. 2009).

The anoctamin family consists of 10 members, all of which are predicted to have 8 transmembrane domains with cytosolic N- and C-termini. With the possible exceptions of Ano8 and Ano10, anoctamins are predicted to have a reentrant loop between transmembrane domains 5 and 6 that has been suggested to participate in the ion selectivity filter (Das et al. 2008; H. C. Hartzell et al. 2009; Milenkovic et al. 2010; Y. D. Yang et al. 2008). While the predicted structural homology between family members is conserved, evolutionary analysis suggests that anoctamins have evolved distinctive functional properties (Milenkovic et al. 2010). Furthermore, the diversity of endogenous CaCCs in various tissues indicates that CaCCs may be mediated by more than one protein molecule. Although other anoctamin family members are, in fact, expressed in epithelial tissues, it is not known whether these function as CaCCs. We find that unlike Ano1 and

Ano2, Anos 3-7 do not generate Cl<sup>-</sup> currents activated by intracellular Ca<sup>2+</sup> when expressed in HEK293 cells, as determined by whole-cell patch clamp electrophysiology. Localization studies demonstrate that several anoctamin family members do not traffic to the plasma membrane in HEK293 cells and may reside in the ER. We took a chimeric approach to determine which regions are important for anoctamin trafficking and function, with an emphasis on Anos 5 and 7. We chose to focus on Ano5 and Ano7 because of their roles in disease. Ano5 was originally identified as the gene responsible for the rare bone disease gnathodiaphyseal dysplasia (GDD1) (Chien and Hartzell 2007; Tsutsumi et al. 2004), and has more recently been linked to several limb girdle muscular dystrophies (Bolduc et al. 2010; Hicks et al. 2011; Mahjneh et al. 2010). Ano7 is implicated in prostate cancer, as it was discovered in a search for genes whose expression patterns mimicked those of known prostate cancer genes (Kiessling et al. 2005).

## **Results**

### **Expression of Anos 3-7 do not generate Ca<sup>2+</sup>-activated Cl<sup>-</sup> currents in HEK293 cells**

We performed whole-cell recordings on HEK293 cells transiently transfected with anoctamin constructs (Ano 1-7) (Fig. 1). Cells transfected with GFP alone had negligible Cl<sup>-</sup> currents (<100 pA in amplitude at +100 mV). Expression of GFP-tagged Ano1 produced currents that were Ca<sup>2+</sup>-dependent. Ano1 currents were outwardly rectifying at intracellular [Ca<sup>2+</sup>] < 1 μM and nearly linear at higher [Ca<sup>2+</sup>] (Figs. 1A, B). Ano2 currents were also Ca<sup>2+</sup>-dependent but activated more quickly and exhibited more pronounced outward rectification at high Ca<sup>2+</sup> (Figs. 1A, B). The mean peak amplitudes of currents at +100 mV with 24 μM intracellular Ca<sup>2+</sup> were 13 nA ± 1.8 for Ano1 and 4 nA

$\pm 1.2$  for An $\alpha$ 2. In contrast, cells transfected with An $\alpha$ s 3-7 had currents that were the same as GFP controls (Fig. 1C). An $\alpha$ 7 has been reported to support a very small iodide flux in transfected FRT cells (R. Schreiber et al. 2010), but in our hands expression of An $\alpha$ 7 in FRT cells did not yield significant Ca $^{2+}$ -activated currents at +100mV, as measured by whole cell patch clamp electrophysiology (31pA  $\pm$  12, n=3).

Because many ion channels are heteromeric, we tested whether the absence of currents could be explained by the absence of another subunit. We co-expressed An $\alpha$ 7, which is not detected in HEK cells by RT-PCR or western blot, with An $\alpha$ 1, An $\alpha$ 2, An $\alpha$ 4, An $\alpha$ 5, An $\alpha$ 6, and An $\alpha$ 10. Combinations that included An $\alpha$ 1 were tested at 180 nM Ca $^{2+}$  to avoid maximal current activation, whereas combinations with other An $\alpha$ s were tested at 24  $\mu$ M Ca $^{2+}$ . None of these anoctamin combinations generated Cl $^{-}$  currents, with the exception of co-expression of An $\alpha$ 7 with An $\alpha$ 1 or An $\alpha$ 2 (Fig. 1D). mAn $\alpha$ 1+hAn $\alpha$ 7 produced currents of similar amplitude as mAn $\alpha$ 1 alone at the same [Ca $^{2+}$ ] (~180 nM). Similarly, mAn $\alpha$ 2+hAn $\alpha$ 7 produced currents of similar amplitude to mAn $\alpha$ 2 alone at the same [Ca $^{2+}$ ] (~24  $\mu$ M).

### **Plasma membrane trafficking of An $\alpha$ s in various cell lines**

An $\alpha$  constructs with a C-terminal EGFP tag were overexpressed in HEK293, CHO, and COS-7 cells, and analyzed using confocal microscopy (Fig. 2). Multiple cell lines were used in the event that HEK cells lacked an essential subunit or chaperone for proper trafficking. These cell lines originate from different species and tissues, and therefore provide a different proteomic background for favorable expression and trafficking. Similar results were obtained with all cell lines tested. An $\alpha$ 1 is clearly localized to the plasma membrane (Fig. 2A). In contrast, EGFP-tagged An $\alpha$ s 3, 4, 5, 6, 7, and 10 are localized intracellularly (Fig. 2B). The intracellular localization of An $\alpha$ s 3, 4,

5, 6, 7, and 10 is consistent with electrophysiology data, which shows that these Anos do not produce  $\text{Ca}^{2+}$ -activated  $\text{Cl}^-$  currents when expressed in HEK293 cells.

To test whether the intracellular localization of Ano7 was possibly caused by the EGFP tag, we examined the localization of a myc-tagged construct. The myc tag is considerably shorter than the 238 amino acid EGFP tag, and may be less likely to interfere with protein folding or trafficking. The localization of Ano7-myc was also intracellular like Ano7-EGFP (Fig. 2C). In Fig. 2C, the difference in localization between Ano1 and Ano7 is shown clearly where Ano7-myc was co-expressed with Ano1-EGFP; Ano1 is localized to the plasma membrane, while Ano7 is intracellular. We consistently observed these distinctive subcellular distributions of Ano1 and Ano7 when expressed in several cell lines, including HeLa and CHO cells.

### **Subcellular localization of anoctamins**

In cells transfected with fluorescently-tagged Anos 3, 4, 5, 6, 7, and 10, a reticular pattern characteristic of ER is observed (Fig. 2B). Colocalization of Ano7 with an ER marker, mCherry-17, supports the conclusion that most of Ano7 is localized in the ER (Fig. 3A). Co-labeling of cells for Ano7 and another ER marker, calnexin (CNX), reveal that while a portion of Ano7 co-localizes with CNX, some Ano7 is localized in a compartment adjacent to the CNX. These data indicate that some Ano7 is localized to an ER subdomain distinct from that of calnexin. Ano7 does not co-localize with other markers, including the KDEL receptor (cis-golgi), EEA1 (endosomes), or TGN46 (trans-golgi) (Fig. 3B). While we cannot rule out potential artifacts of overexpression in a heterologous system, these results suggest that intracellular anoctamins may be ER proteins.

Because the localization of heterologously expressed proteins might be abnormal for a variety of reasons, we examined the endogenous expression of Ano7 in prostate using an antibody against the C-terminus of the long form of Ano7 (5, 6). The specificity of the antibody for the long form of Ano7 was confirmed by both immunoblot and immunofluorescence (Fig. 4). The antibody recognizes a 133kD band in HEK cells transfected with GFP-tagged Ano7, and a 106kD band corresponding to non-tagged Ano7 in a stable cell line, 22Rv1-Ano7 (Fig. 4A). No signal is detected in nontransfected HEK293 cells, or in 22Rv1 cells stably transfected with the empty vector. Furthermore, pre-incubation of the antibody with immunizing peptide abolishes the Ano7 signal (Fig. 4B). The antibody is also suitable for immunofluorescent staining, as antibody staining co-localizes with myc-tagged Ano7 (Fig. 4C). The staining can be abolished upon pre-incubation with the immunizing peptide.

### **Localization of endogenous Ano7 in human prostate**

Staining of human prostate tissue with the Ano7 antibody revealed that Ano7 was highly expressed in the prostatic epithelium when examined at low power (Fig. 5). At higher power, a significant portion of endogenous Ano7 appeared to be localized intracellularly. Basolateral membrane markers, aquaporin 3 and Na<sup>+</sup>-K<sup>+</sup>-ATPase, are clearly confined to the basolateral plasma membrane. In contrast, Ano7 appears to be localized intracellularly at the apical end of the cell. Much of the Ano7 staining is punctuate, and there is no clearly defined apical staining (Fig. 5). We have tried to no avail to find a good apical plasma membrane marker, but none of the antibodies that we have tried (anti-aquaporin 3, anti-Na<sup>+</sup>-K<sup>+</sup>-ATPase, anti-H<sup>+</sup>-K<sup>+</sup>-ATPase) were localized apically (Fig. 5). As in HEK cells, Ano7 staining overlaps with that of calnexin, but the two proteins do not precisely co-localize.

### **Sequence homology across Anos**

There are 10 members of the anoctamin family. However, Ano1 and Ano2 comprise a distinct branch of the family tree. Protein sequence conservation analysis reveals that Ano1 displays the highest degree of conservation (~57% identical) with Ano2, the only other anoctamin shown clearly to be a CaCC. The percent identity between Ano1 and other anoctamin family members is lower, with Ano5 and Ano7 being ~30% identical to Ano1. If one includes structurally similar amino acids, Ano1 is 51% similar to Ano7 and 59% similar to Ano5. Although anoctamins have a similar predicted membrane topology and display sequence conservation in TMDs, it is not clear if all anoctamins are associated with Cl<sup>-</sup> currents.

Evolutionary analysis using DIVERGE suggests that anoctamins may have diverse physiological functions. The regions exhibiting the highest functional divergence are the N-terminus and the hydrophilic loops between transmembrane domains (Fig. 6). However, divergent amino acids are scattered throughout the protein and clustering provides little clue to identifying key amino acids that could account for differences in trafficking or function of the proteins. We therefore took a chimeric approach to identify regions between Ano1 and Ano5 or Ano7 critical for channel trafficking and function.

### **Chimeras between Ano1 and Ano5 or Ano7 do not generate Ca<sup>2+</sup>-activated Cl<sup>-</sup> currents**

Because protein N- and C-termini frequently contain targeting signals important for protein trafficking and were identified as being different among Ano1 or 2 and Ano5 or 7 in the DIVERGE analysis, we generated chimeras containing either N- or C-terminal sequences from Ano1. Functionality and localization of chimeras between Ano1 and Ano5 or Ano7 were analyzed using whole cell patch clamp electrophysiology and confocal

microscopy. Chimeras produced by replacement of the N- or C-terminus of Ano7 with the corresponding sequences from Ano1 (Fig. 7, chimeras 7-2 and 7-3 respectively) did not produce currents and were not trafficked to the plasma membrane. A chimera composed of Ano7 with an Ano1 N-terminus and first transmembrane domain (chimera 7-4) was not trafficked to the plasma membrane. The inverse chimera, composed of Ano1 with an Ano7 N-terminus and first transmembrane domain (chimera 7-5) also was retained intracellularly. These data suggest that there are multiple trafficking signals in Ano7 that are involved in preventing trafficking to the plasma membrane. Analogous results were obtained with Ano1–Ano5 chimeras (Fig. 8). An Ano5 chimera containing the Ano1 N-terminus plus the first 2 transmembrane domains and first intracellular loop (chimera 5-2) was localized intracellularly and did not generate current (Fig. 8).

One possible explanation for the absence of currents generated by Ano5 and Ano7 is that these channels are not activated by  $\text{Ca}^{2+}$  but are activated by other mechanisms. We have found that the sequence 444EEEEAVK452 in the first intracellular loop of mAno1 is important in determining the  $\text{Ca}^{2+}$  sensitivity of the channel (Ferrera et al. 2009; Xiao et al. 2011). In both Ano5 and Ano7, the EAVK sequence is not conserved. Therefore, we inserted EAVK after amino acid 462 to test whether the EAVK sequence was important in channel trafficking or activation. The Ano7 construct containing the EAVK sequence (chimera 7-1) did not produce current when expressed in HEK293 cells and did not traffic to the plasma membrane (Fig. 7). Similar results were found with a chimera of Ano5, in which the entire first intracellular loop is composed of Ano1 sequence (chimera 5-1) (Fig. 8).

Because neither N- and C-terminal sequences from Ano1 nor the EAVK sequence were sufficient to traffic Ano5 or Ano7 to the plasma membrane, we took a slightly different approach. We sought to determine if the putative pore of Ano5 is functional

when inserted into Ano1. The reentrant loop between TM5 and TM6 in Ano1 is thought to form, at least in part, the conduction pathway of the channel (4, 42). If replacement of the Ano1 putative pore with that of Ano5 yields a functional channel, this would strongly suggest that Ano5 also functions as a CaCC. We initially replaced TM5 through TM6 of Ano1 with the corresponding sequence from Ano5 (chimera 5-3). This construct was not trafficked to the plasma membrane and did not generate current (Fig. 8). We then shortened the substituted Ano5 sequence to include only the putative reentrant loop (chimera 5-4). This chimera was also not trafficked to the plasma membrane and did not generate current. Surprisingly, Ano1 containing only 58 amino acids of Ano5 sequence in the reentrant loop (chimera 5-5) failed to be targeted to the plasma membrane or to generate current. Likewise, Ano5 chimeras containing the Ano1 pore region (chimera 5-2) were intracellular (Fig. 8). These data suggest that the reentrant loop of Ano1 and Ano5 is sufficiently divergent, such that substitution of the Ano1 sequence with the corresponding sequence from Ano5 results in structurally aberrant protein. That none of the chimeras between Ano1 and Ano5/7 trafficked to the membrane indicates that Anos 5 and 7 may have topologies that differ from Ano1.

## **Discussion**

### **Anoctamin family homology**

Expression of Ano1 in several different cell types produces Ca<sup>2+</sup>-activated Cl<sup>-</sup> currents that resemble those of endogenous CaCCs. Ano2, which is ~57% identical in primary sequence to Ano1, has also been shown to produce Ca<sup>2+</sup>-activated Cl<sup>-</sup> currents. The conservation of sequence among the anoctamins suggests that other Anos may also function as Cl<sup>-</sup> channels. However, homology is not a certain predictor of protein

function as shown by recent examples: certain voltage-gated  $\text{Ca}^{2+}$  channels in skeletal muscle are non-conductive to  $\text{Ca}^{2+}$  (Schredelseker et al. 2010), the  $\delta 2$  glutamate receptor is not activated by glutamate (Matsuda et al. 2010), and some of the ClC proteins are  $\text{Cl}^-$  channels and others are  $\text{H}^+$ - $\text{Cl}^-$  exchangers (Accardi and Picollo 2010). Although we have come to expect that similar sequence implies common function, it is clear that many structurally related proteins have different functions; for example, the *E. coli* RecA protein, the bovine F1-ATPase, and *S. typhimurium* adenosylcobinamide kinase all share the same highly conserved core, yet perform widely different functions of genetic recombination, ATP synthesis, and phosphorylation (8).

The topology of An07 has been studied using epitope tag insertion (Das et al. 2008). The results of these experiments support an 8 transmembrane topology model of An07 in which N- and C- termini are cytoplasmic. The topology of other Anos has not been explored experimentally, but it is thought that they are similar to An07 because of the primary amino acid sequence is highly conserved and the proteins exhibit very similar hydropathy profiles. However, we have data that the topology of An01 is not as predicted in the region of the putative reentrant loop (Yu et al. 2012). Small differences in sequence among the family members are likely to account for the differences in their trafficking and possibly also function.

The most notable difference between An01 and An05 or An07 is their localization. An01 is clearly expressed on the plasma membrane. However, Anos 3-7 and An010 are intracellular in several expression systems as confirmed by whole-cell patch clamp electrophysiology and confocal microscopy. We found that An07 co-localized with the ER marker mCherry-17, and displayed partial overlap with calnexin. However, An07 did not co-localize with markers for Golgi or endosomes in transfected cells. A search for ER retention signals within An05 and An07 revealed that neither contained the classical ER

retention signal KDEL (Munro and Pelham 1987). However, Ano5 and Ano7 do have several RXR/KKXX potential retention signals which are not present in Ano1. These potential signals are mainly located in the N-terminus, but replacement of the Ano5 or Ano7 N-terminus with the Ano1 N-terminus did not result in plasma membrane localization.

Further examination of the localization of Ano7 reveals that the majority of endogenous Ano7 in prostate is intracellular, but it remains unclear exactly in which subcellular structures it resides. We cannot rule out the possibility that some Ano7 is trafficked to the plasma membrane because we have not been able to identify a reliable apical membrane marker. Surprisingly, although the Na<sup>+</sup>-K<sup>+</sup>-ATPase has been reported to be apical in some studies (Mobasher et al. 2001) but not others (Mobasher et al. 2003), in our hands it is clearly basolateral in human prostate. Similarly, H<sup>+</sup>-K<sup>+</sup>-ATPase, which has been reported to be apical in mouse (Pestov et al. 2002) is intracellular punctate in human. One possibility, although unlikely, is that the apical membrane has been destroyed during preparation of the tissue. Additional experiments are needed to refine the subcellular localization of endogenous Ano7, but our results indicate that Ano7 is primarily intracellular, and is likely expressed in the ER. The fact that we find no current in transfected cells and no membrane localization in transfected cells or prostate, and that others have reported essentially background iodide fluxes in cells transfected with Ano7 (R. Schreiber et al. 2010) argues strongly that the primary function of Ano7 is not a plasma membrane Cl<sup>-</sup> channel.

A similar situation exists with Ano5. Transient expression of Ano5 results in ER localization of the protein, but subcellular fractionation indicates that endogenous Ano5 resides in intracellular membrane vesicles (Mizuta et al. 2007; Tsutsumi et al. 2004). Mizuta et al. report that Ano5 resides predominantly in fractions that contain

membranes from Golgi apparatus, secretory vesicles, endosomes, endoplasmic reticulum, and trans-Golgi network, and to a lesser degree in the plasma membrane fraction. However, the precise nature of the intracellular compartments in which it resides has not been determined (Mizuta et al. 2007).

### **Ano5 and Ano7 may have significant structural and functional differences from Ano1**

We constructed several chimeras between Ano1 and Ano5 or 7 in an attempt to traffic Ano5 and Ano7 to the plasma membrane. However, relatively short sequences from Ano5 or 7 are sufficient to prevent Ano1 trafficking to the plasma membrane. Remarkably, replacement of a stretch of 58 amino acids within the predicted reentrant loop of Ano1 with corresponding sequences from Ano5 resulted in intracellular localization. This result is surprising in that the substituted region falls within the DUF590, an ~200 amino acid domain of unknown function that is relatively well conserved across all members of the anoctamin family. These data highlight the importance of the DUF590 in anoctamin function, and reveal notable differences between anoctamins in this region. One explanation of these results is that substitution of Ano1 sequences with sequences from Ano5 introduces targeting sequences which prevent trafficking to the plasma membrane. However, introduction of the corresponding Ano1 sequences to Ano5 did not result in functional plasma membrane channels. Similarly, chimeras between Ano1 and Ano7 were intracellular. These results demonstrate that Ano5 and Ano7 are significantly different, both structurally and functionally, from Ano1.

### **Are Ano5 and Ano7 CaCCs?**

Based on our findings, it is still unclear whether Ano5 and Ano7 are CaCCs. The intracellular localization of Ano 3-7 in several systems precludes the use of whole-cell patch clamp electrophysiology to examine channel function. In a previous study by Schreiber et al. (R. Schreiber et al. 2010) it was suggested that Ano7 functioned as a CaCC. However, in iodide flux assays, the ATP- or ionomycin- stimulated flux carried by Ano7 was less than 10% as large as Ano1. Although a small fraction of Ano7 may traffic to the membrane, Ano7 is predominantly intracellular and generates currents indistinguishable from background. It is possible that anoctamins function as intracellular CaCCs.

It is possible that the iodide flux experiments are more sensitive than patch clamp, as it measures anion influx over a period of time. Nonetheless, it is surprising that the short form of Ano7 (Ano7S), which is a 179 amino acid protein with no predicted transmembrane domains, produced approximately the same iodide flux as the long form of Ano7. It is clear that Anos3-10 likely have roles in physiology distinct from that of Ano1, and may produce currents with properties very different from those of Ano1.

## **Materials and Methods**

### **Cell culture and transfection.**

HEK293 and COS-7 cells were cultured in DMEM supplemented with 10% fetal bovine serum and 0.5% penicillin-streptomycin at 37°C. Chinese hamster ovary (CHO) and Fischer rat thyroid (FRT) cells were cultured in Ham's F-12 medium supplemented with 2 mM L-glutamine, 10% fetal bovine serum, and 0.5% penicillin-streptomycin at 37°C. The 22Rv1-Ano7 cell line (generously provided by Ira Pastan, NIH) was cultured in

RPMI 1640 containing 10% FBS, 1 mmol/l pyruvate, 2 mmol/l glutamine, and 100 µg/ml penicillin, and 100 µg/ml streptomycin. For electrophysiology, low-passage HEK293 cells were transfected using Fugene 6 with 1 µg of green fluorescent protein (GFP)-tagged anoctamin constructs. For cotransfections, 0.5 µg of each construct were used. Transfected cells were then plated at low density and used for electrophysiology 24–48 h after transfection. Cells expressing the GFP-fusion proteins were patched. For immunofluorescence, all cell types were transfected with 1 µg of DNA using lipofectamine 2000 (Invitrogen). For colocalization with the mCherry-17 ER marker (Brambillasca et al. 2006; Ronchi et al. 2008) (generously provided by Catherine Hartzell, Stanford University), cells were transfected with 1 µg of the 17-mCherry construct in addition to 1 µg of the Ano7-myc construct.

### **Electrophysiology.**

Recordings were performed using the whole cell patch clamp configuration. Patch pipettes had resistances of 2–4 MΩ. Data were acquired by an Axopatch 200A amplifier controlled by Clampex 8.2 via a Digidata 1322A data acquisition system (Molecular Devices). Voltage ramps of 200 ms from –100 to +100 mV were applied at 10-s intervals, followed by a voltage-step protocol from –100 to +100 mV in 20-mV intervals applied every 10 s. Data were analyzed using ClampFit 8.2 software (Molecular Devices).

### **Solutions.**

The high Ca<sup>2+</sup> (24 µM free Ca<sup>2+</sup>) intracellular pipette solution contained (in mM) 146 CsCl, 2 MgCl<sub>2</sub>, 5 Ca-EGTA, 10 sucrose, and 8 HEPES, pH 7.3 with NMDG. Different free [Ca<sup>2+</sup>] solutions were made by mixing the high Ca<sup>2+</sup> solution with a Ca<sup>2+</sup>-free solution containing 5 mM EGTA as described previously (Kuruma and Hartzell 2000). The

extracellular solution contained (in mM) 140 NaCl, 5 KCl, 2 CaCl<sub>2</sub>, 1 MgCl<sub>2</sub>, 15 glucose, and 10 HEPES, pH 7.4 with NaOH. Osmolarity was adjusted with sucrose to 303 mOsm for all solutions.

### **Anoctamin constructs.**

mAno1 tagged with enhanced GFP (EGFP) on the COOH-terminus was generously provided by Prof. Uhtaek Oh, Seoul National University. hAno7 tagged with myc on the COOH-terminus was provided by Ira Pastan, NIH, and was tagged on the COOH-terminus with EGFP or mCherry by subcloning into pEGFP-N1 or pmCherry. The hAno5 construct was purchased from Open Biosystems (I.M.A.G.E. ID: 100061756) and tagged with EGFP on the COOH-terminus by subcloning into pEGFP-N1. All other Ano constructs were cloned from mouse tissues using RT-PCR and subsequently subcloned into pEGFP-N1 (mAno2, NM\_153589.2; mAno4, NM\_178773.4; mAno6, NM\_175344.3; mAno10, NM\_133979.2).

### **Generation of chimeric constructs.**

Chimeras were constructed using overlapping PCR (Horton et al. 1989). After PCR, the products were digested and subsequently ligated into the pEGFP vector.

### **Immunoblot.**

Cells in culture were homogenized in lysis buffer containing 1% Triton X-100, 1 mM EDTA, 50 mM Tris·HCl (pH 7.4), and protease inhibitor cocktail III (Calbiochem) plus 10 μM phenylmethylsulfonyl chloride. Samples were diluted in SDS Laemmli buffer, and aliquots were run on 7.5% reducing SDS-PAGE and transferred to nitrocellulose. Ano7

antibody was used at a 1:1,000 dilution and detected by enhanced chemiluminescence (Super Signal, Thermo Scientific).

### **Immunofluorescence.**

Cells were plated on poly-D-lysine-coated coverslips. One to two days after transfection, cells were fixed for 20 min in 4% paraformaldehyde. Cells were then washed in PBS, incubated in a PBS blocking solution containing saponin (0.025%) and either BSA (3%) or 1% cold fish water gelatin for 30 min at room temperature, and subsequently incubated with primary antibodies (1:1,000) overnight at 4°C. Primary antibodies were used against the following antigens: hAno7 (generously provided by Dr. Ira Pastan, NIH, directed against amino acids 875–933, IPES. . .QLQQ), mAno1 (amino acids 878–960 MSDF. . .GDAL, SDIX custom Genomic Antibody, Newark DE), mouse anti-myc (1:1,000, Invitrogen), rabbit anti-calnexin (1:300, Enzo Life Sciences), mouse anti-calnexin (1:50 BD Biosciences), sheep anti-TGN46 (1:150, AbD Serotec), KDEL receptor (1:200, Stressgen), and mouse anti-EEAI (1:100 BD Biosciences). For determining Ano7 antibody specificity, antibody was preincubated with immunizing peptide for 1 h at room temperature. The cells were then washed and incubated with a mixture of Alexa 488- or Alexa 568-conjugated (1:1,000) secondary antibodies for 1 h at 4°C, and either rhodamine-conjugated wheat germ agglutinin (2 µg/ml) (WGA, Invitrogen) for 10 min at room temperature, or Alexa 633-conjugated phalloidin (1:1,000, Invitrogen) for 1 h at 4°C. Coverslips were mounted on glass slides using ProLong Gold (Invitrogen).

### **Human prostate tissue.**

Sections of frozen tissue from radical prostatectomy specimens were obtained from the Prostate Tissue Satellite Bank of the Human Tissue Procurement Service of Emory

University. Formalin-fixed paraffin-embedded tissues from the same patients were also obtained. All the sections utilized for this study were from areas composed exclusively of benign prostatic tissue. Frozen sections (20  $\mu$ m thick) were fixed for 1 h in 4% paraformaldehyde in 0.1 M phosphate buffer, pH 7.3, rinsed 3 $\times$  in PBS, and blocked with 1% cold fish water gelatin in PBS for 1 h. Paraffin-embedded sections were deparaffinized with two washes in xylene for 5 min followed by rehydration with serial dilutions of ethanol. Sections were heated in a water bath (20 min at 85°C) in citrate buffer for antigen retrieval. Both frozen and paraffin-embedded sections were incubated with primary antibodies overnight at 4°C. Antibodies were used against the following antigens: anti-alpha Na<sup>+</sup>-K<sup>+</sup>-ATPase, (a6F-c, 1:100, Developmental Studies Hybridoma Banks, University of Iowa), calnexin (1:50, BD Biosciences), rabbit anti-ATP12A (1:50, Sigma), and aquaporin-3 (Santa Cruz Biotechnology). Use of human tissue was approved by the Emory University Institutional Review Board. Tissue samples were deidentified and impossible for us to trace back to the patient's identity.

### **Bioinformatic analysis.**

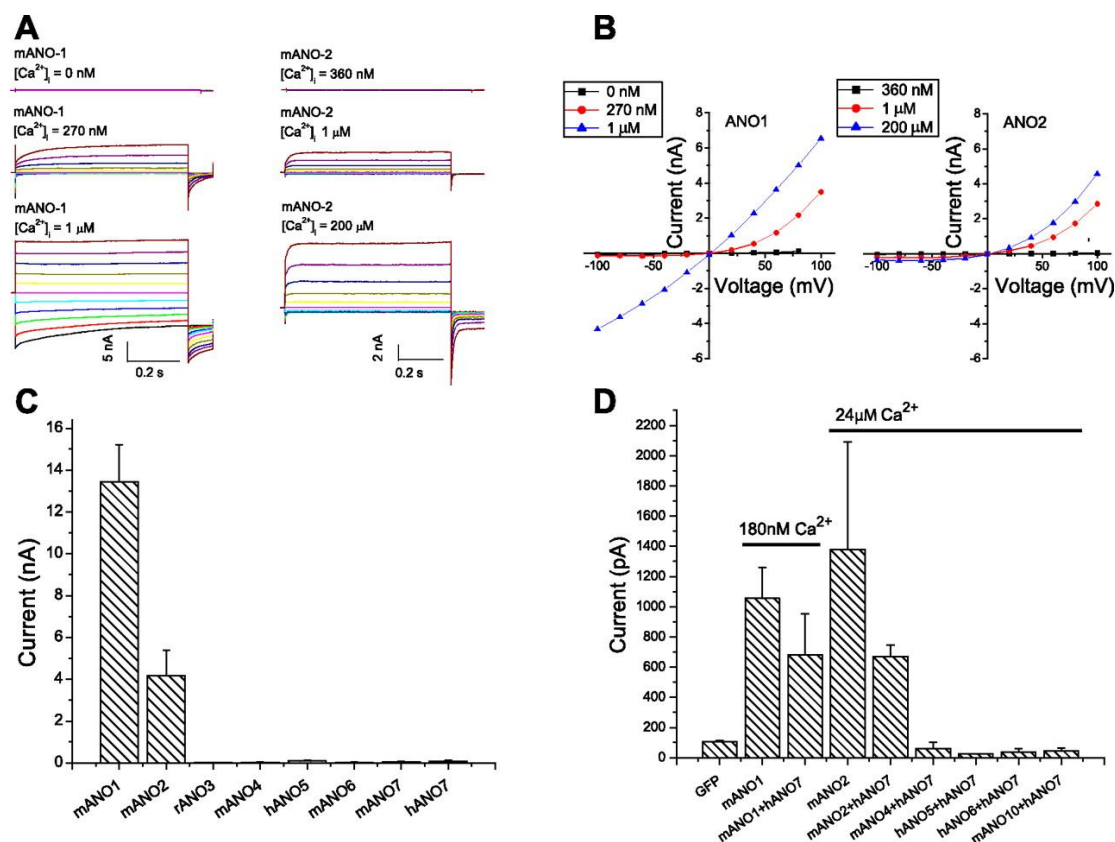
Protein and nucleotide alignments and pairwise comparisons were performed using Lasergene 7.0 and CLC Main Workbench 5.6. Transmembrane helices were predicted using MemBrain, which integrates sequence representation by multiple sequence alignment matrix, optimized evidence-theoretic K-nearest neighbor prediction, fusion of multiple prediction window sizes, and classification by dynamic threshold (Shen and Chou 2008). Type-II divergence was determined using DIVERGE 2.0 (<http://xgu.zool.iastate.edu/software.html>). GENBANK accession numbers of sequences used for the DIVERGE analysis were the following: An01: NP\_001101034, NP\_848757, XP\_610636, NP\_060513, XP\_854489, XP\_002194623,X

P\_421072, NP\_001128709, NP\_001123799, NP\_001155062;

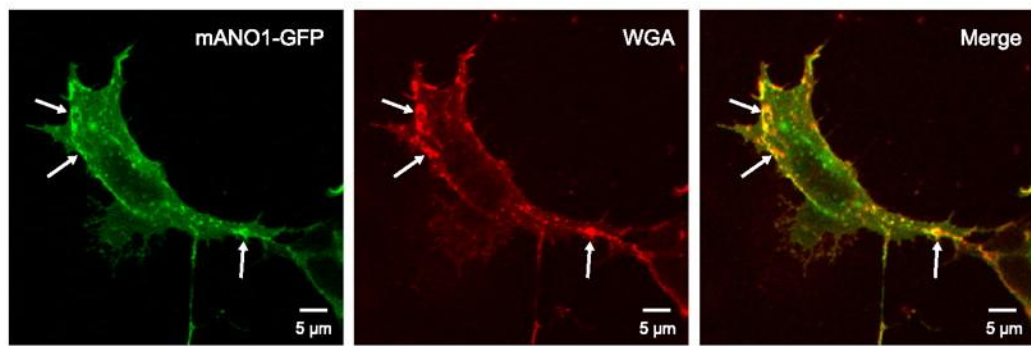
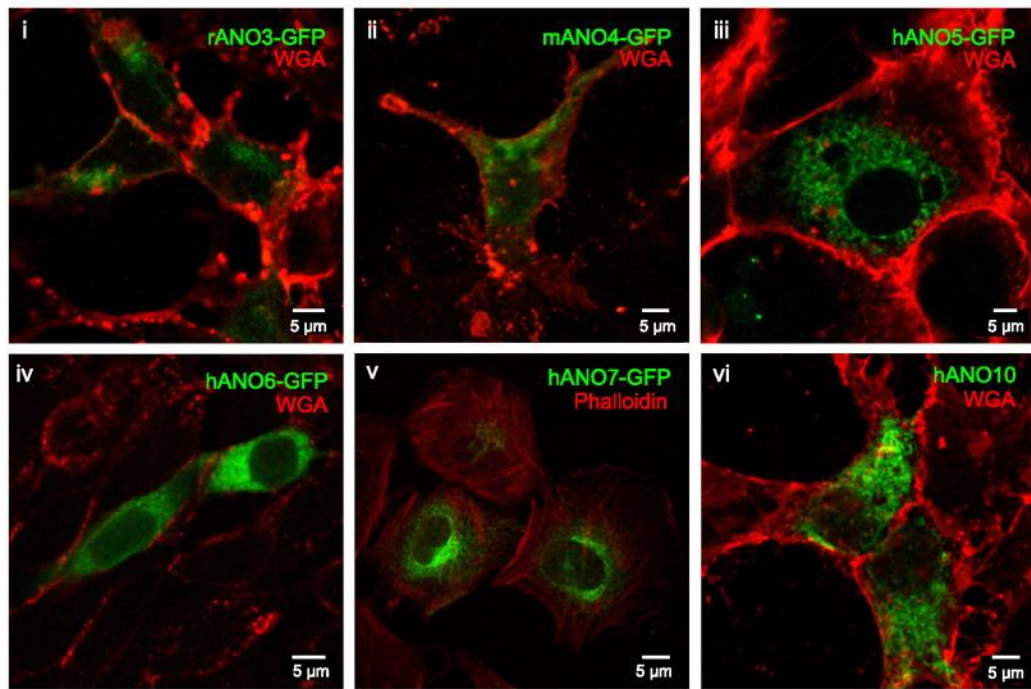
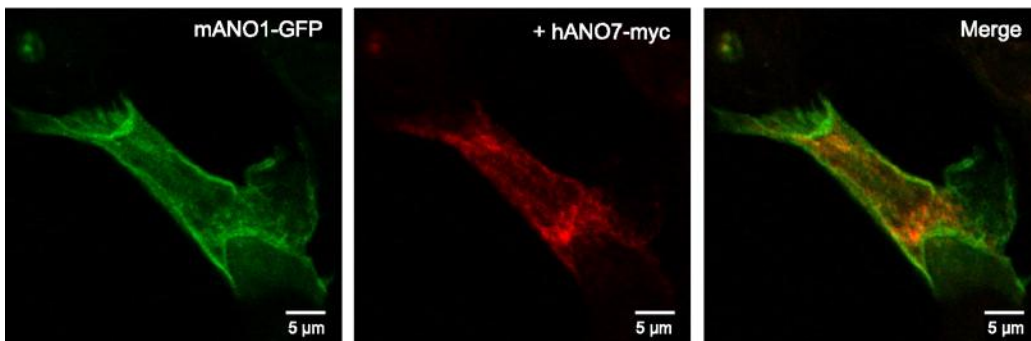
Ano2: XP\_508944, NP\_065106, XP\_001495378, XP\_001066367, NP\_70581, XP\_001118212, XP\_590066, XP\_001368614, XP\_002188249;

Ano5: NP\_998764, XP\_001918124, NP\_808362, NP\_001086810, NP\_001073452;

Ano7: NP\_996914, NP\_001004071, NP\_001001891, XP\_684890, XP\_001377095.



**Figure 2-1.** Anoctamin whole cell current response to intracellular [Ca<sup>2+</sup>]. **A)** Representative current traces for mAno1 and mAno2 at different intracellular [Ca<sup>2+</sup>]. Different free [Ca<sup>2+</sup>] solutions were made by mixing the high Ca<sup>2+</sup> solution with a Ca<sup>2+</sup>-free solution containing 5 mM EGTA (Kuruma and Hartzell 2000). **B)** Mean current-voltage (*I-V*) relationship for AnO1 and AnO2 in response to different intracellular [Ca<sup>2+</sup>]. **C)** Current amplitude at +100 mV of mAno1, mAno2, rAno3, mAno4, mAno7, hAno5, mAno6, and hAno7 as indicated with an intracellular solution containing 5 mM Ca-EGTA (24 μM free Ca<sup>2+</sup>). *N* = 3–7 for each condition. **D)** Current amplitude at +100 mV of hAno7 coexpressed with various Anos in response to 24 μM intracellular [Ca<sup>2+</sup>] or 180 nM [Ca<sup>2+</sup>] for coexpression with AnO1. For transfection with individual AnO constructs, 1 μg DNA was used; cotransfections were performed using 0.5 μg of each AnO construct.

**A****B****C**

**Figure 2-2.** Immunofluorescence confocal microscopy of various cell types expressing Anos 1, 3, 4, 5, 6, 7, and 10. **A)** HEK293 cells transiently transfected with green fluorescent protein (GFP)-tagged mAno1 alone. Arrows indicate colocalization of Ano1 with the membrane marker wheat germ agglutinin (WGA). **B)** Various cell lines transiently transfected with GFP-tagged Ano constructs. Different cell types are shown for illustration, but these results are typical of all cell lines tested. *i, ii, vi*: HEK293 cells; *iii, v*: COS-7 cells; *iv*: CHO cells. Cells in *B,v* were counterstained with phalloidin for actin; all other cells were counterstained with a plasma membrane marker WGA. **C)** GFP-tagged mAno1 (green) coexpressed with myc-tagged hAno7 (red) in HEK293 cell.

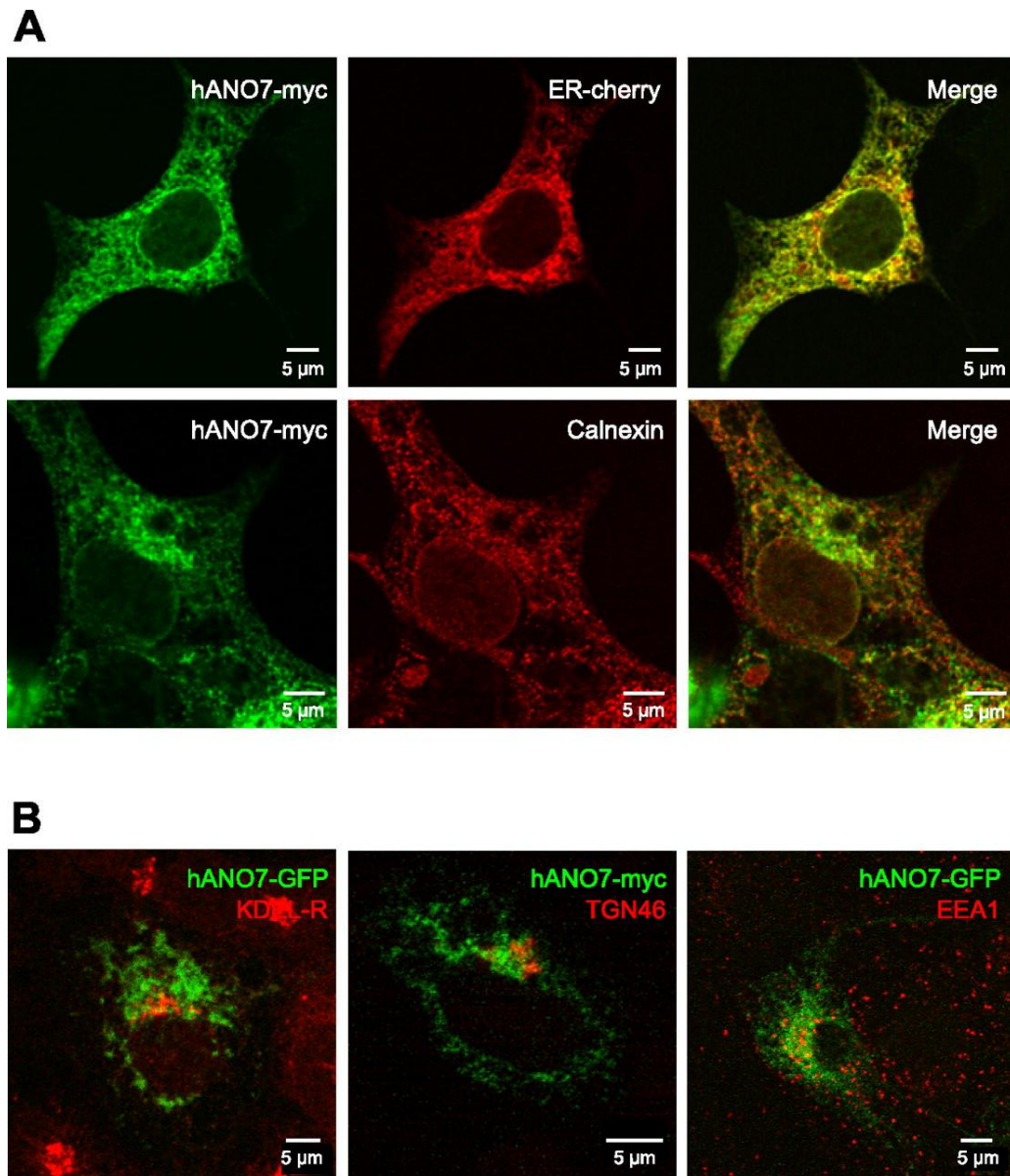


**Figure 2-3.** Subcellular localization of Ano7. **A)** Ano7-myc colocalizes with endoplasmic reticulum (ER) marker mCherry-17, and partially colocalizes with the ER protein calnexin (CNX) in HEK293 cells. **B)** Ano7 does not colocalize with markers for KDEL Receptor (cis-golgi), TGN46 (trans-golgi), or EEA1 (endosomes) when expressed in HEK293 cells.

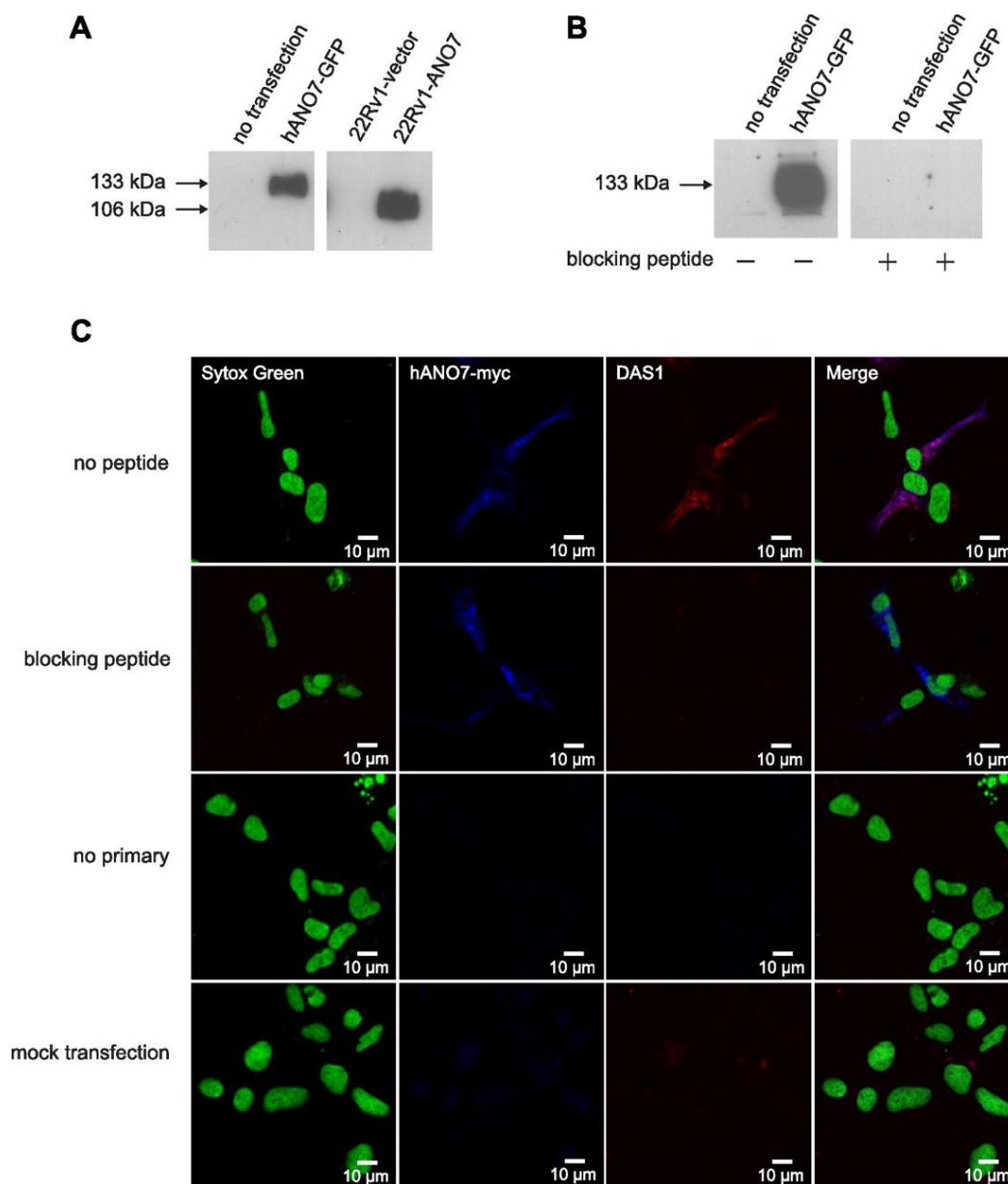


**Figure 2-4.** Characterization of An7 antibody specificity. **A)** An7 antibody recognizes GFP-tagged An7 protein in transfected HEK293 cells and nontagged An7 in a stably transfected cell line 22Rv1-ANO7. No signal is detected in nontransfected HEK293 cells or 22Rv1 cells stably transfected with the empty vector. **B)** Immunoblot showing that preincubation of An7 antibody with the immunizing peptide abolishes An7 staining in HEK293 cells transfected with GFP-tagged hAno7. **C)** An7 antibody

(DAS1) staining in transfected HEK293 cells demonstrates that it colocalizes with myc-tagged Ano7. The staining is abolished upon preincubation of the antibody with immunizing peptide.

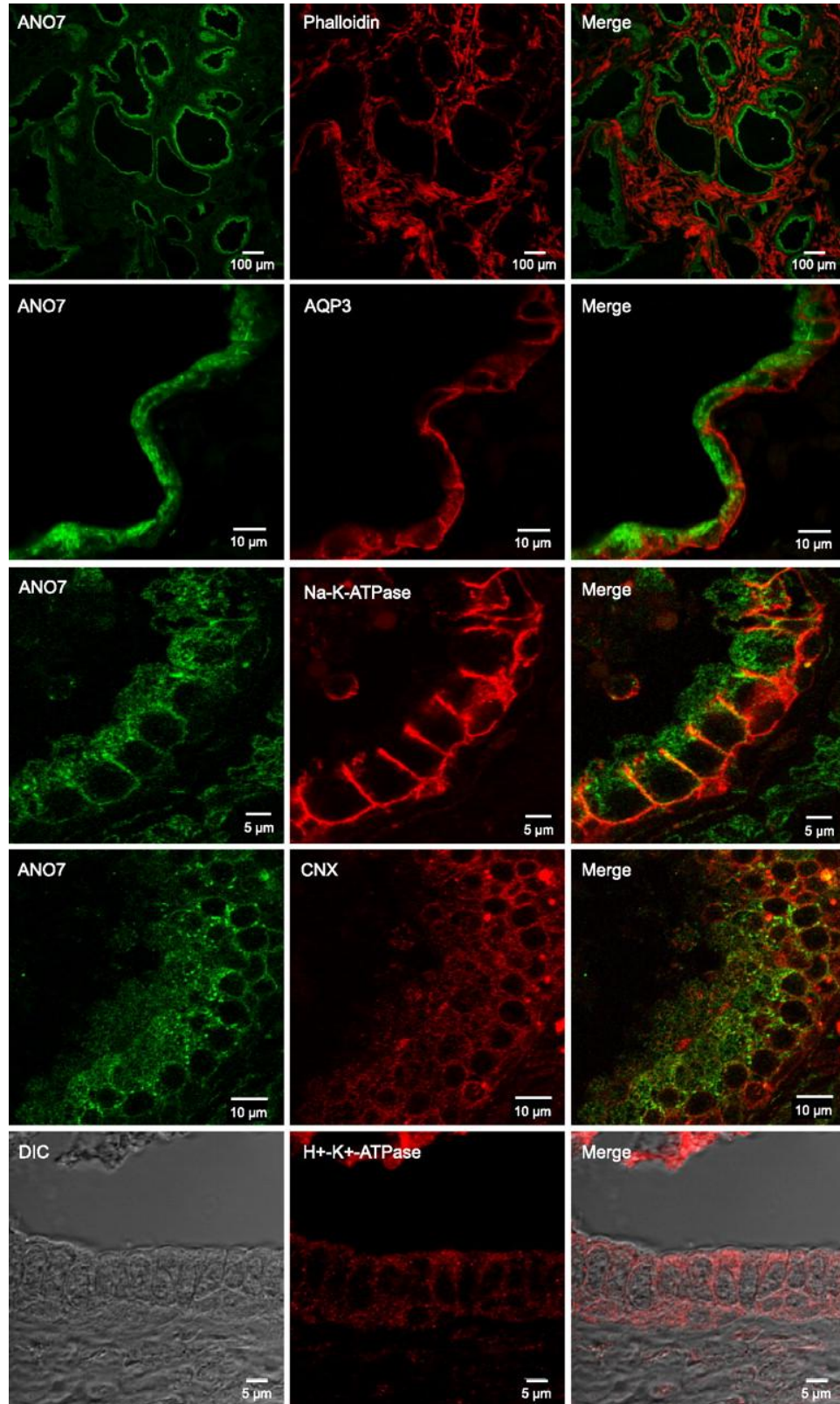


**Figure 2-5.** Immunofluorescence confocal microscopy of human prostate expressing endogenous Ano7. Endogenous Ano7 (green) in prostate gland epithelium with various counterstains: phalloidin, aquaporin-3, Na<sup>+</sup>-K<sup>+</sup>-ATPase, CNX, and H<sup>+</sup>-K<sup>+</sup>-ATPase.

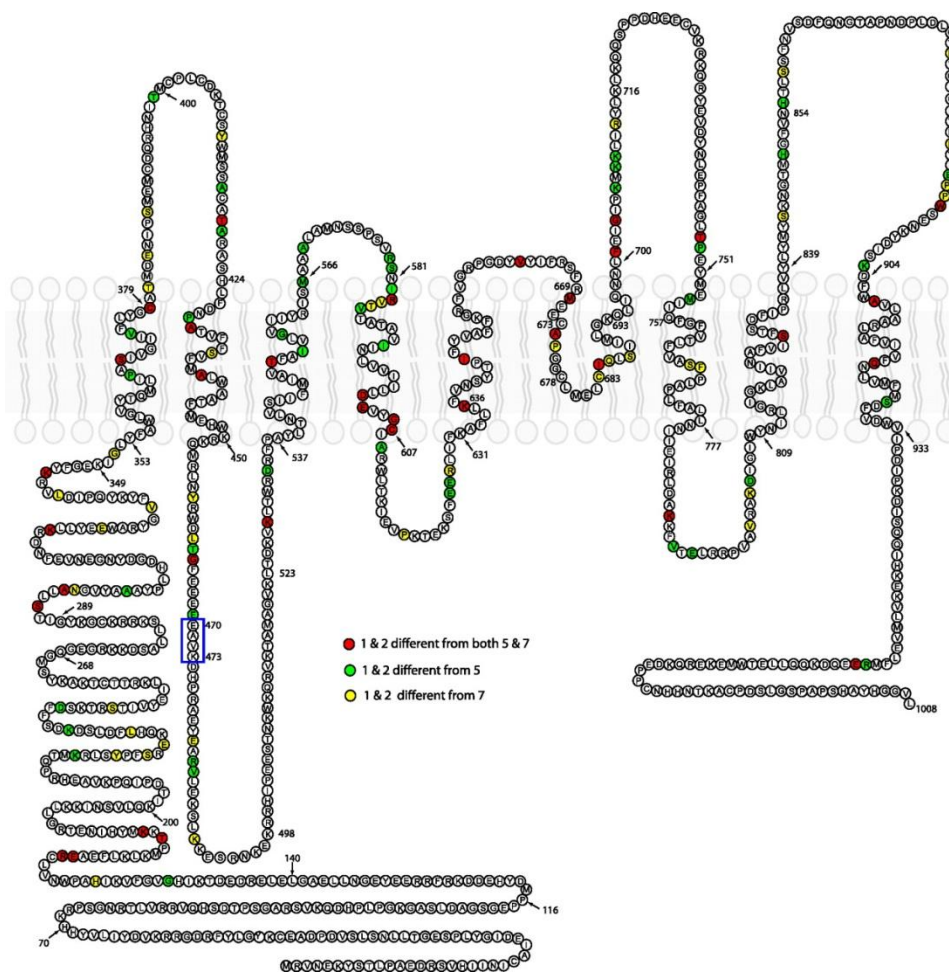


**Figure 2-6.** Evolutionary divergence between An01 and 2 and An05 and 7. mAno1 sequence is shown. Available vertebrate An01, An02, An05, and An07 sequences were aligned and analyzed by DIVERGE 2.0 for type-II divergence to identify conserved amino acids of difference between An01/2 and An05/7. Amino acids colored red are amino acids that are conserved in both An01 and 2 that differ from conserved amino acids in both An05 and 7. Green: amino acids conserved in An01 and 2 that are different from conserved amino acids in An05 but not An07. Yellow: amino acids conserved in An01 and 2 that are different from conserved amino acids in An07 but not An05. Amino

acids boxed in blue are unique to Ano1 and are critical for Ca<sup>2+</sup> sensitivity, but are not conserved in Ano5 and Ano7.

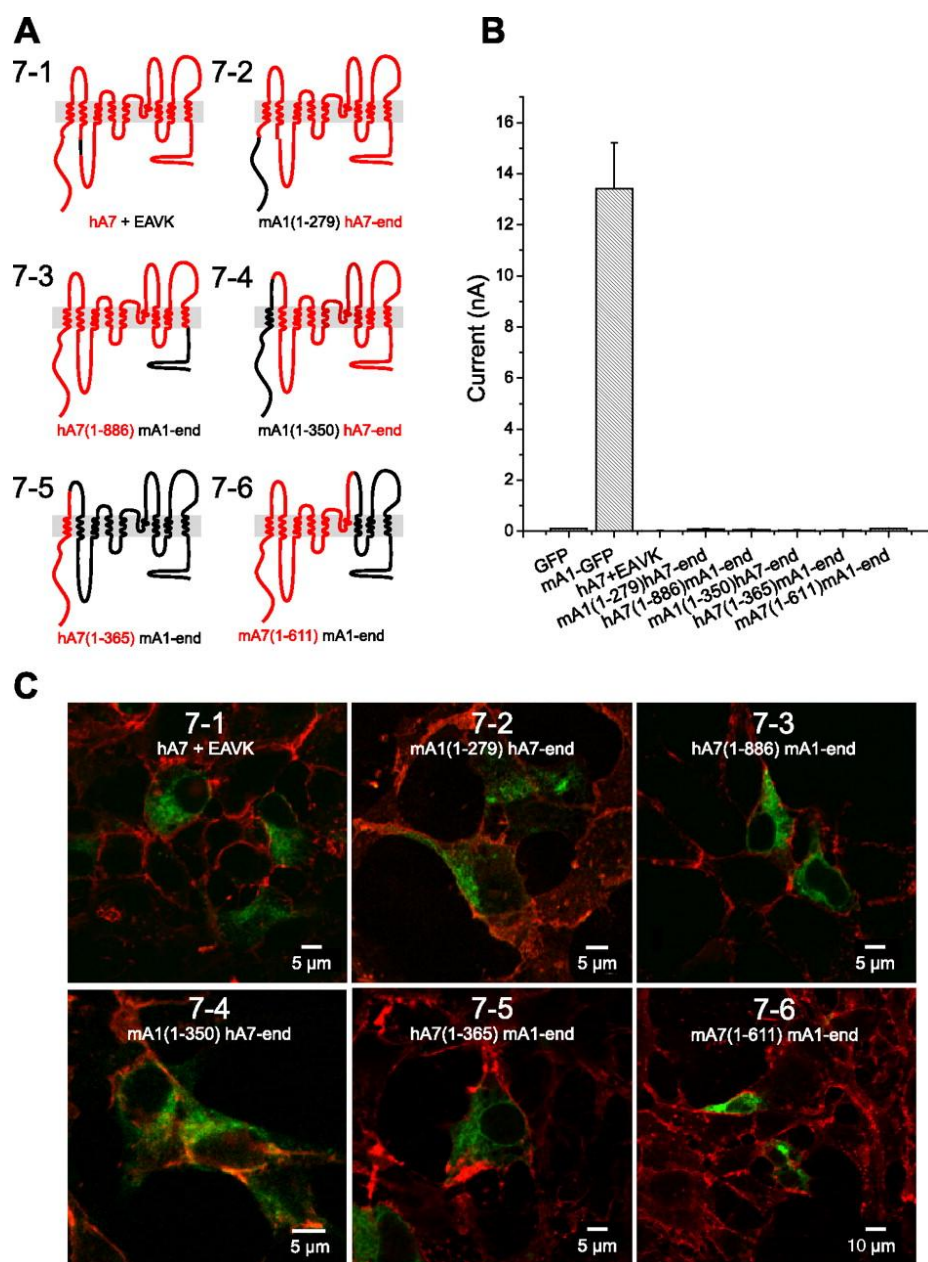


**Figure 2-7.** Trafficking and  $\text{Cl}^-$  currents of chimeras between Ano1 and Ano7. **A)** Cartoon of chimeric constructs. Ano1 (black). Ano7 (red). Chimeras are named based on the position of the residues included from either Ano1 (A1) or Ano7 (A7); for example, mA1(1-279)hA7-end includes the first 279 residues from Ano1 with the remaining residues belonging to Ano7. **B)** Average current amplitudes of Ano1-Ano7 chimeras in

transiently transfected HEK293 cells in response to 24  $\mu\text{M}$  intracellular  $[\text{Ca}^{2+}]$ . **C)**  
Confocal images showing localization of GFP-tagged Ano1-Ano7 chimeras  
counterstained with WGA.

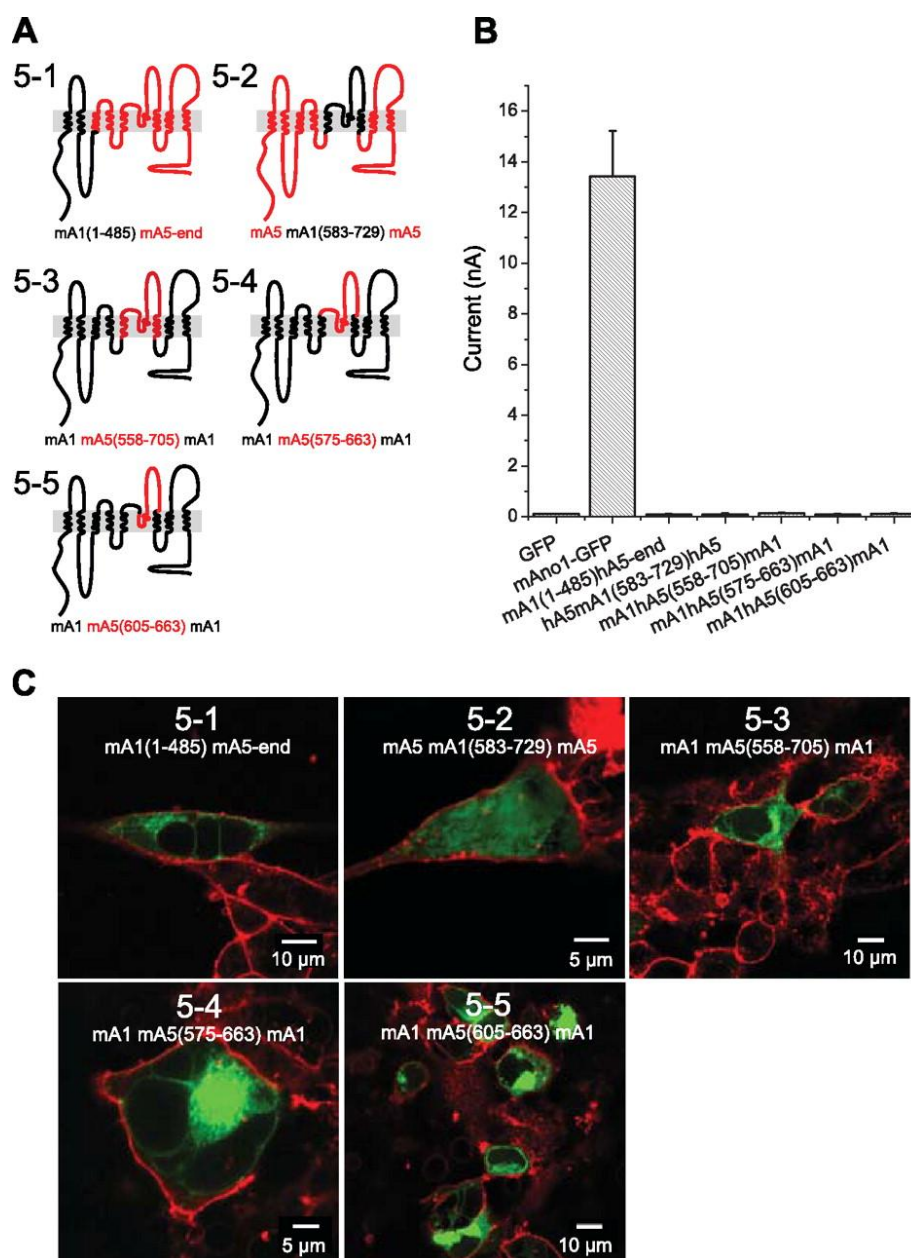


**Figure 2-8.** Properties of Ano1-Ano5 chimeras. **A)** Cartoon of Ano1-Ano5 chimeras. Ano1 (black). Ano5 (red). **B)** Average current amplitudes of Ano1-Ano5 in transiently transfected HEK293 cells in response to 24  $\mu$ M intracellular  $[Ca^{2+}]$ . **C)** Localization of GFP-tagged Ano1-Ano5 chimeras in transiently transfected HEK293 cells. Cells were counterstained with WGA.

## **CHAPTER 3**

# **EPITOPE ACCESSIBILITY AND MUTAGENESIS STUDIES IMPLICATE THE SIXTH TRANSMEMBRANE DOMAIN AND ADJACENT RESIDUES IN REGULATION OF ANOCTAMIN 1 BY $Ca^{2+}$ AND VOLTAGE<sup>4</sup>**

## Summary

Ca<sup>2+</sup>-activated chloride channels (CaCCs) are critical for many physiological functions such as cellular excitability, epithelial secretion, and sensory signal transduction. Since the discovery that Ano1 is an essential subunit of CaCCs, multiple studies have demonstrated the important functions of Ano1 in multiple tissues including fluid secretion in salivary gland, regulation of smooth muscle contraction, and control of cellular excitability. Understanding the physiological function of Ano1 requires knowledge of how the channel is activated by Ca<sup>2+</sup> and voltage. The objective of this study was to examine the mechanisms underlying Cl<sup>-</sup> permeation of Ano1, and also to identify regions critical for Ca<sup>2+</sup> and voltage sensitivity. Here we experimentally determined the transmembrane topology of Ano1, and showed that the predicted fourth intracellular loop is localized intracellularly as evidenced by HA-epitope accessibility. Mutagenesis studies in this region revealed that E702 and E705 are critical for Ca<sup>2+</sup> sensitivity of the channel. In addition, a point mutation within the sixth transmembrane domain, T714V, altered the voltage sensitivity of Ano1. These data present an alternative model to the predicted reentrant loop model of Ano1, and identify regions of Ano1 involved in regulation by Ca<sup>2+</sup> and voltage.

## Introduction

Ca<sup>2+</sup>-activated chloride channels (CaCCs) are involved in numerous physiological functions including epithelial secretion, sensory signal transduction, and cellular excitability. The mechanisms underlying CaCC regulation and activation are not well understood because native CaCCs are heterogeneous in their regulatory mechanisms, and the molecular identity of CaCCs has been elusive. Recently however, three labs independently identified *Tmem16a*, also known as anoctamin-1 (*Ano1*) as the gene encoding an essential subunit of CaCCs (Caputo et al. 2008; Schroeder et al. 2008; Y. D. Yang et al. 2008). *Ano1* is a member of a 10-gene family, of which only *Ano1* and *Ano2* definitively encode CaCCs. Since the identification of *Ano1* and *Ano2* as CaCCs, their important functions in various tissues have been elucidated, including fluid transport in salivary gland (Romanenko et al. 2010; Y. D. Yang et al. 2008), slow wave activity in the gut (S. J. Hwang et al. 2009), regulation of smooth muscle contraction (Manoury et al. 2010), control of cellular excitability (W. C. Huang et al. 2012b), and nociception (Cho et al. 2012).

Understanding the physiological function of *Ano1* requires knowledge of how the channel is activated by Ca<sup>2+</sup>. The biophysical properties of *Ano1* are dependent on both the concentration of Ca<sup>2+</sup> and the membrane potential (Xiao et al. 2011). Submicromolar concentrations of Ca<sup>2+</sup> yield currents that are strongly outwardly rectifying and time dependent, whereas higher concentrations result in linear time independent currents; furthermore, *Ano1* is more sensitive to Ca<sup>2+</sup> at positive membrane potentials. These factors may determine whether epithelial CaCCs mediate secretion or absorption, and whether neuronal CaCCs pass depolarizing or hyperpolarizing current. The mechanism underlying Ca<sup>2+</sup> and voltage-dependent gating are not understood, largely because the

topology of Ano1 and the location of Ca<sup>2+</sup> binding sites and the anion-selective pore are unknown.

Structure-function studies of Ano1 have been based on a predicted topology model of eight transmembrane  $\alpha$ -helices with a reentrant loop between transmembrane helices 5 and 6. While this model has been verified experimentally for Ano7 (Das et al. 2008), the topology of Ano1 is less certain. Furthermore, the amino acid sequence of Ano1 and Ano7 are only 32% identical, and Ano7 has not been shown to be a Cl<sup>-</sup> channel. The function of several anoctamins is still unknown. Identifying residues indispensable for Ano1 channel function will aid future studies examining functional differences across anoctamins. Previous mutagenesis studies on Ano1 suggest that the reentrant loop lines the channel pore, because mutations in this region reportedly alter anion:cation selectivity of the channel. The goal of the following study was to identify residues critical for activation of Ano1 by Ca<sup>2+</sup> and voltage, and regions critical for anion permeation.

## **Results**

### **Determinants of anion:cation permeability of Ano1**

The region between F620 and N650 is thought to be important in forming the Ano1 pore because mutagenesis of positively charged amino acids, R621 and K668, are reported to drastically alter ion selectivity (Y. D. Yang et al. 2008). In these experiments, reversal potentials were measured from whole cell recordings using intracellular and extracellular solutions containing 70mM NaCl and 210mM NaCl respectively. The R621E mutant was reported to exhibit a  $P_{Na}/P_{Cl}$  ratio of 0.87 compared to 0.03 for wild-type (Y. D. Yang et al. 2008). We have tried without success to confirm these observations using several different methods. We were unable to perform these

experiments under the exact same conditions, because the stability of whole cell patches was very poor in these solutions. It is likely that the high osmolarity of the 210mM NaCl extracellular solution, which was >100mOsm higher than the intracellular solution, resulted in unfavorable recording conditions.

Alternatively, we determined  $P_{Na}/P_{Cl}$  and  $P_{Cs}/P_{Cl}$  by the dilution potential method (Figure 3-1). In the dilution potential method, the anion:cation permeability is determined by measuring changes in the reversal potential as the solution on one side is diluted. If a channel is permeable only to  $Cl^-$ , the reversal potential shifts will follow the Nernst potential for  $Cl^-$ . If however, the channel is also permeable to the respective cation in solution, the reversal potential will display a shift towards the Nernst potential of the cation. Using a form of the Goldman Hodgkin Katz equation, the relative anion:cation permeability can be calculated from the reversal potential shifts. Because the permeability of channels to particular ions can be dependent on the atomic radius and hydration state of the ion, we performed the dilution potential method using two different solutions containing either NaCl or CsCl. The anion:cation permeability ratios were not significantly different for NaCl or CsCl, and were identical for WT ( $P_{Na}/P_{Cl} = 0.13$ ;  $P_{Cs}/P_{Cl} = 0.08$ ) and R621E ( $P_{Na}/P_{Cl} = 0.14$ ;  $P_{Cs}/P_{Cl} = 0.1$ ). These results suggest that R621 is not critical for the selectivity filter of the channel, but does not rule out the possibility that this region may in part form the pore. For example, within the selectivity filter of ClC channels,  $Cl^-$  ions bind to multiple sites within the pore via electrostatic interactions with helix dipoles and partial charges of amino acid residues. Therefore, it is possible that mutagenesis of a single residue may not be sufficient to significantly alter channel selectivity. The R621E mutation did, however, require a higher concentration of intracellular  $Ca^{2+}$  to generate measurable currents, suggesting this region is important for channel function. Cysteine accessibility studies on the reentrant loop by Yu et. al

corroborate results from the dilution potential studies in that no mutations in amino acids at positions 620-646 significantly altered the ionic selectivity of Ano1 (Yu et. Al, 2012). However, these residues may be implicated in the permeation pathway; accessibility of amino acids 625 to 630 to various thiol reagents suggests that this region contributes to an outer vestibule that is accessible to the extracellular fluid, with amino acids after 635 being located deep within the pore.

Hydropathy analysis of mAno1 identifies between 7 and 9 transmembrane segments depending on the algorithm used. However, the topology of Ano1 has not been experimentally verified. The topology of Ano7 has been determined experimentally, and is consistent with the predicted 8 transmembrane domain topology with cytosolic N- and C- termini (Figure 3-2). Although hydropathy analysis indicates that Ano1 and Ano7 have similar topologies, we sought to experimentally verify the topology of mAno1 using epitope tag insertion and confocal microscopy. HA epitopes were introduced into mAno1 at various positions (570, 614, 672, 700, or 824), and then evaluated for their accessibility to extracellularly applied antibodies in permeabilized and nonpermeabilized cells (Figure 3-3). mAno1-HA constructs were evaluated using whole cell patch clamp electrophysiology to verify functionality of modified channels. All constructs exhibited currents characteristic of Ano1, indicating that the HA insertions did not significantly alter the structure of the channel. In non-permeabilized cells HA epitopes at positions 614 and 824 were accessible to extracellular anti-HA antibody, whereas all other positions were inaccessible. These data suggest that the putative fourth extracellular loop (amino acids 650-706) is oriented intracellularly. The intracellular localization of this region raises possibilities for the mechanism of channel gating by  $Ca^{2+}$ .

### **E702 and E705 contribute to Ca<sup>2+</sup> gating**

We sought to identify regions within Ano1 critical for channel function, including residues that may be important for channel gating and ion permeation. The role of the sixth transmembrane domain and adjacent N-terminal sequence in channel function was further investigated because of the high level of conservation in this region (Figure 3-4). Amino acids 650 to 706, which immediately precede the predicted sixth transmembrane domain, contain a sequence that is highly conserved among all members of the Ano superfamily: [E/D]-[Y/F]-[M/L/Q]-E-[M/T/L/Q]. In Ano1 and Ano2, this sequence is invariably <sub>702</sub>EYMEM. Although amino acids 650 to 706 were previously thought to comprise an extracellular loop, our topology studies place this region intracellularly. The intracellular localization of this region suggests new possibilities for the mechanism of Ano1 channel gating by Ca<sup>2+</sup>.

Several mutations in this region produced marked changes in Ca<sup>2+</sup> and voltage sensitivity. E702Q, E705Q, and P724S mAno1 mutants all displayed reduced Ca<sup>2+</sup>-dependent activation compared to WT Ano1 (Figure 3-5A). WT Ano1 is outwardly rectifying at submicromolar concentrations of intracellular Ca<sup>2+</sup>. This IV relationship becomes increasingly linear with higher intracellular [Ca<sup>2+</sup>] (Figure 3-5B). In contrast, the E705Q mutant was outwardly rectifying with 23μM intracellular [Ca<sup>2+</sup>] (Figure 3-5C). Even at an intracellular [Ca<sup>2+</sup>] of 126μM, the E705Q mutant maintained outward rectification. E702Q and P724S mutations had similar effects, as 23μM [Ca<sup>2+</sup>] elicited an outwardly rectifying, time dependent response. Because P724 is predicted to lie within the sixth transmembrane domain, it is unlikely that it is directly involved in Ca<sup>2+</sup> binding; therefore, this residue was not as extensively studied.

The importance of E702 and E705 in Ca<sup>2+</sup>-dependent gating is further supported by experiments performed by Yu et al. in which inside-out excised patches were rapidly

switched between zero and high  $\text{Ca}^{2+}$  (Yu et al. 2012) (Figure 3-6). The time constant of deactivation ( $\tau_{\text{off}}$ ) was measured by fitting current decay with an exponential equation.  $\tau_{\text{off}}$  is likely representative of  $\text{Ca}^{2+}$  dissociation from the binding site, because deactivation is strongly dependent on the ligand used to activate the channel ( $\text{Ca}^{2+}$  or  $\text{Ba}^{2+}$ ) (Xiao et al. 2011). This suggests that ligand binding and unbinding are the rate limiting steps for channel opening/closing.  $\tau_{\text{off}}$  was greatly accelerated by the E702Q and E705Q mutations, and was voltage dependent. At +120mV,  $\tau_{\text{off}}$  was  $408.4 \pm 67.3$ ms for WT, vs  $40.4 \pm 4.1$ ms for E702Q, and  $96.3 \pm 6.6$  ms for E705Q. The time constant of activation ( $\tau_{\text{on}}$ ) of Ano1 current was slower for E705Q than WT ( $13.1 \pm 20.2$ ms and  $5.1 \pm 1.1$ ms respectively). E702Q, unlike E705Q, did not have a dramatic effect on  $\tau_{\text{on}}$ ; however,  $\tau_{\text{on}}$  is close to the switching time of the perfusion system and therefore not quantitatively reliable. Lower  $\text{Ca}^{2+}$  concentrations could not be tested for the E702Q mutant because current amplitudes were too small to be accurately measured.

The E702Q and E705Q mutations also alter the apparent  $\text{EC}_{50}$  for  $\text{Ca}^{2+}$ . The apparent  $\text{EC}_{50}$  for  $\text{Ca}^{2+}$  can be calculated as  $\text{EC}_{50} = \alpha/\beta$ , for which  $\alpha = 1/\tau_{\text{off}}$  and  $\beta = (1/\tau_{\text{on}}) - \alpha/[\text{Ca}^{2+}]$ . These calculations assume that the predominant rate-limiting steps in Ano1 current activation and deactivation are  $\text{Ca}^{2+}$  binding and unbinding. The calculations were performed with data utilizing different  $\text{Ca}^{2+}$  concentrations that provided reliable on-rates for WT and mutant channels. The E705Q mutation increases the  $\text{EC}_{50}$  at all voltages (Figure 3-6F), suggesting that it plays a key role in  $\text{Ca}^{2+}$  sensing. The E702Q also increases the  $\text{EC}_{50}$ , but has a greater effect at more negative potentials.

### **Mutations within TM6 affect channel gating by voltage**

The sixth transmembrane domain may also be implicated in voltage-dependent gating of Ano1. Mutation of T714 to valine significantly increases the sensitivity of Ano1

to voltage in the absence of intracellular  $\text{Ca}^{2+}$  (Figure 3-7). Ano1 does generate currents similar to T714V mutants in response to strong depolarization, but requires higher voltages ( $>+100\text{mV}$ ) to exhibit measurable currents. Average current amplitude of WT Ano1 in response to  $+100\text{mV}$  was  $17 \pm 4\text{pA}$ , whereas the T714V mutant response was  $349 \pm 49\text{pA}$ . The response of the T714V mutant to intracellular  $\text{Ca}^{2+}$  was similar to WT, except that the current amplitude at positive voltages was larger. There was no apparent shift in the  $\text{EC}_{50}$  for  $\text{Ca}^{2+}$ , suggesting that the larger current amplitude may be attributed to the increased sensitivity of the T714V mutant to depolarization (data not shown). While this mutation produced a measurable increase in the amplitude of voltage dependent current, a comparable mutation, T714A, surprisingly had little effect (Figure 3-7). Similarly, several other substitutions at this position (714K, 714E, 714W, 714Y) only slightly increased current amplitude in response to voltage.  $\text{Ca}^{2+}$ -induced responses of T714X mutants were similar to WT (Figure 3-8).

## **Discussion**

### **Revised topology places $\text{Ca}^{2+}$ and voltage sensors near pore**

Understanding the mechanisms underlying  $\text{Ca}^{2+}$  and voltage sensitivity of CaCCs is difficult, because unlike typical voltage-gated or ligand-gated channels, CaCCs exhibit strongly coupled voltage dependence and  $\text{Ca}^{2+}$ -gating. In this study, we have identified several residues within the highly conserved region near the sixth transmembrane domain that are important for  $\text{Ca}^{2+}$  and voltage sensitivity of Ano1. Given the strong coupling between voltage and  $\text{Ca}^{2+}$ -dependence of Ano1, it is not surprising that these residues are implicated in both  $\text{Ca}^{2+}$  and voltage sensitivity of Ano1. These results, taken together with cysteine accessibility studies (Yu et al. 2012), suggest an appealing model

for Ano1 that places the pore within close proximity to determinants of  $\text{Ca}^{2+}$  and voltage sensitivity.

### **$\text{Ca}^{2+}$ -dependent gating of Ano1**

The mechanisms underlying  $\text{Ca}^{2+}$ -dependent gating of Ano1 are unknown. Some studies suggest that the sensitivity of the channel is dependent on calmodulin, although the involvement of CaM may be specific to particular isoforms of Ano1 (Tian et al. 2011). Other studies implicate a stretch of five glutamic acids located in the first intracellular loop which resembles the  $\text{Ca}^{2+}$  bowl of the large-conductance channel. A naturally occurring splice variant that deletes the fifth glutamic acid ( $\Delta_{448}\text{EAVK}_{451}$ ) increases the  $\text{EC}_{50}$  for  $\text{Ca}^{2+}$  by approximately 50-fold; however, neutralization of the first four glutamic acids have little effect on  $\text{Ca}^{2+}$  sensitivity, and also renders the channel insensitive to voltage-dependent gating in the absence of  $\text{Ca}^{2+}$  (Xiao et al. 2011). In addition, the  $\text{Ca}^{2+}$   $\text{EC}_{50}$  for  $\Delta_{448}\text{EAVK}_{451}$  appears to be convergent with WT values at positive voltages. While this region may couple  $\text{Ca}^{2+}$  and voltage, it is unlikely to be a  $\text{Ca}^{2+}$  binding site.

### **E702 and E705 are critical for $\text{Ca}^{2+}$ -regulation of Ano1**

Our data implicate conserved sequences near the sixth transmembrane domain in  $\text{Ca}^{2+}$  regulation. Although this region was previously predicted to be an extracellular loop based on hydropathy analysis, topology studies from our lab indicate that it is intracellular. The revised topology is supported by both introduced HA epitope accessibility, and accessibility of specific residues to either intracellular or extracellular MTS reagents. Specifically, E702C and E705C mutants were accessible to MTS reagents applied on the cytoplasmic face of inside-out excised patches (Yu et al. 2012). This revised topology, in parallel with our functional data, implicates this region in channel

gating by intracellular  $\text{Ca}^{2+}$ . Rapid  $\text{Ca}^{2+}$  perfusion experiments show that E705Q has a slower time constant of activation, and that both the E705Q and E702Q mutants display a faster time constant of dissociation.

It is difficult to unambiguously determine if these mutations alter  $\text{Ca}^{2+}$ -binding or  $\text{Ca}^{2+}$ -gating, because these processes are allosterically coupled. The apparent affinity of a ligand for a receptor is dependent on both the ability of the ligand to bind the receptor, as well as the ability of the receptor to change conformation to its active state. Hence, distinguishing between effects of mutations on ligand binding versus effects on channel gating is a reoccurring problem in ion channel research (Colquhoun 1998). However, we believe these results most likely reflect changes in  $\text{Ca}^{2+}$  dissociation from the binding site, because previous studies on Ano1 indicate that  $\tau$ -off reflects ligand dissociation (Xiao et al. 2011). In theory, channel deactivation consists of at least two steps: dissociation of  $\text{Ca}^{2+}$  from the binding site, followed by channel closure. For Ano1, the time constant of dissociation for  $\text{Ba}^{2+}$  is markedly decreased compared to  $\text{Ca}^{2+}$ . This could be because coordination of  $\text{Ba}^{2+}$  at the binding site is not as stable as  $\text{Ca}^{2+}$ ;  $\text{Ba}^{2+}$  has been shown to be a less effective ligand for activating CaM-dependent phosphodiesterase, and is ineffective at displacing  $\text{Ca}^{2+}$  from the ligand binding site of CaM (Chao et al. 1984). Because  $\tau_{\text{off}}$  for Ano1 is strongly dependent on the ligand used, the process of deactivation is likely dominated by ligand dissociation. Therefore, these data are most simply interpreted in terms of changes in  $\text{Ca}^{2+}$  binding, and suggest that E702 and E705 are critical for  $\text{Ca}^{2+}$  binding of Ano1. However, Ano1 may have multiple  $\text{Ca}^{2+}$  binding sites. It is still unknown how many  $\text{Ca}^{2+}$  binding sites there are, and if these lie within Ano1 or on an accessory subunit.

### **The role of TM6 in voltage sensitivity of Ano1**

These studies also reveal a potential role for the sixth transmembrane domain in voltage sensitivity of Ano1. This region was examined because it is one of the most highly conserved regions across anoctamins. Mutation of T714 to valine resulted in channels that produced significantly larger currents in response to strong depolarization in the absence of intracellular  $\text{Ca}^{2+}$ . Various other amino acid substitutions at this position slightly increased channel current response to voltage, but not to the extent of the T714V mutant. It is difficult to explain why only the T714V mutation had a dramatic effect. Amino acid side chain size at this position does not appear to be important because threonine and valine are similar molecular weights, and substitution with amino acids of very small (alanine) or large (tryptophan) side chain volumes had no substantial effect on Ano1 currents. Amino acid side chain charge also did not seem to be important, as currents from T714K and T714E were similar to WT. There are, however, differences in the hydrophobicity of the residues substituted. With the exception of tryptophan, valine is the most hydrophobic residue substituted at this position (Monera et al. 1995). It is possible that substitution of a more hydrophobic residue at position 714 induces a specific conformational change in this region that accounts for the effects of the T714V mutation. Although tryptophan is more hydrophobic than valine, it differs significantly from valine in that it is energetically unfavorable at the membrane center and tends to be found near membrane-water interfaces. This hypothesis remains to be tested, as substitution of other significantly hydrophobic residues such as isoleucine and phenylalanine were not examined.

Evidence from other labs also implicates the sixth transmembrane domain in voltage dependence. Q757A (corresponding to Q709 in the splice variant used for our studies) markedly alters the IV curve and time dependence of Ano1 current (Caputo et al.

2008). In comparison with WT Ano1, the Q757A mutant displays a linear IV curve at the same intracellular  $[Ca^{2+}]$  and also exhibited a reduction in the time-dependence of activation. These data suggest a role for TM6 in voltage dependence, but it is unlikely to be the sole determinant of voltage sensitivity. Neutralization of a stretch of five glutamic acids in the first intracellular loop completely abolishes voltage activation of Ano1 in the absence of  $Ca^{2+}$  (Xiao et al. 2011). Therefore, TM6 and the first intracellular loop may concurrently confer voltage sensitivity to the channel.

### **Ano1 may have a complex transmembrane topology**

Our studies reveal an alternative transmembrane topology for Ano1 in which the fourth extracellular loop is localized intracellularly. Using epitope tag insertion, we found that residues 672 and 700 were inaccessible to extracellular antibody. These results are supported by cysteine accessibility studies. When positions 702 or 705 are mutated to cysteine, application of membrane-impermeant MTS reagents to the cytosolic face of the membrane results in a rapid change in current amplitude or  $Ca^{2+}$  sensitivity. This provides evidence for a transmembrane domain somewhere between position 614 and 672. It is possible that part of the putative reentrant loop constitutes a membrane spanning segment, because some transmembrane prediction algorithms identify a transmembrane domain located between positions 629 and 653.

The topology between positions 700 to 824 is less certain, because HA tags inserted at several positions in this region yielded channels that were nonfunctional or poorly expressed. There must be an odd number of transmembrane domains between these positions, because 700 is intracellular and 824 is extracellular. However, transmembrane prediction algorithms consistently identify two transmembrane domains in this region, corresponding to TM6 and TM7 in the original model of Ano1

topology. While hydropathy analysis is a useful tool for predicting hydrophobic segments that potentially span the membrane, it cannot reliably distinguish between membrane spanning segments and those that only partially cross the lipid bilayer. Epitope tag insertion analysis has a similar limitation. Our results may best be explained if Ano1 has a more complex membrane topology between 700 and 824 than originally predicted. The complex transmembrane topology of ClCs resulted in a similar uncertainty regarding their topology. Until the crystal structure was solved, biochemical topology analysis yielded confusing results (Jentsch et al. 2002). The crystal structure revealed that in contrast to the predicted 13 transmembrane domains, ClCs possess 18 alpha helices of varying lengths. Many of these helices only partially cross the membrane and are tilted at different angles relative to the plane of the membrane. It is possible that Ano1 has a similarly complex membrane topology within this region, although more direct structural studies will be needed to understand the transmembrane organization of Ano1.

The alternative topology model presented here differs from that previously reported for Ano7, in which the fourth loop is placed extracellularly. It was originally thought that Ano1 shared a similar topology with Ano7 based on hydropathy analysis and experimental results from topology studies on Ano7. Given that there is no convincing evidence that Ano7 is a Cl<sup>-</sup> channel, this result is not surprising. Furthermore, we have found that Ano7 does not traffic to the plasma membrane or generate currents in transfected cells, and that it is localized predominantly intracellularly in prostate where it is endogenously expressed. A difference in topology between Ano1 and Ano7 may explain our previous results with Ano1-Ano7 chimeras. Many Ano1-Ano7 chimeras containing relatively short sequences from Ano7 were not able to traffic to the plasma membrane. Interestingly, replacement of 58 residues within the putative reentrant loop

of Ano1 with the corresponding sequence from Ano7 dramatically reduced the amplitude and time dependence of  $\text{Ca}^{2+}$  activated currents (unpublished data). These functional data coupled with our topology results indicate that Ano1 and Ano7 have significant structural differences in this region.

### **Determinants of Ano1 $\text{Cl}^-$ selectivity are still unknown**

Using the dilution potential method, we were unable to confirm previous results indicating that two mutations in the putative reentrant loop, R621E and K668E significantly altered cation-anion permeability of Ano1. There are several questions regarding the discrepancy, in part due to an incomplete description of the methods employed by Yang et al (Y. D. Yang et al. 2008). It is unclear how many cells were tested or the statistical significance of these findings, as no statistics were reported. It is also unknown what voltage protocol was used to determine the reversal potential, or the variability of the reversal potentials measured. This is important because it was previously reported that Ano1 has multiple open states that differ in anion selectivity (Schroeder et al. 2008). There are, in fact, two dramatically different  $P_{\text{Na}}/P_{\text{Cl}}$  values reported for the K668E mutant, 0.98 and 0.10.

While it seems that residues within the putative reentrant loop contribute to the permeation pathway, the determinants of  $\text{Cl}^-$  selectivity have yet to be identified. In general, the principles underlying the selectivity of anion channels is channels is poorly understood. This may be in part because anion channels are relatively nonselective. While there are some examples, notably the glycine receptor, whose selectivity can be switched from anionic to cationic via mutagenesis of a few residues (Keramidas et al. 2000; Keramidas et al. 2002), this approach may not be feasible for other anion channels.  $\text{Cl}^-$  channels, for example, have multiple  $\text{Cl}^-$  binding sites within the pore that

are important for anion permeation. Cl<sup>-</sup> ions are coordinated not by full positive charges, but rather by partial positive charges contributed by helix dipoles and main chain and side chain nitrogen and oxygen atoms (Dutzler et al. 2002). Because the permeability and selectivity of ClC channels is governed by anion association to and dissociation from multiple anionic binding sites within the pore, single charge switch mutations may not have dramatic effects on anion:cation permeability ratios. Identification of residues that are critical for anoctamin channel function is further complicated by the fact that anoctamins do not share significant sequence homology with any other known channels, nor is there a crystal structure available. Here we have identified regions critical for channel function based on their conservation across anoctamins. These findings may provide insight into the structure/function of other anoctamins family members, although it remains to be determined if anoctamins 3-10 function as channels, and if they have a similar topology to Ano1.

## **Materials and Methods**

### **Site directed mutagenesis.**

The *a,c* splice variant of mAno1 (Accession: Q8BHY3) was used for all experiments. mAno1 tagged with enhanced green fluorescent protein (EGFP) at the C-terminus was provided by Dr. Uhtaek Oh, Seoul National University. Mutations were made using the Quickchanger PCR-based mutagenesis kit (Quickchanger; Stratagene, La Jolly, CA).

### **Electrophysiology.**

1 $\mu$ g of total DNA of WT or mutant mAno1 was transfected into HEK 293 cells using Fugene-6 (Roche Molecular Biochemicals). Single cells identified by EGFP fluorescence

were used for whole-cell patch clamp experiments within 72 hours. Transfected HEK293 cells were recorded using conventional whole-cell and excised inside-out patches. The zero  $\text{Ca}^{2+}$  intracellular solution contained 146 mmol/L CsCl, 2 mmol/L  $\text{MgCl}_2$ , 5 mmol/L EGTA, 10 mmol/L HEPES, and 10 mmol/L sucrose, pH 7.3, adjusted with NMDG. High- $\text{Ca}^{2+}$  pipette solution contained 5 mmol/L  $\text{Ca}^{2+}$ -EGTA, instead of EGTA (free  $\text{Ca}^{2+}$  approximately 20  $\mu\text{mol/L}$ ). The standard extracellular solution contained 140 mmol/L NaCl, 5 mmol/L KCl, 2 mmol/L  $\text{CaCl}_2$ , 1 mmol/L  $\text{MgCl}_2$ , 15 mmol/L glucose, and 10 mmol/L HEPES, pH 7.4, with NaOH. Borosilicate pipette tips were fire-polished to a final resistance of 3-5M $\Omega$ . Permeability of  $\text{Na}^+$  or  $\text{Cs}^+$  relative to  $\text{Cl}^-$  was determined using the “dilution potential” method; changes in the zero-current reversal potential ( $E_{\text{rev}}$ ) were measured when the concentration of extracellular NaCl or CsCl was changed (Barry, 2006). Data is presented as mean  $\pm$  SEM. Statistically significant differences between means were evaluated by two-tailed t-test, with a p value of  $< 0.05$ .

### **Rapid perfusion.**

Fast application of  $\text{Ca}^{2+}$  to excised inside-out patches was performed using a double-barreled theta tubing (1.5mm o.d.; Sutter Instruments) with a tip diameter of  $\sim 50\mu\text{m}$  attached to a piezobimorph on a micromanipulator. One barrel was filled with standard zero  $\text{Ca}^{2+}$  solution described above, and the other barrel was filled with intracellular solution containing the indicated free  $\text{Ca}^{2+}$ . Excised patches were switched between zero  $\text{Ca}^{2+}$  and free  $\text{Ca}^{2+}$  solutions by applying  $\sim 100$  V to the piezobimorph. The time course of solution exchange across the laminar flow interface was estimated by liquid junction potential measurements, which were found to be 0.5ms (10-90% rise time) for a 10-fold difference in ionic strength. The onset of current in response to  $\text{Ca}^{2+}$  was fit to an exponential.

**HA-tagged mAno1.**

Tandem HA epitopes (YPYDVPDYA) were introduced into various locations in mAno1 where EcoRI restriction endonuclease sites had been added via PCR-based mutagenesis. mAno1 constructs with engineered EcoRI sites were digested with EcoRI and ligated with two primers that encoded the HA tag. Only constructs that generated currents were used for immunofluorescent staining and epitope tag accessibility analysis.

**Immunofluorescence.**

mAno1 with HA epitopes inserted at various positions were used to examine the topology of Ano1 by evaluating the accessibility of HA epitopes to extracellularly applied antibody in permeabilized and non permeabilized conditions. Following fixation for 15 min at room temperature in 1% paraformaldehyde in 0.1mol/L phosphate buffer pH 7, cells were washed 3 X 15 min in blocking buffer (PBS with 1% cold water fish gelatin (Sigma)). For permeabilization, cells were incubated in blocking buffer containing 0.15%-0.3% Triton-X100. Cells were then incubated with anti-HA antibody (1:750) for 2 hrs at room temperature. Following 3 X 15min washes in blocking buffer, cells were incubated with Dylight-549 conjugated goat-anti-rabbit IgG (1:1000) (Jackson Immunochemicals). All antibodies were diluted in blocking buffer. Images were acquired using a Zeiss LSM 710 confocal laser-scanning microscope.

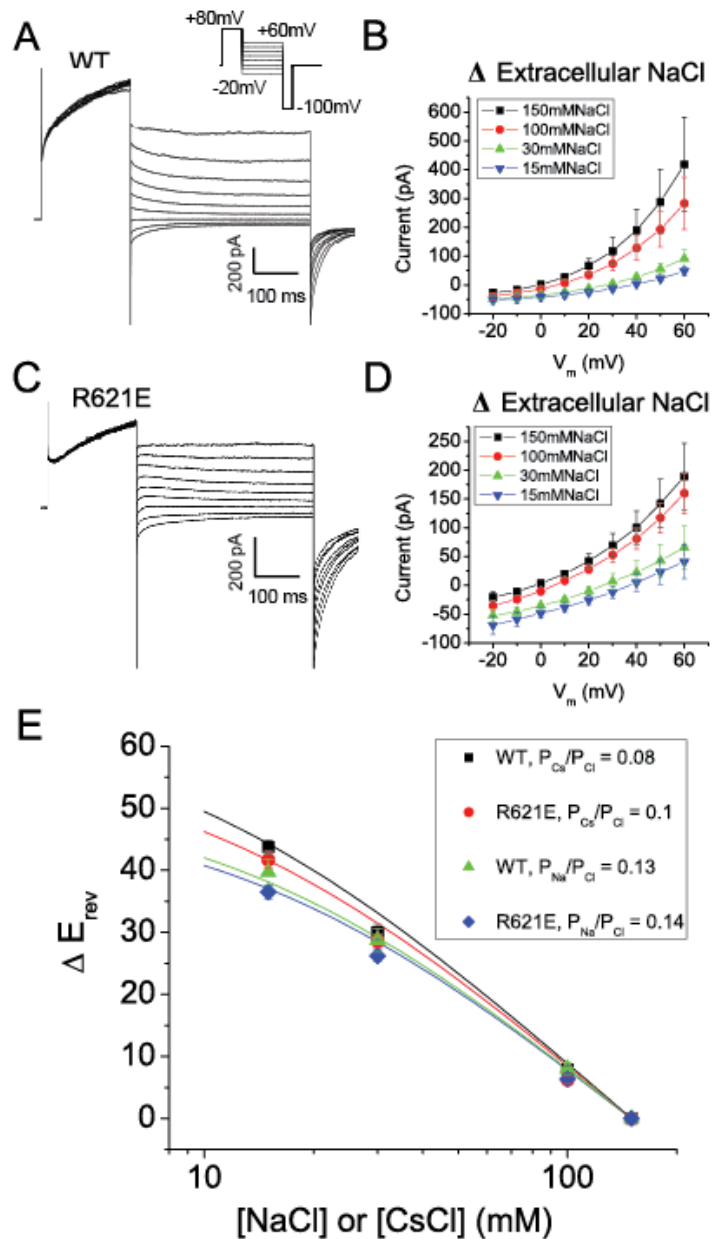


**Figure 3-1:** Effect of R621E mutation on anion:cation permeability of mAno1. Whole-cell recordings of **A**) WT mAno1 in symmetrical 150 mmol/L NaCl with 180 nmol/L  $Ca_i$  and **B**) R621E mAno1 in symmetrical 150 mmol/L NaCl with 1.1  $\mu$ mol/L  $Ca_i$ . The R621E mutation decreased the  $Ca^{2+}$  sensitivity of the channel, requiring a larger  $Ca^{2+}$  concentration to generate a measurable current. Current–voltage relationships of **C**) WT

mAno1 and **D**) R621E mAno1 with different extracellular [NaCl]. **E**) Change in reversal potential ( $\Delta E_{rev}$ ) for different extracellular [NaCl] or [CsCl] determined from experiments like those in **C** and **D**. Lines are best fits to the Goldman-Hodgkin-Katz equation. Reprinted from Circulation Research 110: 7, Yu K, et al, Explaining Calcium-Dependent Gating of Anoctamin-1 Chloride Channels Requires a Revised Topology, Copyright (2012)

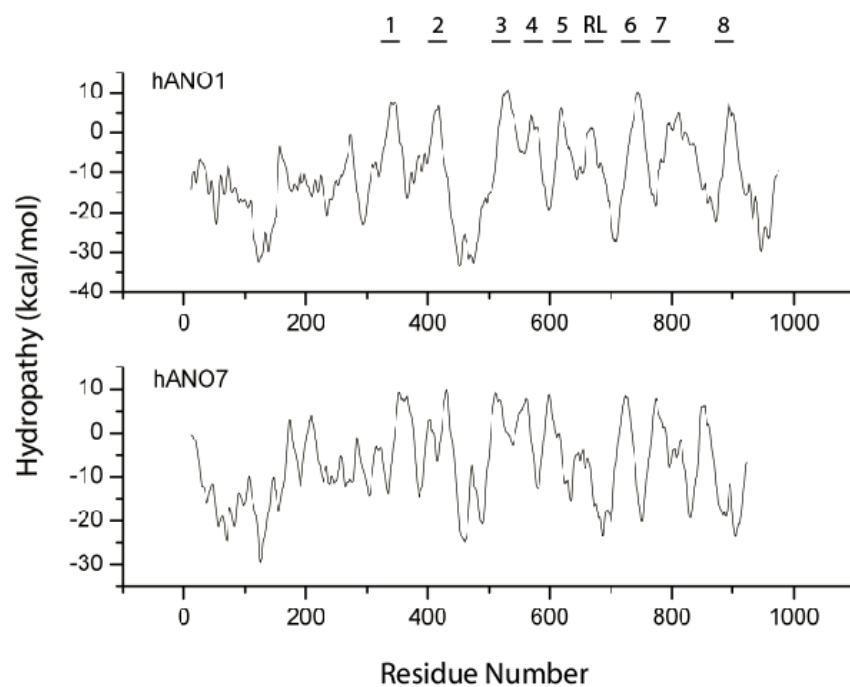


**Figure 3-2:** Hydropathy analysis of An01 and An07. Hydropathy analysis reveals eight hydrophobic peaks that are strongly conserved across anoctamins. Position of predicted transmembrane domains and putative reentrant loop (RL) are indicated by dashes above the plot. The predicted transmembrane topology is based on hydropathy analysis and experimental evidence for An07. Hydropathy plot was generated by MPEX (<http://blanco.biomol.uci.edu/mpex/>).

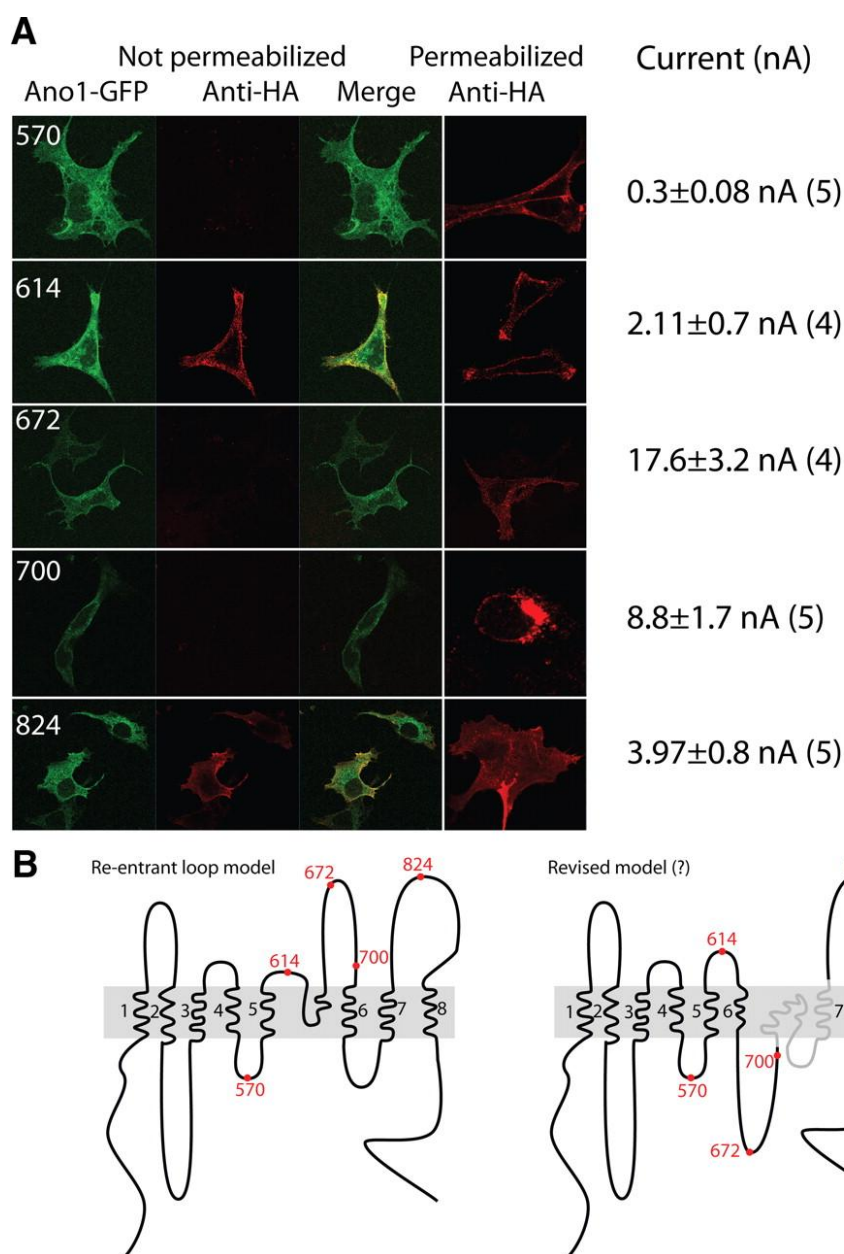


**Figure 3-3:** Immunofluorescent staining of mAno1 containing tandem hemagglutinin (HA) epitopes inserted at various locations. **A)** HA tags were inserted into mAno1-EGFP at amino acids 570, 614, 672, 700, and 824. After transient expression, nonpermeabilized intact cells were stained with antibody for HA epitope. Green: Ano1-GFP; red: anti-HA and merged image. Duplicate cover slips were permeabilized before

incubation with HA antibody (red: permeabilized, anti-HA). For each construct, images were acquired at the same gain and settings, but settings may differ between constructs that were imaged on different days. Raw images from the Zeiss Zen acquisition software from permeabilized and nonpermeabilized cells were assembled in Adobe Photoshop CS5 and brightness-adjusted and contrast-adjusted for all four panels equally.

Anoctamin-1 (Ano1) currents for each construct were recorded with 20  $\mu\text{mol/L}$  Ca.

Average peak amplitude at +100 mV and the number of recorded cells are listed. **B)**

Topological models of mAno1. The locations of HA tags are indicated with red numbers.

**Left**, reentrant loop model. **Right**, revised model. The topology of the sequence depicted in gray remains in question. Reprinted from Circulation Research 110: 7, Yu K, et al, Explaining Calcium-Dependent Gating of Anoctamin-1 Chloride Channels Requires a Revised Topology, Copyright (2012)

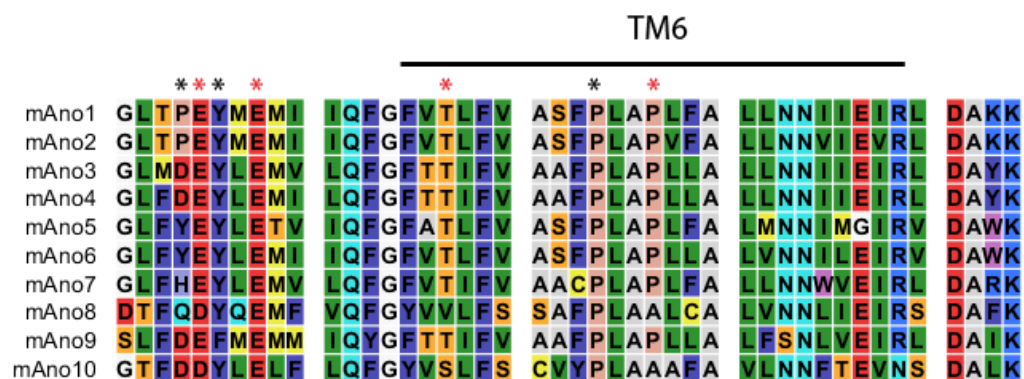


**Figure 3-4:** Sequence alignment of the region previously predicted to comprise the sixth transmembrane domain. Sequence alignment of residues 698-741 of mouse anoctamins 1-10 showing high level of conservation across the anoctamin family. Red asterisks indicate mutations found to affect mAno1 channel function. Black asterisks indicate mutations that had currents similar to WT mAno1.

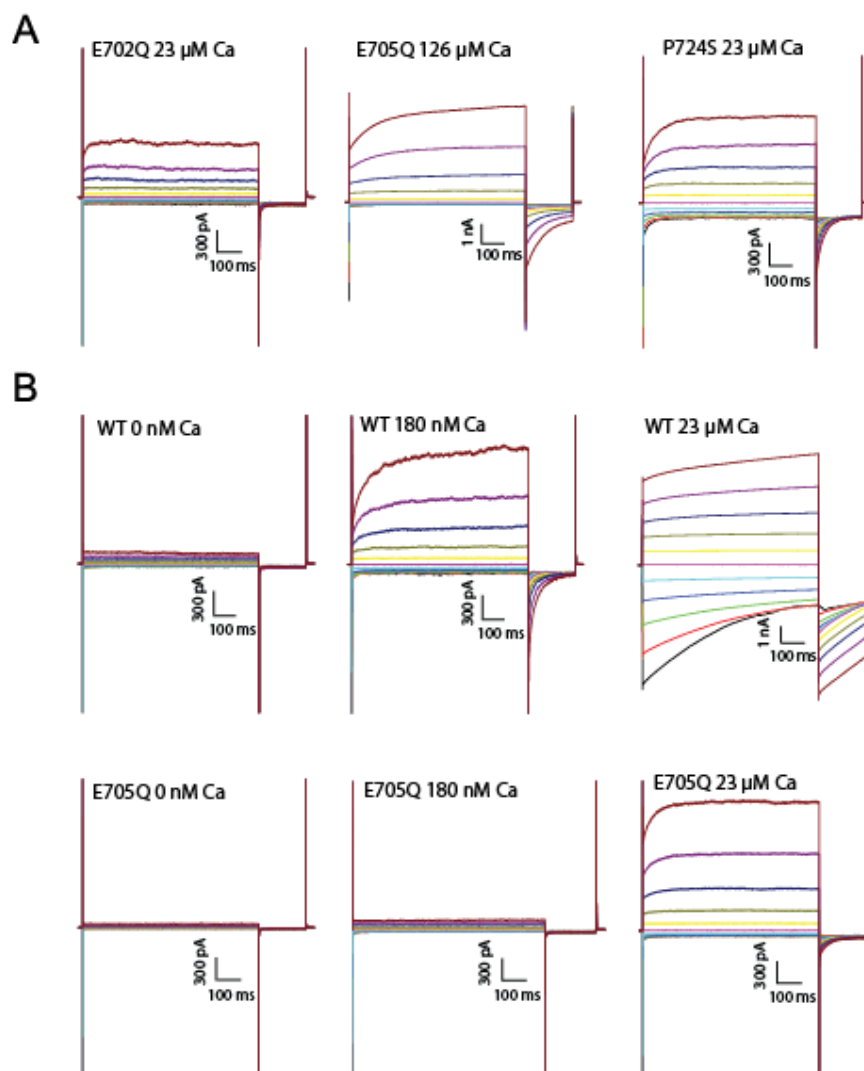


**Figure 3-5:** Representative whole-cell recordings of Ano1 constructs in transfected HEK293 cells at the indicated free  $[\text{Ca}^{2+}]_i$ . **A)** E702Q, E705Q, and P724S mutants maintain outward rectification even in the presence of high intracellular  $[\text{Ca}^{2+}]_i$ . **B)** Comparison of current responses to various  $[\text{Ca}^{2+}]_i$  of WT Ano1 and E705Q mutant ANO1. A voltage protocol from -100 to +100 mV in 20 mV intervals was applied for all records.

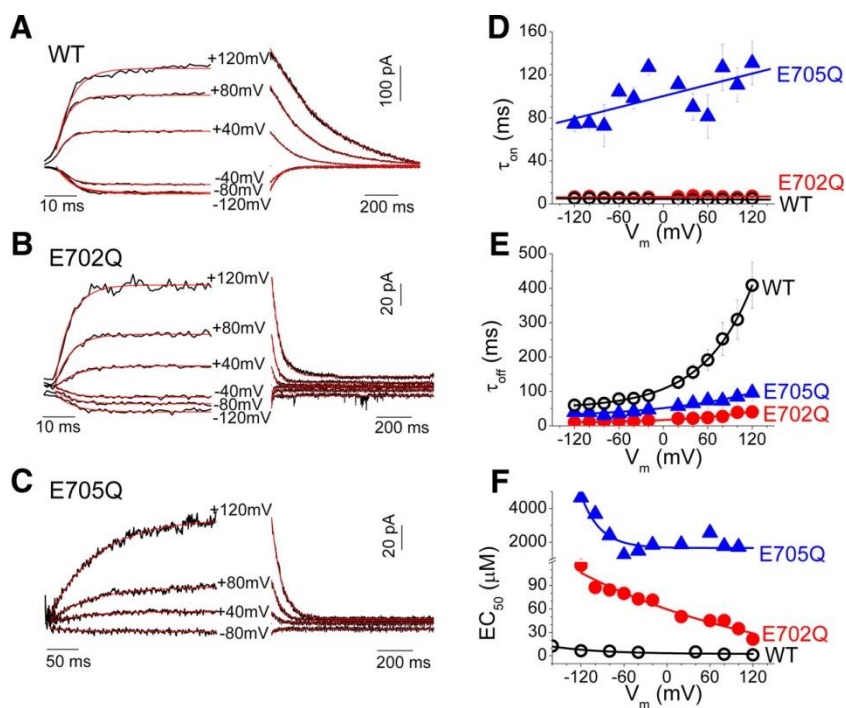


**Figure 3-6:** Activation and deactivation kinetics of anoctamin-1 (Ano1) with rapid Ca<sup>2+</sup> perfusion in inside-out excised patches. Representative traces of Ano1 current in response to application (**left**) and washout (**right**) of Ca<sup>2+</sup> at the indicated holding potentials. **A)** WT-mAno1. **B)** E702Q mANO1. **C)** E705Q mANO1. **D–F)** V<sub>m</sub> dependence of τ<sub>on</sub>, τ<sub>off</sub>, and EC<sub>50</sub> for WT Ano1 (open circles), E702Q (filled circles), and E705Q (filled triangles). Reprinted from Circulation Research 110: 7, Yu K, et al, Explaining Calcium-Dependent Gating of Anoctamin-1 Chloride Channels Requires a Revised Topology, Copyright (2012)

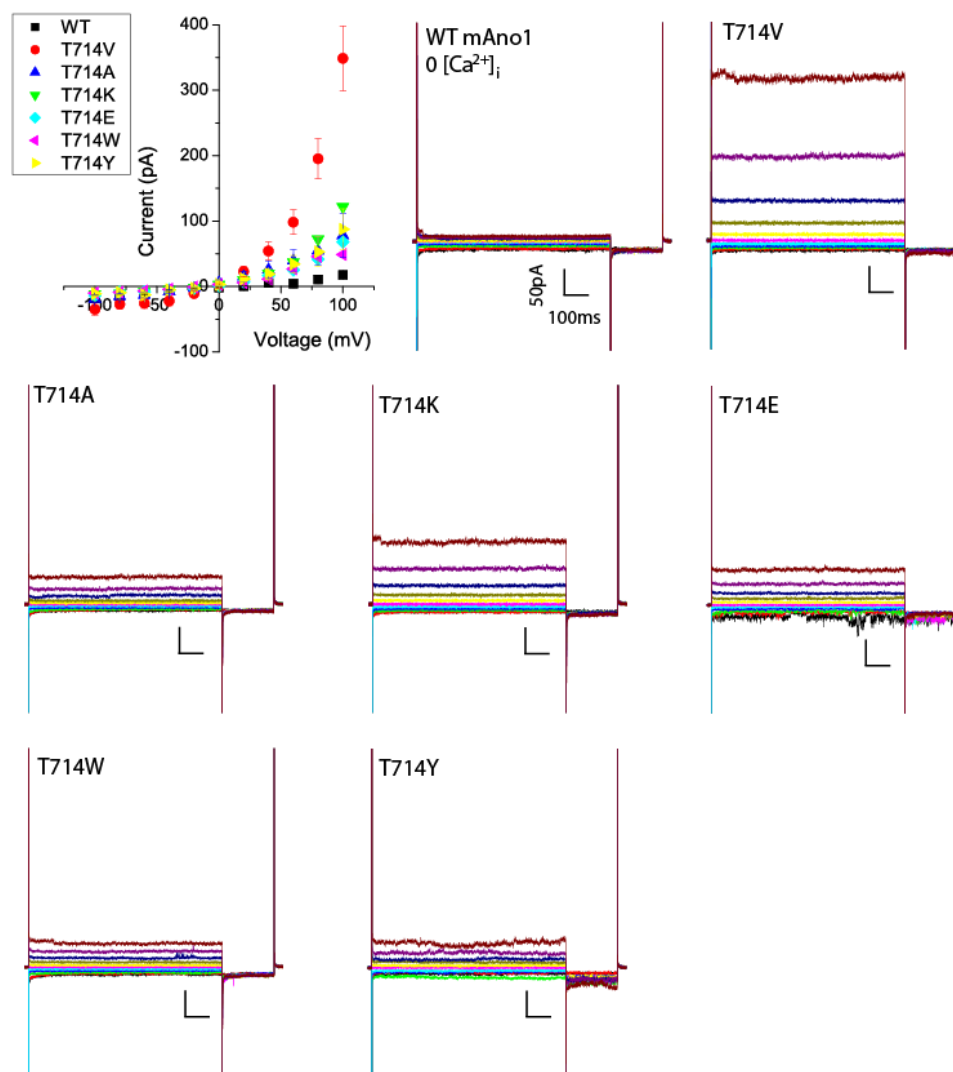


**Figure 3-7:** Voltage sensitivity of mAno1 T714X mutants. Average current responses of WT and T714X mAno1 mutants and representative whole cell current records in response to voltage in the absence of intracellular  $\text{Ca}^{2+}$ . A voltage step protocol from -100mV to 100mV was applied in 20mV intervals. In response to positive voltages, the T714V mutant exhibits current that is time independent and outwardly rectifying, while WT Ano1 does not elicit a response. Other mutations had a much smaller effect on voltage sensitivity compared with the T714V mutant.

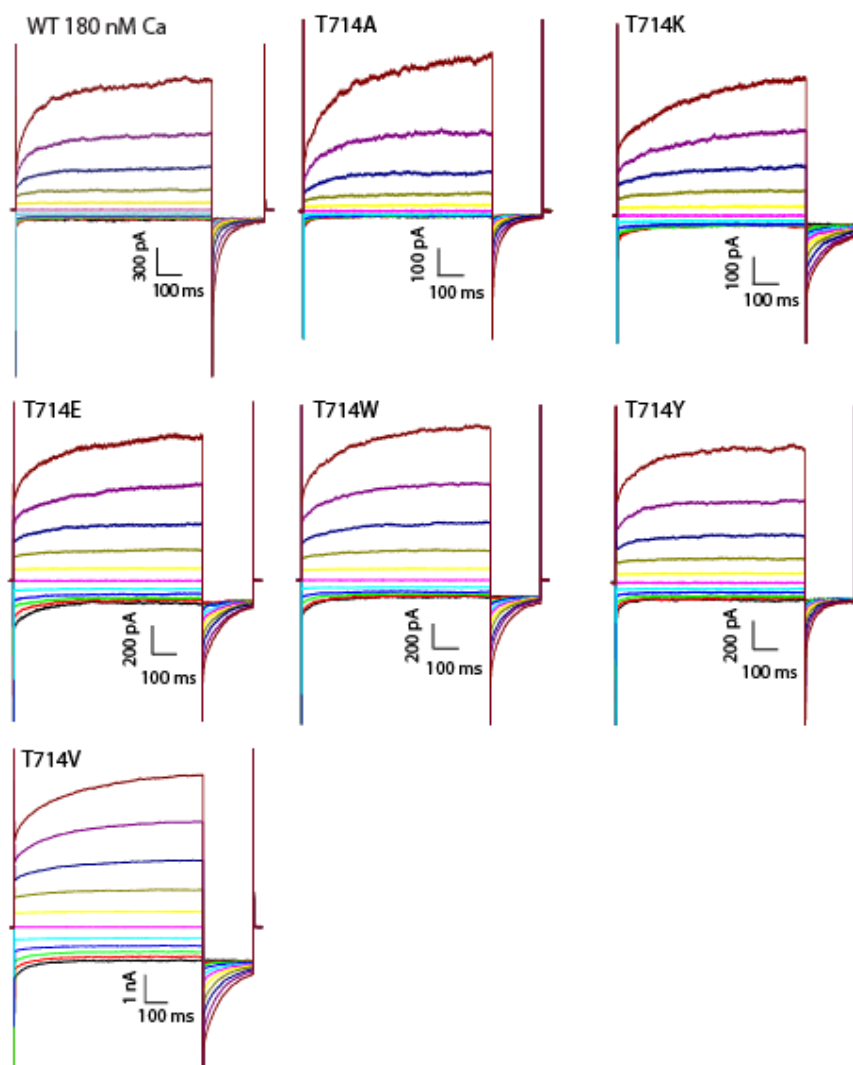


**Figure 3-8:** Response of mAno1 T714X mutants to intracellular  $\text{Ca}^{2+}$ . Representative whole cell current records in response to 180nM intracellular  $\text{Ca}^{2+}$ . A voltage step protocol from -100mV to 100mV was applied in 20mV intervals. All mutants displayed currents comparable to WT.

**CHAPTER 4**

***DROSOPHILA* BESTROPHIN-1 CURRENTS ARE REGULATED BY  
PHOSPHORYLATION VIA A CAMKII DEPENDENT MECHANISM**

## Summary

Cell swelling induced by hypo-osmotic stress results in activation of volume-regulated anion channels (VRAC) that drive a compensatory regulatory volume decrease. We have previously shown that the Best1 gene in *Drosophila* encodes a VRAC that is also activated by increases in intracellular  $\text{Ca}^{2+}$ . The role of Best1 as a VRAC has recently been confirmed in an RNAi screen (Stotz et al. 2012). Although dBest1 is clearly a volume-regulated channel, its mechanisms of regulation remain unknown.

Furthermore, it has been proposed that another  $\text{Cl}^-$  channel, anoctamin 1 (Ano1) is a VRAC. Here we investigate these questions using the *Drosophila* S2 cell model system to study *Drosophila* Best1 (dBest1) regulation. Previous studies indicate that human Best1 (hBest1) activity is directly regulated by phosphorylation (Xiao et al. 2009), suggesting that dBest1 may also be regulated via phosphorylation. We evaluate the effect of various kinase inhibitors on endogenous dBest1 currents expressed in *Drosophila* S2 cells.

Nonspecific kinase inhibitors reduce current amplitude of dBest1 currents. Application of  $\text{Ca}^{2+}$ /calmodulin dependent kinase II (CaMKII) specific inhibitors dramatically inhibits dBest1 current activation. Neither PKA specific inhibitors nor nonfunctional CaMKII inhibitor analogs have an effect on dBest currents, indicating that inhibition of dBest currents occurs specifically through CaMKII inhibition. Furthermore, we use RNAi to demonstrate that *Drosophila* anoctamin orthologs do not contribute to S2 cell  $\text{Ca}^{2+}$ -activated  $\text{Cl}^-$  currents. Our results demonstrate that dBest1, which is predominantly responsible for CaCC currents in S2 cells, is regulated by phosphorylation via a CaMKII dependent mechanism.

## Introduction

Volume-regulated anion channels (VRACs) are critical for the homeostasis of cell volume via a process called regulatory volume decrease (RVD). RVD is a process by which a cell returns to its normal volume in response to osmotic pressure differences across the plasma membrane. During RVD, activation of VRAC and other channels or transporters results in an efflux of ions followed by water, thereby returning the cell to its normal volume (Hoffmann and Simonsen 1989; Lang et al. 1998; Nilius et al. 1997). Several molecular candidates have been proposed to mediate VRAC (d'Anglemont de Tassigny et al. 2003; Eggermont et al. 2001). Best1 is one such candidate that has received considerable support for being a VRAC in *Drosophila* S2 cells.

We have previously shown that the Best1 gene in *Drosophila* S2 cells encodes an anion channel. The Best1 current can be activated by increases in intracellular  $\text{Ca}^{2+}$  (Chien et al. 2006), and is abolished by RNAi directed against Best1. The Best1 current is also activated by extracellular hypo-osmotic solutions and thus was considered to be a candidate for the volume-regulated anion channel (VRAC) in these cells. Evidence in support of this hypothesis was that the VRAC current was abolished by RNAi directed against Best1 (Chien and Hartzell 2007). Furthermore, cells with Best1 expression knocked down by RNAi failed to undergo regulatory volume decrease in response to cell swelling. The effect of Best1 RNAi was rescued by over-expression of dBest1 (Chien and Hartzell 2008). Furthermore, it was possible to rescue the Best1 currents with a mutant Best1 that exhibited altered anion selectivity. This showed conclusively that the VRAC current was mediated by Best1. Recently, Stotz et al. (2012) performed a genome-wide RNAi screen to identify the VRAC in S2 cells and concluded that Best1 was the most likely candidate.

Cell volume and  $\text{Ca}^{2+}$  may independently regulate Best1 function, because  $\text{Ca}^{2+}$  can activate the current in the absence of cell volume changes. However, the mechanisms underlying ion channel regulation by cell volume are very complex, and multiple signaling pathways have been implicated (Lang et al. 1998; Nilius et al. 1997). It is unknown if cell volume and  $\text{Ca}^{2+}$  converge on a common regulatory pathway to activate Best1, as very little is known about other mechanisms that contribute to *Drosophila* bestrophin current regulation. Previous studies indicate that that human Best1 is regulated by phosphorylation, suggesting that *Drosophila* Best1 may also be regulated via phosphorylation (L. Y. Marmorstein et al. 2002; Xiao et al. 2008; Xiao et al. 2009).

To further examine the role of phosphorylation in bestrophin regulation, whole cell patch clamp recordings were taken from *Drosophila* S2 cells. The effect of various kinase inhibitors on dBest1 current was examined. Although several studies have demonstrated that S2 cell CaCCs are mediated by dBest1 (Chien et al. 2006; Chien and Hartzell 2008; Dutzler et al. 2002; ), a new family of chloride channels, called anoctamins, has been discovered (Yang et al. 2008; Caputo et al. 2008; Schroeder et al. 2008). It has been suggested that Ano1 is a VRAC (Almaca et al. 2009). *Drosophila* have five anoctamin genes (CG13010 (Axs), CG16718, CG10353, CG6938, and CG15270 ). Because *Drosophila* anoctamins may also mediate VRACs or  $\text{Ca}^{2+}$ -activated chloride channels (CaCCs) in S2 cells, we used RNAi knockdown to evaluate the contribution of *Drosophila* anoctamin orthologs to CaCCs in S2 cells.

## Results

### **dBest currents are regulated by phosphorylation**

*Drosophila* Best1 currents are activated by increases in intracellular  $\text{Ca}^{2+}$ .

However, the mechanisms underlying  $\text{Ca}^{2+}$  regulation of dBest are unknown. There are three basic models which could explain activation of dBest1 by  $\text{Ca}^{2+}$  (Figure 4-1). Firstly,  $\text{Ca}^{2+}$  may bind directly to dBest1 to induce a conformational change which gates the channel open. An alternative scenario is that  $\text{Ca}^{2+}$  binds to and activates  $\text{Ca}^{2+}$ -dependent kinases, which subsequently regulate dBest1 activation via phosphorylation. There is also the possibility that dBest activity is regulated by both mechanisms. To examine the potential role of phosphorylation in dBest1 activation, we first performed whole cell patch clamp in the presence or absence of intracellular ATP. In the presence of high intracellular  $\text{Ca}^{2+}$  ( $4.5\mu\text{M}$ ) and 3mM ATP, dBest1 currents activate over a period of 4-5 min before reaching a plateau (Figure 4-2A). Exclusion of ATP from the intracellular solution significantly decreases the rate of  $\text{Ca}^{2+}$ -dependent current activation of dBest1 (Figure 4-2B, C). The slow time course of activation and its dependence on intracellular ATP would suggest that phosphorylation is implicated in dBest current activation. To test this hypothesis, we first examined the effect of non-specific protein kinase inhibitors on dBest1 currents (Figure 4-3). K252a and staurosporine are potent nonselective kinase inhibitors that bind to the ATP binding site of various kinases. When applied to the bath solution, both k252a and staurosporine caused a dramatic slowing of Best1 current activation by  $\text{Ca}^{2+}$  and a decrease in the maximal amplitude of  $\text{Ca}^{2+}$  activated dBest currents.

### **Regulation of dBest currents by phosphorylation is CaMKII-dependent**

We next set out to determine which specific kinases regulate dBest1 activity. Because regulation of CaCC currents by CaMKII has been observed in several cell types (Holevinsky et al. 1994; Nishimoto et al. 1991; Schlenker and Fitz 1996; Wagner et al. 1991), we examined the effect of CaMKII inhibitors on dBest1 currents (Figure 4-4). Application of KN-93, a selective and potent CaMKII inhibitor, significantly reduced dBest1 current amplitude. An inactive structural analogue of KN-93, KN-92, had no effect on dBest1 currents. These results indicate that the effects of KN-93 are mediated through inhibition of CaMKII, rather than through nonspecific effects of the drug. In addition to KN-93, myristoylated autocalcinein-2 related inhibitory peptide (AIP) dramatically inhibits dBest currents. AIP is a highly-specific and potent inhibitor of CaMKII, further supporting the participation of CaMKII in dBest regulation. The effects of two other selective kinases were examined as well (Figure 4-5). The PKA specific inhibitor, H7, did not have any effect on dBest current amplitude. A CaMKII specific inhibitor, KN-62, slightly decreased dBest1 current amplitude; however, it did not reduce currents to the same extent as KN-93. Because KN-62 and KN-93 were used at the same concentration, this result is in agreement with the fact that KN-62 is a relatively less potent CaMKII inhibitor than KN-93, with  $K_i$ 's of 370nM and 900nM respectively (Tokumitsu et al. 1990) (Sumi et al. 1991; Tokumitsu et al. 1990). The relative effects of various kinase inhibitors on dBest1 current are presented in Figure 4-6.

### ***Drosophila* anoctamin orthologs do not contribute to S2 cell CaCC current**

Multiple studies demonstrate that the  $Ca^{2+}$  sensitive  $Cl^-$  current expressed in *Drosophila* S2 cells is mediated by the hBest1 ortholog, dBest1 (Chien et al. 2006; Chien and Hartzell 2008; Dutzler et al. 2002). However, the recent discovery that anoctamins

are CaCCs raises the possibility that *Drosophila* anoctamin orthologs may contribute to S2 cell CaCCs. A Flybase blast search (<http://flybase.org>) using the peptide sequence for human Ano1 as the input (NP\_060513.5) identified several *Drosophila* anoctamin orthologs: *CG16718*, *CG6938*, *CG10353*, *CG15270*, and *Axs*. Of the genes identified, *CG16718* had the highest sequence similarity to hAno1. *Axs* is responsible for abnormal X segregation in *Drosophila* and is most similar to Anos8/10 (Zitron and Hawley 1989). To examine the possible contributions of these *Drosophila* anoctamins to S2 cell CaCCs, we generated siRNA against *CG16718* and *Axs* transcripts, which will be referred to as dAno1 and dAno8/10 for the purpose of this study. Treatment of S2 cells with dAno1 siRNA significantly reduced the endogenous CaCC current, but did not completely abolish it (Figure 4-7A). siRNA against dBest1, however, completely eliminated CaCC current. siRNA knockdown of dAno8/10 or treatment with control siRNA had no effect on S2 cell CaCCs.

Because knockdown of dAno1 reduced the CaCC current, we cloned and expressed dAno1 (NM\_142563.1) in HEK293 cells to examine its channel function. Expression of dAno1 generated currents with biophysical properties distinct from those of the endogenous dBest1 current (Figure 4-7B, C). Unlike dBest1 currents, dAno1 currents are strongly outwardly rectifying and generate tail currents in response to voltage steps from positive voltages to -100mV. In addition, dAno1 currents are time dependent and activate slowly, while dBest1 currents display no time dependence. These results suggest that endogenous S2 cell CaCCs are mediated primarily by dBest1 and not dAno1. While dAno1 knockdown may regulate dBest1 activity, dAno1 is unlikely to be the molecular correlate underlying S2 CaCC currents because its biophysical properties are significantly different. Furthermore, dBest1 expression in HEK293 cells generates currents similar to those of endogenous S2 CaCCs (Chien et al. 2006). However, these

data do suggest some interaction between Ano1 and Best1, as knockdown of Ano1 significantly decreased Best1 currents.

## **Discussion**

### ***Drosophila* anoctamins do not mediate S2 cell CaCCs**

We used RNAi to evaluate the contribution of various anoctamin orthologs to S2 cell CaCCs. Knockdown of dAno1 resulted in a dramatic decrease in CaCC current amplitude, but did not completely abolish currents as did siRNA against dBest1. Because we have not yet determined the efficiency of dAno1 knockdown, we cannot definitively conclude that dAno1 affects dBest1 function. However, based on the biophysical properties of dAno1, we believe that dAno1 does not contribute to S2 cell CaCC currents. dAno1 expressed in HEK cells has biophysical properties significantly different from those of dBest1, further suggesting that S2 cell CaCCs are not mediated by dAno1. Although it is possible that differential expression of regulatory subunits in S2 and HEK293 cells alters the biophysical properties of dAno1 currents, expression of dBest1 in HEK cells yields currents similar to those seen in S2 cells (Chien et al. 2006). These results suggest that while dAno1 knockdown might regulate dBest1 expression or function, it does not directly contribute to S2 cell CaCC currents. Knockdown of dAno8/10 had no effect on S2 cell CaCC currents, which is not surprising because murine Ano8 and Ano10 are intracellularly localized proteins that do not generate CaCCs when expressed in HEK cells (Duran et al. 2012). Future work will be aimed at evaluating the efficiency of siRNA knockdown of anoctamin orthologs, and determining the reproducibility of the effect of dAno1 siRNA on S2 cell CaCC currents.

Although more work is needed to determine the significance of this interaction, these results could have implications for Best vitelliform macular dystrophy (BVMD). BVMD, which is caused by mutations in Best1, is characterized by a chloride channel deficit in the retinal pigment epithelium. In mice this chloride current is not mediated by Best1, suggesting that Best1 is instead a regulator of this current (L. Y. Marmorstein et al. 2006; Zhang et al. 2010). Ano1 now represents the most promising candidate for mediating this current (see Chapter 5). Therefore, future work examining S2 cell CaCC regulation could provide important information regarding the interaction between Ano1 and Best1.

#### **dBest1 currents are regulated via a CaMKII dependent mechanism**

The effects of various kinase inhibitors on dBest1 reveals that current activation by intracellular  $\text{Ca}^{2+}$  is regulated by phosphorylation, which is primarily mediated via CaMKII. These are the first reports of Best1 regulation by CaMKII. While our results suggest that dBest1 activity is mostly dependent on CaMKII phosphorylation, we cannot rule out regulatory contributions by other kinases or phosphatases. Notably, PKC has been shown to phosphorylate hBest1 to regulate channel activity (Xiao et al. 2008). The phosphorylation state of serine 358, which lies within the C-terminus of bestrophin, regulates rundown of hBest1 currents and is responsible for hypertonic stress induced inhibition of Best1 currents. Phosphorylation of S358 by PKC slows channel rundown, while dephosphorylation via PP2A accelerates channel rundown (L. Y. Marmorstein et al. 2002; Xiao et al. 2009). The effect of PKC or PP2A inhibitors on dBest current was not examined here. However, S358 is not conserved in dBest1, suggesting that dBest1 and hBest1 may be differentially regulated by phosphorylation.

It is possible that for Best1, phosphorylation sites exist for multiple kinases or phosphatases, and that these mechanisms are dependent on the system in which Best1 is expressed. Axotomy of DRG neurons, for example, results in up-regulation of a CaCC current mediated by Best1 that is specific to a subset of DRG neurons (Boudes et al. 2009). Transfection of Best1 in naïve neurons yields currents that are significantly smaller than those induced by injury, suggesting differences in regulatory mechanisms between naïve and axotomized neurons. Furthermore, transfection of DRG neurons with Best1 generates CaCC currents only in a subset of these neurons. Variations in Best1 current expressed in different neuronal populations could potentially be related to its phosphorylation state or its association with other regulatory subunits. This is also true of endogenous CaCCs, for which regulation by CaMKII is cell-type dependent, as is whether CaMKII has an inhibitory or stimulatory effect on CaCC currents (C. Hartzell et al. 2005; Holevinsky et al. 1994; Nishimoto et al. 1991; Schlenker and Fitz 1996; Wagner et al. 1991). It is important to note, however, that this could also be due to heterogeneity in the proteins that underlie endogenous CaCCs in these systems.

### **The mechanism of dBest regulation by CaMKII is unknown**

We used two different phosphorylation site identification programs to determine regions potentially implicated in regulation of dBest1 by CaMKII. One phosphorylation site identification program, Phosphomotif finder, identified several potential CaMKII phosphorylation sites within the C-terminus of dBest1 (Amanchy et al. 2007) (Figure 4-8). An alternative phosphorylation site identification program, Scansite, did not identify any high stringency CaMKII phosphorylation sites within dBest1. However, using less stringent cutoff criteria, one CaMKII phosphorylation site was identified in dBest1 at position S440, which was also predicted by Phosphomotif finder. In contrast to Scansite,

Phosphomotif finder does not employ algorithms or computational strategies to predict phosphorylation sites, but rather reports the presence of any literature-derived motifs.

Given the importance of the C-terminus in the regulation of hBest1 by phosphorylation, it is plausible that a CaMKII phosphorylation site exists within the C-terminus of dBest1. However, it is unknown if CaMKII directly phosphorylates dBest1, or if there are intermediate signaling events involved in dBest1 activation by CaMKII. Like dBest1, there are no high stringency CaMKII phosphorylation sites within hBest1. However, there are no published data on the regulation of hBest1 by CaMKII. Because the C-terminal sequences of dBest1 and hBest1 are not highly conserved, the regulatory mechanisms governing channel activity may differ between hBest1 and dBest1. None of the potential CaMKII phosphorylation sites identified within dBest1 are conserved in hBest1. The PKC phosphorylation site of hBest1 is also not conserved in dBest1, and none of the predicted CaMKII phosphorylation sites are near this region. Furthermore, truncation of hBest1 at position 390 yields channels that function similarly to wild type, suggesting that this region is not critical for hBest1 function (Xiao et al. 2008). The lack of predicted high stringency CaMKII sites conserved in both dBest1 and hBest1 could indicate a species specific difference in Best1 regulation by CaMKII. However, these results could also indicate that there are no CaMKII phosphorylation sites in Best1, and that CaMKII regulates dBest1 through an indirect mechanism. Future studies should be aimed at determining whether CaMKII regulates dBest1 via direct phosphorylation, or through intermediate signaling events.

### **Future Directions**

These preliminary studies provide future directions for examining the regulatory mechanisms of Best1. The foremost question posed by this study is: can dBest1 be

directly phosphorylated, and if so, is phosphorylation directly mediated by CaMKII? Alternatively, if dBest1 is not directly phosphorylated by CaMKII, CaMKII may act on a regulatory subunit of dBest1. There are several possible mechanisms for how phosphorylation could regulate dBest1 activity. First, the phosphorylation state of Best1 may directly regulate its channel function, as has been shown for hBest1. Phosphorylation of Best1 could also alter its trafficking to the plasma membrane. Or, phosphorylation of Best1 could affect its association with regulatory subunits, and vice versa. Studying Best1 regulation in a native system is important for several reasons. First, if the phosphorylation state of Best1 alters its plasma membrane expression, studies in over-expression systems where Best1 typically traffics to the membrane may be inadequate. In addition, many commonly used heterologous systems, such as HEK293 cells, are dedifferentiated cells that likely do not express the same milieu of regulatory subunits. Future studies examining the mechanisms of Best1 regulation in *Drosophila* S2 cells may therefore yield critical information about Best1 function, and accordingly dysfunction, in retinal diseases.

## **Materials and Methods**

### **Cell Culture**

*Drosophila* S2 cells were cultured at room temperature (22-24°C) in Schneider's *Drosophila* Medium (GIBCO BRL) containing 10% heat-inactivated FBS (GIBCO BRL), 50ug/ml penicillin, and 50 µg/ml streptomycin (GIBCO BRL). HEK293 cells were maintained at 37°C in DMEM supplemented with 10%FBS (GIBCO), and 50 U/ml penicillin and 50 µg/ml streptomycin (GIBCO).

### **RNA interference**

dsRNA was synthesized from dBest, dAno1, or dAno8/10 cDNAs using the Ambion Mega-script High-Yield Transcription Kit. 40ug of double-stranded interfering RNA was applied to S2 cells in serum-free medium for 30min at room temperature. Cells were patch clamped 4-5 days after RNAi treatment. Primer pairs for RNAi synthesis are as follows: Control, 5'-TCGGGGCTGTGGCTGAGGT-3' and 5'-TGGTGCTTCGCGTTGATGTGT-3'; dBest1, 5'-TGTTTGTCTAAGCCCTTCTACCTC-3' and 5'-ATTGCTGTTCTTCTTTCCGACTGT-3'; dAno1, 5'-CTGGCGCGTTTGGAGCACA-3' and 5'-ACAGCCGCCCGATGAGCACT-3'; dAno8/10, CACGGCTGCATCTCGGACTTTCTA and 5'-CCGGCACACTTACGCTTCCACAAC-3'. To ensure specificity each primer was BLASTed against the *Drosophila* nucleotide database.

### **Phosphorylation site prediction**

Phosphorylation sites were predicted using either Phosphomotif Finder ([http://www.hprd.org/PhosphoMotif\\_finder](http://www.hprd.org/PhosphoMotif_finder)) or Scansite (<http://scansite.mit.edu/>). Identification of CaMKII phosphorylation sites with Scansite were performed using the medium stringency scan. Accession number for the dBest1 peptide sequence analyzed is AAL29094.

### **Electrophysiology**

Whole cell patch-clamp was performed at room temperature (22-24°C). Patch pipettes were fire polished to resistances of 2-3 MΩ. The standard extracellular solution used for patch clamping S2 cells contained (mM) 150NaCl, 2 CaCl<sub>2</sub>, 1 MgCl<sub>2</sub>, HEPES (pH7.2 with NaOH), and 10 glucose. The standard intracellular solution contained (mM) 143 CsCl, 10 Ca-EGTA-NMDG, 8 MgCl<sub>2</sub>, 10 HEPES (pH 7.2 with NaOH), 10 glucose, and 3 ATP.

For both extracellular and intracellular solutions, pH was adjusted to 7.2 with NMDG, and osmolarity was adjusted to 320 mOsm with water or sucrose. Cells were voltage clamped with ramps from -100mV to 100mV run at 10-s intervals. Recording continued until the current reached a plateau. For HEK293 cell recordings, cells were transfected using Fugene 6 with 0.4 $\mu$ g DNA of dAno1-PIRES. The dAno1 sequence (NM\_142563.1) was subcloned into the PIRES-II vector. Transfected cells were then plated at low density and recorded from 24–48 h after transfection. Cells expressing GFP-were patched.

### **Pharmacology**

Kinase inhibitors were diluted to their final concentrations in extracellular and intracellular recording solutions, and were included in both the bath and patch pipette for whole-cell recordings. S2 cells were pre-exposed to extracellular solution containing drug for at least 6 minutes prior to recording. For cells treated with myristoylated-AIP, a longer 20 min pre-incubation was required due to its relative impermeability to the membrane.

### **Data Analysis**

Data were analyzed using pClamp 8.2 software and Origin 7.0. One way ANOVA with a Bonferonni post test was used to determine significant differences in maximum current. Data is expressed as mean  $\pm$  SEM.

**Acknowledgement**

I would like give a special thanks to Li-Ting Chien who made a significant contribution to the S2 cell RNAi studies, and who initiated the studies examining the role of phosphorylation in dBest activation.

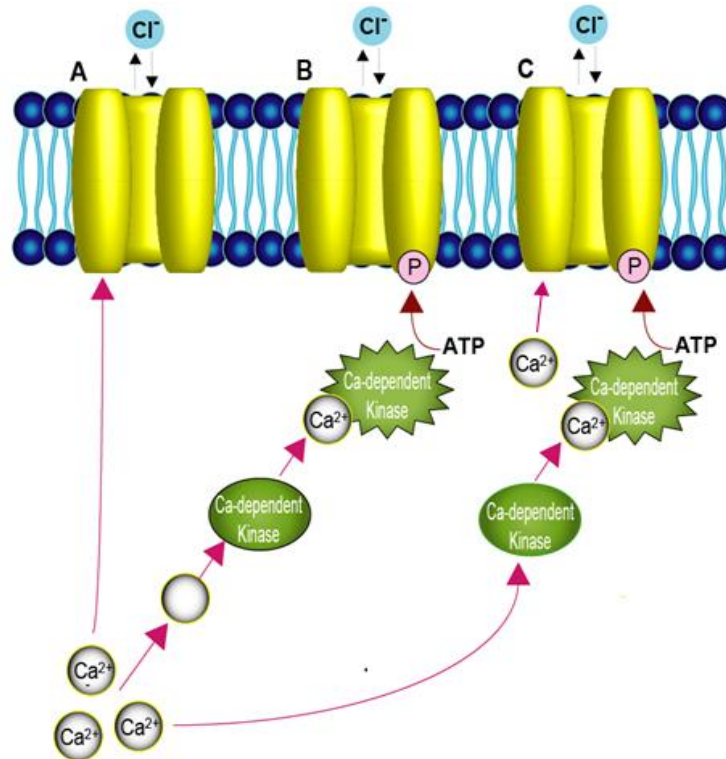


**Figure 4-1:** Models of *Drosophila* Bestrophin mechanisms of activation/regulation. *Drosophila* bestrophin channels can be activated **A)** by Ca<sup>2+</sup> alone, **B)** by Ca<sup>2+</sup>-dependent protein kinases, or **C)** by both Ca<sup>2+</sup> and Ca<sup>2+</sup>-dependent protein kinases.

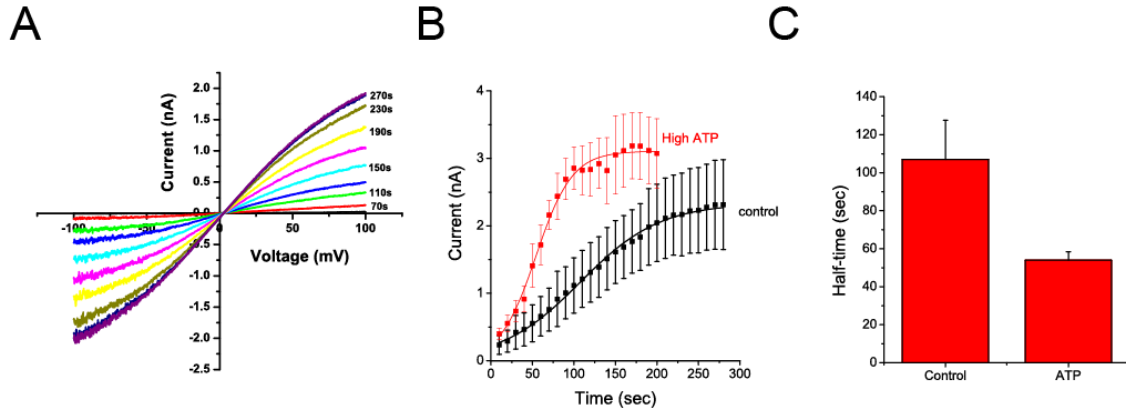


**Figure 4-2:** Time-dependent activation of S2 Cl<sup>-</sup> currents in response to high [Ca<sup>2+</sup>]<sub>i</sub>.  
**A)** Typical IV traces of *Drosophila* S2 cell Ca<sup>2+</sup>-activated bestrophin currents with high Ca<sup>2+</sup> (4.5 μM) and 3mM ATP. Cells are voltage clamped with ramps from -100 to 100 mV at 10-s intervals until the current reaches a plateau. **B)** Time-dependent activation of *Drosophila* S2 cell Ca<sup>2+</sup>-activated bestrophin currents in the presence or absence of 3mM intracellular ATP. **C)** Half-time of dBest1 current activation with or without intracellular ATP.

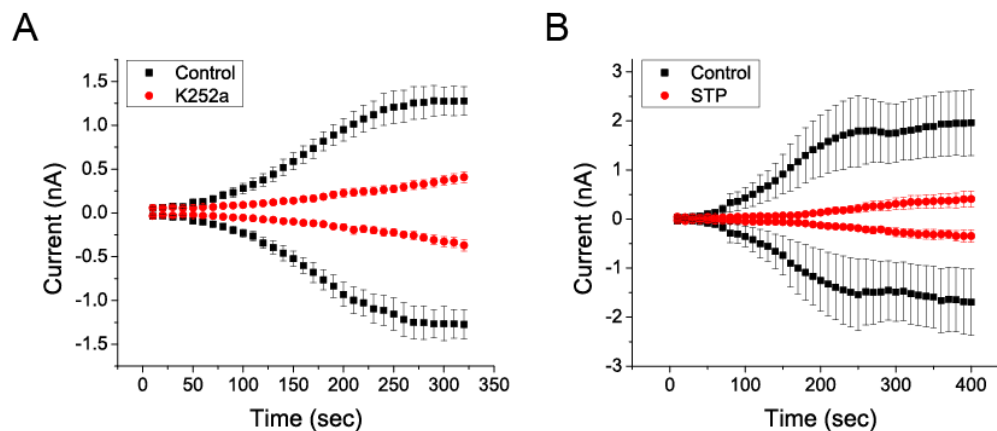


**Figure 4-3:** Nonselective kinase inhibitors inhibit *Drosophila* S2 Ca<sup>2+</sup>-activated currents. Cells were pre-incubated with either k252a or staurosporine before being recorded with pipette solutions containing the inhibitor in addition to high Ca<sup>2+</sup> and ATP. Bestrophin currents are inhibited by **A)** K252a (1 μM) and **B)** staurosporine (10 μM).

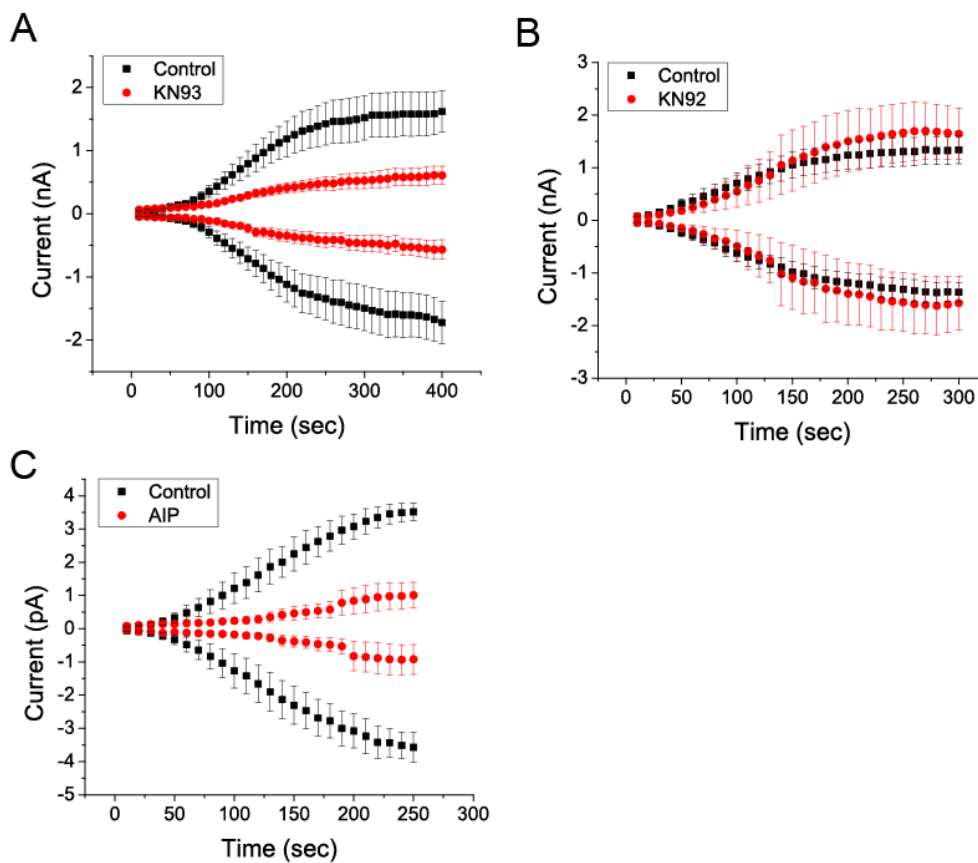


**Figure 4-4:** Reduction in bestrophin currents by kinase inhibitors occurs through inhibition of CaMKII, not a nonspecific interaction. *Drosophila* Ca<sup>2+</sup>-activated bestrophin currents are modulated by a potent CaMKII inhibitor, KN-93. **A)** KN-93, (10 $\mu$ M), reduces current amplitude, whereas its inactive structural analogue, **B)** KN-92 (10 $\mu$ M), has no effect on dBest currents. **C)** A very specific peptide inhibitor of CAMKII, myristoylated AIP, also inhibits dBest currents.

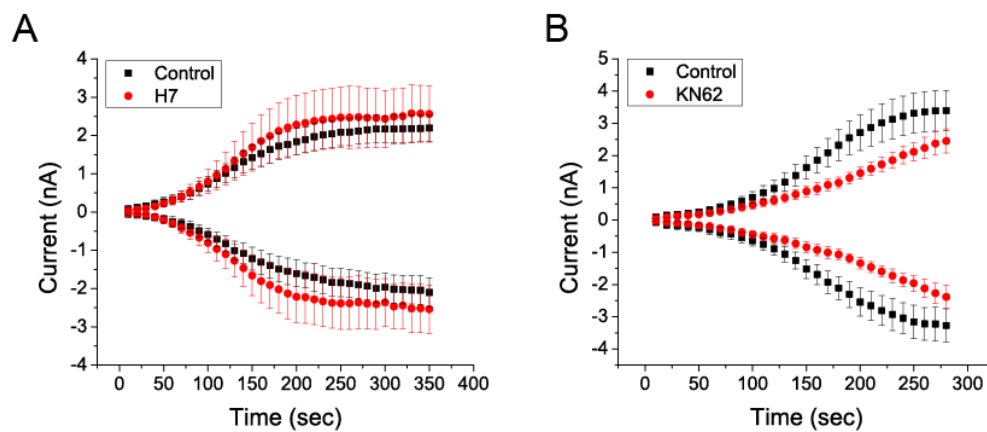


**Figure 4-5:** Dihydrochloride (H7) and KN-62 do not significantly reduce dBest currents. **A)** H7 (10 $\mu$ M), which selectively inhibits PKA at this concentration, has no effect on dBest currents. **B)** KN-62 (10 $\mu$ M) also does not have a significant effect on dBest currents. KN-62 is a relatively less potent CAMKII inhibitor than KN-93.

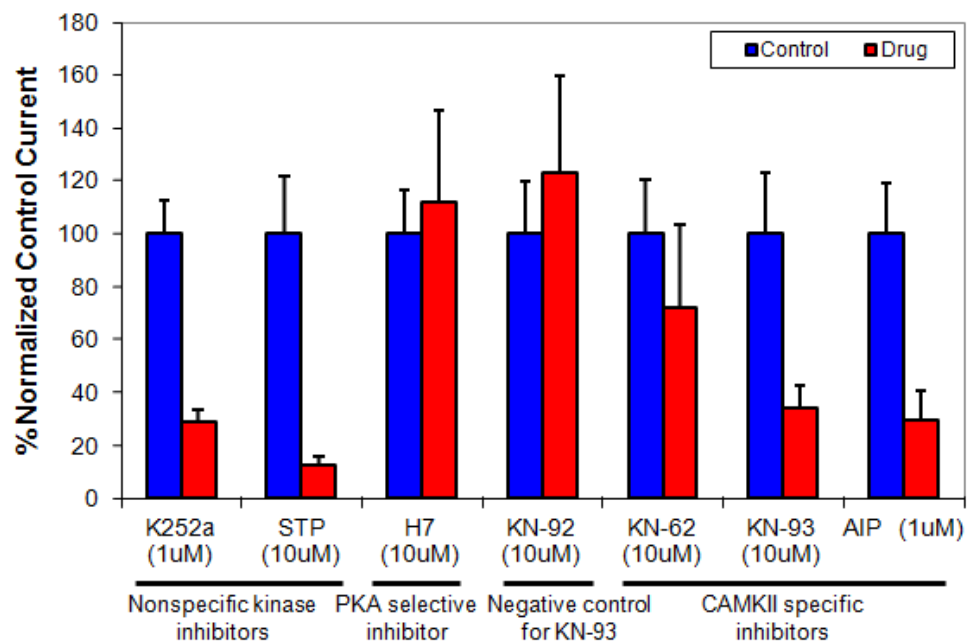


**Figure 4-6:** Comparison of the effects of various kinase inhibitors. Currents were measured at 100 mV 300-s after break-in. Data represent the percentage of the normalized control current. Error bars indicate  $\pm$  SEM. Asterisks denote currents that are significantly different from control currents.

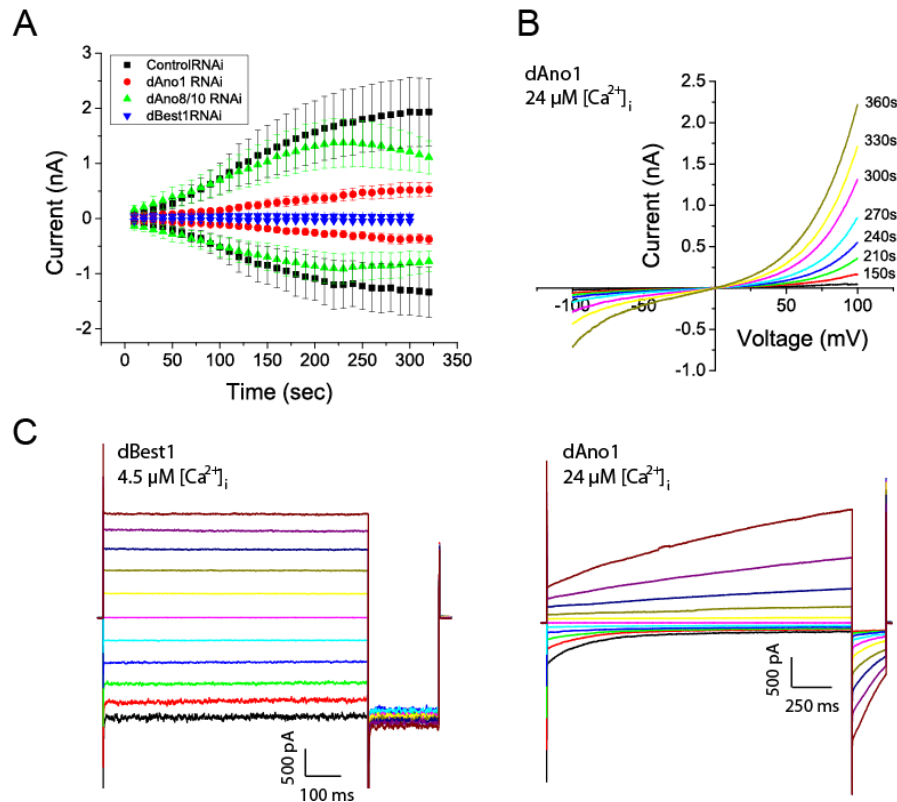


**Figure 4-7:** Contribution of *Drosophila* anoctamin orthologs to CaCC currents in S2 cells. **A)** Effect of siRNA knockdown of dTMEM16 orthologs or dBest1 in S2 cells on CaCC currents. Knockdown of dBest1 abolishes current, while siRNA against dAno1 significantly reduces, but does not abolish current. Treatment with control or dAno8/10 siRNA had no effect. Error bars indicate +/- SEM. **B)** Representative current traces of dAno1 expressed in HEK293 cells. Voltage ramps from -100 to +100mV were applied. **C)** Comparison of endogenous dBest1 current in S2 cells with dAno1 currents expressed in HEK293 cells using a step protocol from -100 mV to +100 mV in 20 mV intervals. dBest1 and dAno1 currents have distinct biophysical properties.

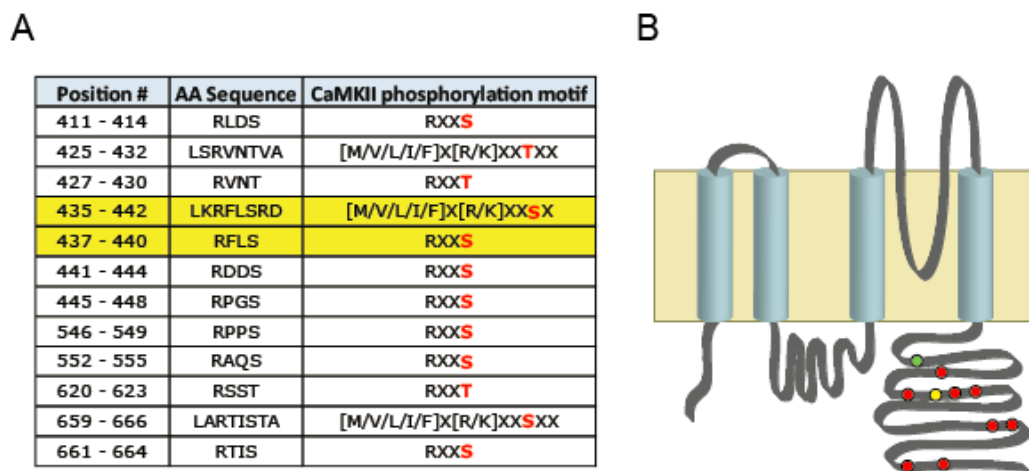


**Figure 4-8:** Potential CaMKII phosphorylation sites in dBest1 identified by Phosphomotif finder and Scansite. **A)** Table listing potential CaMKII phosphorylation sites within dBest1 (AAL29094.1). Sites identified by Phosphomotif finder are indicated in red. The phosphorylation site identified by both Phosphomotif finder and Scansite is highlighted in yellow. **B)** Topology model of dBest1 based on hBest1 (Tsunenari 2003) showing relative positions of predicted CaMKII phosphorylation sites. Sites identified by Phosphomotif finder are indicated by red circles. S440, which was identified by both programs, is indicated in yellow. S358, which is critical for regulation of hBest1 by PKC, is indicated in green.

**CHAPTER 5**

**ANOCTAMIN 1 MAY MEDIATE CACCS IN MOUSE RETINAL  
PIGMENT EPITHELIUM**

## Summary

Mutations in Best1 result in a form of macular degeneration called Best Vitelliform Macular Dystrophy (BVMD). The hallmark feature of BVMD is a deficit in the light peak (LP) of the electrooculogram (EOG). Therefore, identifying the protein that mediates the LP is critical for understanding the pathogenic mechanisms of BVMD. The LP is thought to be mediated by a basolateral  $\text{Ca}^{2+}$ -activated  $\text{Cl}^-$  channel (CaCC). The discovery that anoctamins mediate classical CaCCs in several tissues raises the possibility that anoctamins may contribute to the LP. Here we evaluate the suitability of various model systems for examining RPE CaCC electrophysiology. An inducible conditional Ano1 knockout mouse model is the most promising model for examining the contribution of Ano1 to RPE CaCCs. Whole cell patch clamp recordings suggest that Ano1 contributes to RPE CaCCs in mice, although future work is needed to determine the efficiency of Ano1 knockdown. Because Best1 mutants have previously been shown to inhibit WT Best1 currents, we also examined the effect of a Best1 mutant on Ano1 currents. Coexpression of Best1  $\Delta\text{I}295$  with Ano1 had no effect on Ano1 function. Although speculative at this point, Best1 could potentially regulate Ano1 currents through an indirect mechanism, such as modulation of intracellular  $\text{Ca}^{2+}$  signaling.

## Introduction

Best Vitelliform Macular Dystrophy (BVMD) is an autosomal dominant form of macular degeneration caused by mutations in the Best1 gene. The Best1 gene encodes for a Ca<sup>2+</sup>-activated Cl<sup>-</sup> channel (CaCC) expressed in the retinal pigment epithelium. Although there is heterogeneity in the clinical presentation of BVMD, patients share one common feature: a deficit in the light peak (LP) of the electrooculogram (EOG) (Blodi and Stone 1990; Cross and Bard 1974; Duran et al. 2010; Wajima et al. 1993). Because the LP is likely mediated by a CaCC expressed in RPE, it was originally hypothesized that Best1 mediated the LP, and that mutations in Best1 resulted in channel dysfunction (Sun et al. 2002). However, there is mounting evidence against the idea that Best1 mediates RPE CaCC currents. Best1 is indeed a CaCC, but it is not required for generating the LP, as Best1 KO mice display no deficits in the LP and have normal CaCC currents (L. Y. Marmorstein et al. 2006).

An alternative hypothesis is that Best1 serves as a modulator of the CaCC responsible for generating the LP. The identity of the Ca<sup>2+</sup>-dependent Cl<sup>-</sup> conductance in RPE is currently unknown. The recently discovered anoctamins are promising candidates for mediating RPE CaCCs. Anos 1 and 2 generate CaCC currents with biophysical properties similar to those in native epithelial tissues, and are critical for CaCC activity in various epithelia (Caputo et al. 2008; Schroeder et al. 2008; Y. D. Yang et al. 2008). Given the important role of anoctamins in other epithelia, anoctamins may play important roles in RPE physiology as well. Because the hallmark feature of bestrophinopathies is a reduction in the LP, identifying the molecular correlate of the LP will be an important first step for understanding the pathology and progression of bestrophinopathies.

## Results

### Model systems for studying RPE electrophysiology

The study of CaCC function has been hampered by the fact that there are no RPE cell lines available that express endogenous CaCCs (A. D. Marmorstein et al. 2000). Using cultured RPE cells is also troublesome because they quickly lose their differentiated phenotype and cease to express RPE markers such as bestrophin (Rak et al. 2006). We therefore set out to identify a model system in which to study CaCC function. First, we examined the electrophysiological properties of human induced pluripotent skin stem cell derived RPE. These cells recapitulate many of the morphological features of native RPE including pigmentation and apical microvilli (Li et al. 2012). In addition, they also express RPE specific markers such as Best1. Following digestion with TrypLE, hiPS RPE cells were plated on Matrigel coated coverslips and allowed to recover for at least 1 hr before recording. Based on whole cell patch clamp recordings, hiPS RPE cells fell into one of four categories electrophysiologically; these groups were morphologically indistinguishable. First, most cells exhibited a  $\text{Ca}^{2+}$ -independent current that was present at the time of break in (Figure 5-1A). The mean peak amplitude of this current at +100mV was  $1.8 \pm 0.26$  nA. In addition, replacement of extracellular  $\text{Cl}^-$  with a  $\text{NaSO}_4$  solution had no effect, indicating that this current was not carried by  $\text{Cl}^-$ . A second type of current was observed in 4/21 cells that was outwardly rectifying (Figure 5-1B). This current was not dependent on intracellular  $\text{Ca}^{2+}$ , and was present at the time of break in. The average current amplitude was  $509 \pm 110$  pA at +100mV. This current was carried by  $\text{Cl}^-$ , as replacement of extracellular  $\text{NaCl}$  with  $\text{NaSO}_4$  dramatically reduced current amplitude. In addition to these cells, there were cells that did not express any currents (Figure 5-1C). One cell expressed an outwardly

rectifying current that activated gradually over the course of 2 minutes; however, we were unable to determine if this current was carried by  $\text{Cl}^-$  because the patch was lost. Although hiPS RPE cells may be a useful tool for studying RPE physiology, they may not be ideal for whole-cell patch clamp recording due to the prevalence of the large  $\text{Ca}^{2+}$ -independent current present at break in, which may obscure other currents. Another issue is that trypsinization reportedly reduces Best1 protein expression (unpublished data). If Best1 is a regulator/mediator of CaCCs in RPE, the effect of enzymatic digestion of Best1 expression poses a serious caveat to interpreting electrophysiological data from these cells. Unfortunately, because these cells grow in tight clusters, enzymatic digestion is required to adequately dissociate hiPS RPE cells for patch clamp.

Next we examined the electrophysiological properties of human fetal RPE cells (hFRPE). hFRPE maintained in culture on Transwell filters form confluent monolayers that exhibit morphological and physiological characteristics of native RPE; they form tight junctions, have apical microvilli, are heavily pigmented, and express various RPE markers (Ablonczy et al. 2011; Maminishkis et al. 2006). After being maintained in culture for > 3 months on Transwell filters, hFRPE cells were enzymatically dissociated and used for whole cell patch clamp electrophysiology. No currents were detected in response to high intracellular  $\text{Ca}^{2+}$  (24 $\mu\text{M}$ ) (Figure 5-2A). Because enzymatic digestion could potentially digest membrane proteins critical for CaCCs, we recorded from hFRPE cells that were mechanically dissociated without the use of enzyme. Still, no CaCC currents were detected.

Lastly, we characterized CaCC currents in acutely-dissociated mouse RPE cells, which have previously been shown to express CaCCs (Zhang et al. 2010). In response to 1 $\mu\text{M}$  intracellular  $\text{Ca}^{2+}$ , dissociated mouse RPE cells exhibit an outwardly rectifying time dependent current (Figure 5-2A). The protein responsible for this conductance is

currently unknown, but studies in Best1 knockout mice indicate that this current is not mediated by Best1 (L. Y. Marmorstein et al. 2006). Recently it has been shown that members of the anoctamin family mediate native CaCCs in various epithelial tissues, raising the possibility that anoctamins may contribute to CaCCs in RPE (Caputo et al. 2008; Schroeder et al. 2008; Y. D. Yang et al. 2008). Expression of both Ano1 and Ano2 in HEK293 cells generates CaCC currents (Figure 5-2B). In contrast, Anos 3-10 do not generate currents and are localized intracellularly (Duran et al. 2012). It is therefore unlikely that Anos3-10 contribute to CaCCs in RPE. The biophysical properties of Ano1 closely resemble those of native CaCCs in mouse RPE. In response to  $1\mu\text{M}$  intracellular  $\text{Ca}^{2+}$ , Ano1 expression generates an outwardly rectifying  $\text{Cl}^-$  current that activates slowly. In addition, at  $1\mu\text{M}$   $\text{Ca}^{2+}$  both Ano1 and native mouse RPE CaCCs pass an inward current which slowly inactivates. Ano2 activates more rapidly than does the endogenous RPE CaCC, and displays little inward current at  $1\mu\text{M}$   $\text{Ca}^{2+}$ . Therefore, we hypothesize that Ano1 mediates CaCCs in mouse RPE.

### **Expression of anoctamins in mouse RPE**

To further examine the contribution of anoctamins to RPE CaCC currents, we examined RNA expression of Anos 1-10 in both hfrPE and mouse RPE using RT-PCR (Figure 5-3A). Primers used for RT-PCR are listed in Table 6-1. Anos 1, 2, 6, and 10 were detected in mouse RPE. hfrPE also expressed several anoctamin mRNAs, but unlike mouse RPE Ano1 mRNA was not detected. This result is consistent with the hypothesis that Ano1 mediates RPE CaCCs, as we were only able to record CaCC currents in cells isolated from mouse RPE but not hfrPE. Expression of Ano1 in mouse RPE was also detected at the protein level (Figure 5-3B). The specificity of a polyclonal antibody raised against amino acids 878–960 MSDF. . .GDAL of Ano1 was verified by both

overexpression and knockdown of Ano1. The Ano1 antibody detects a band at 137kDa which corresponds to Ano1. This band is absent in tissues from Ano1 knockout mice, and its intensity is reduced in heterozygous mice. In addition, this band is detected in HEK293 cells transfected with Ano1, but not in non-transfected cells. Using this antibody, we detected Ano1 protein in dissociated mouse RPE cells.

### **Generation of Ano1 inducible conditional knockout mice**

To determine if Ano1 expression is critical for CaCCs in mouse RPE, we generated an inducible RPE specific conditional Ano1 knockout mouse. Mice carrying the human vitelliform macular dystrophy-2 promoter ( $P_{VMD2}$ )-directed reverse tetracycline-dependent transactivator, and tetracycline-response element-directed cre were crossed with mice harboring loxP sites flanking exon 12 of Ano1 (Le et al. 2008) (Figure 5-4). Cre expression was induced by administering doxycycline in the drinking water of pregnant mice at embryonic day 17. RPE cells were isolated from mice between the ages of 1-3 months for electrophysiological recordings. Currents from Ano1 floxed mice were compared with those from Ano1 floxed-cre mice. Whole cell patch clamp recordings revealed that compared with control Ano1 floxed mice, conditional knockout mice showed a dramatic reduction in the number of cells expressing CaCC currents (Figure 5-4A). These results suggest that Ano1 is required for CaCCs in mouse RPE. Another important finding from patch clamp studies is that not all RPE cells from control mice express CaCC currents. In >80% of the cells, the currents were >400 pA in amplitude, but in 2 of 12 wild-type cells, the CaCC currents were small (< 200pA). Based on electrophysiology experiments, the expression level of CaCCs seems to vary widely across RPE cells, with current amplitudes ranging between 200pA to 2nA. Because RPE may be comprised of a heterogeneous population of cells, this raises questions about the

interpretation of the absence of currents in knockout mice. An alternative explanation for the differences observed between wild type and knockout mice is that by chance we selected RPE cells with lower levels of CaCC expression for Ano1 KO mice. More recordings are needed to verify the absence of CaCC currents in knockout mice. To quantify the efficiency of the knockout, we performed quantitative RT-PCR of Ano1. Paradoxically, there was no significant difference in Ano1 expression between Ano1 conditional knockout mice and Ano1 floxed mice (Figure 5-4B). There are several possible explanations for this result. First, contamination of the RPE prep with other cells expressing Ano1 could obscure changes in Ano1 expression. Alternatively, the heterogeneity of RPE cells coupled with the fact Best1 may be differentially expressed (Mullins et al. 2007) could mask the knockdown of Ano1. However, it is also possible that there is no change in Ano1 expression, and that the differences observed in CaCC current amplitude is due to chance selection of cells with reduced or absent CaCC expression.

### **Expression of Best1 mutants does not affect Ano1 channel function**

Mutations in Best1 cause BVMD, but the mechanism underlying the pathology of the disease is unclear. It was previously shown that Best1 mutants have a dominant negative effect on wild-type Best1 currents when coexpressed in HEK cells (Yu et al. 2007). While evidence suggests that Best1 itself does not mediate RPE CaCCs, mutant Best1 may negatively regulate the CaCC responsible for the LP. If Ano1 mediates RPE CaCCs, Best1 mutants could possibly inhibit Ano1 function, thus producing the CaCC deficit seen in BVMD. We coexpressed a Best1 construct harboring a common BVMD causing mutation,  $\Delta I295$ , with Ano1 to examine its effect on Ano1 current amplitude. Cells were transfected with empty pEGFP-N1 vector in order to visually identify

transfected cells. Using these constructs, co-expression of Best1 ( $\Delta I295$ ) with Ano1 resulted in a significant decrease in Ano1 current amplitude (Figure 5-5A). However, because we were not able to directly visually verify expression of Ano1 or Best1 ( $\Delta I295$ ), we repeated the experiment using different constructs. Ano1 was inserted into the PIRE5 II vector, which also expresses a fluorescent protein marker, and Best1 ( $\Delta I295$ ) was tagged on its C-terminus with mCherry. We found that using these constructs, co-expression of Ano1 with Best1 ( $\Delta I295$ ) had no effect on Ano1 current amplitude (Figure 5-5B). There are a couple of possibilities that could account for this discrepancy. First, differences in current amplitude could be an artifact caused by variability in Ano1 expression, because Ano1 expression could not be visually verified. Alternatively, tagging Best1 on its C-terminus could potentially disrupt its interaction with Ano1.

## **Discussion**

### **hiPS RPE are not amenable for whole cell patch-clamp electrophysiology**

Similar to dissociated mouse RPE, hiPS RPE appear to be a heterologous population of cells. While it is apparent that hiPS RPE cells are capable of ion transport, it is still unclear how well hiPS RPE cells recapitulate the electrophysiological properties of native RPE. The majority of recordings from hiPS RPE cells reveal a large  $Ca^{2+}$ -independent conductance that is present at the time of break in. This current is not carried by  $Cl^-$ , but the precise nature of the current is unknown. The prevalence of this current increased with recovery time following cell dissociation as cells became more confluent, indicating that this current may be due to the electrical coupling of cells (de Roos et al. 1996). Because this current may obscure other currents expressed in hiPS RPE, future patch clamp studies will require the development of methods for inhibiting

this current. In cells which lacked this current, we were able to identify a  $\text{Ca}^{2+}$  - independent outwardly rectifying  $\text{Cl}^-$  conductance. There were also cells which did not exhibit any currents in response to intracellular  $\text{Ca}^{2+}$  or voltage. One cell expressed an outwardly rectifying current which looked similar to endogenous CaCCs, but we were unable to determine if this current was  $\text{Ca}^{2+}$  dependent and if it was carried by  $\text{Cl}^-$ . Although more work is needed to fully characterize the electrophysiological profile of hiPS cells, technical limitations of using hiPS RPE cells for patch clamp make this model undesirable. The most problematic limitation is that hiPS RPE cells do not grow as single cells, but as tightly coupled clusters. In order to perform whole-cell patch clamp, hiPS cells must be enzymatically digested to acquire a sufficient yield of single cells for recording; however, enzymatic digestion reportedly abolishes Best1 protein expression (unpublished data), suggesting that freshly dissociated cells have phenotypic differences from established cells. Unfortunately, cells must be used for patch clamp studies within 24 hrs following dissociation because they quickly form cell-cell contacts. Therefore, these cells may be better suited for Ussing chamber recordings, in which it is possible to study the electrophysiological properties of confluent monolayers.

### **Whole cell recordings do not detect CaCCs in hFRPE cells**

Several electrophysiological studies have demonstrated that RPE from various sources, including hFRPE, *Xenopus* oocytes, chick embryo, and toad possess a basolateral  $\text{Cl}^-$  conductance (Fujii et al. 1992; Gallemore and Steinberg 1993; H. C. Hartzell and Qu 2003; Kuntz et al. 1994; Quinn and Miller 1992). In hFRPE monolayers specifically, this basolateral  $\text{Cl}^-$  conductance was shown to be dependent on intracellular  $\text{Ca}^{2+}$  (Quinn et al. 2001). Therefore, it was surprising that we did not detect any CaCC currents in dissociated hFRPE cells. However, the hFRPE cells used for this study were maintained

in culture and dissociated before recording, which could result in an altered electrophysiological phenotype relative to intact RPE tissue. To ensure that enzymatic treatment did not digest membrane proteins critical for CaCC function, these experiments were repeated using mechanical dissociation in the absence of enzyme. Regardless of dissociation technique, hFRPE cells did not exhibit CaCCs. Because most electrophysiological studies examining CaCC currents have been conducted using intact RPE preparations or confluent RPE monolayers, one possibility is that dissociation disrupts CaCC function. However, CaCC currents have been observed in enzymatically dissociated cells from both *Xenopus* (H. C. Hartzell and Qu 2003) and murine RPE. The intracellular  $\text{Ca}^{2+}$  concentration used here ( $24\mu\text{M}$ ) is in excess of what is required to evoke measureable CaCC currents in *Xenopus* or murine RPE. Furthermore, RT-PCR demonstrates that hFRPE does not express *Ano1*, which is currently the most likely candidate for mediating CaCCs in mice. Therefore, we suggest that the lack of CaCC currents in hFRPE cells is due to phenotypic changes resulting from culture conditions. Alternatively, the age at which we used the hFRPE cells for electrophysiology experiments could potentially affect the expression of CaCC currents, but this has not yet been experimentally determined.

### **Suitability of mouse models for studying BVMD**

Here we use a mouse model to examine the electrophysiological properties of the RPE. While this model is useful, there are certain limitations. First, while mice are widely used as models for human eye disease, it is important to realize that mice do not possess a macula. Because the mouse retina is predominantly comprised of rod photoreceptors, it is more akin to the peripheral retina in human. Therefore, applicability of mouse retina as a model system for human macular disease should be

viewed with caution. Even so, RPE defects that are not restricted to the macula can be modeled in mice as evidenced by the W93C knock-in mice (Zhang et al. 2010). While these mice do not fully recapitulate the BVMD phenotype, they do manifest changes in the panretinal abnormalities such as the LP deficit and lipofuscin accumulation.

Another important consideration is that mice do not exhibit a Best1 null phenotype, which is represented by autosomal recessive bestrophinopathy in humans. This may indicate species specific differences in the function of Best1; however, the lack of ocular pathology in Best1 knockout mice could also be due to compensatory mechanisms. In light of the fact that there are currently no organisms that are amenable to genetic manipulation that have an anatomic macula, we conclude that a mouse model is the most suitable model for examining the electrophysiological deficits present in BVMD. Here we use an inducible conditional RPE knockout model, thereby circumventing the problem of developmental compensation.

Electrophysiology data from *Ano1* conditional knockout mice indicate that *Ano1* is necessary for normal CaCC currents in RPE. The majority of RPE cells isolated from *Ano1* floxed mice elicited CaCC currents in response to  $1\mu\text{M Ca}^{2+}$ . In contrast, CaCC currents were not observed in RPE cells from *Ano1* conditional knockout mice.

However, because RPE from *Ano1* floxed mice show variation in CaCC expression levels these results must be taken with caution. An alternative explanation is that by chance we recorded from more RPE cells with lower expression levels of CaCCs in the conditional knockout mice than the floxed mice. We are currently breeding more mice for patch clamp experiments to increase the number of recordings and ensure the significance of these results. Another concern of this study is that qRT-PCR did not show a difference in *Ano1* expression across *Ano1* floxed and *Ano1* conditional knockout mice. There are several possible explanations for this inconsistency. First, we isolated RPE cells from eye

cups using a combination of enzymatic and mechanical methods. Although the majority of cells in this preparation are RPE cells, there may be some contamination with other cell types that express Ano1. Photoreceptors, for example, express Ano1 (Y. D. Yang et al. 2008). Contamination with other cell types is not an issue for electrophysiology experiments, because single cells are morphologically identified as RPE cells before they are patched. However, this poses a problem for qRT-PCR experiments in which RNA is extracted from a heterologous population of cells. As previously mentioned, RPE cells themselves appear to be a heterologous population. Electrophysiology studies demonstrate that CaCC expression is variable across RPE cells, and that some RPE cells do not express CaCCs. Additional variability may be introduced because knockdown of Ano1 in our mouse model is contingent on the level of inducible cre expression, which is under the control of the Best1 promoter. Previous studies demonstrate that, at least in humans, Best1 is differentially expressed across RPE cells (Mullins et al. 2007).

Given these caveats, it is possible that differences in Ano1 expression across Ano1 floxed and conditional knockout mice are obscured by these confounding variables. Therefore, we are currently developing a protocol for performing RT-PCR from single RPE cells. By using a low resistance pipette tip, individual RPE cells can be manually selected following enzymatic digestion for RT-PCR analysis. This selection method is more consistent with that used for the patch clamp studies. Performing RT-PCR using this isolation method may yield results that are more congruous with CaCC expression changes observed with patch clamp electrophysiology. Although there are several limitations to using the inducible conditional knockout mice, they are currently the best available model for studying Ano1 function in RPE. In the future, an alternative would be to cross our mice with mice harboring a Rosa-GFP locus that is activated by cre. This method would allow us to identify cre positive cells for patch clamp analysis and qRT-

PCR, and circumvent the question of dox-induced efficiency of cre expression and gene knock-down.

### **Does mBest1 regulate Ano1 channel function, and if so, how?**

Because Best1 mutants inhibit wild-type Best1 currents, we sought to determine if mutant Best1 co-expression could also regulate Ano1 function. We tested the effect of the  $\Delta I295$  mutation, which is a common dominant negative mutation found in BVMD patients usually associated with a reduced LP (F. Kramer et al. 2000; Marquardt et al. 1998; Wabbels et al. 2006). The inhibitory effect of the  $\Delta I295$  mutation on Ano1 current amplitude was dependent on the constructs used for co-expression. Co-expression with the myc-tagged Best1 construct significantly decreased Ano1 current amplitude, while cherry-tagged Best1 construct had no effect. One possible explanation for this discrepancy is that the C-terminal cherry tag on Best1 interferes with its interaction with Ano1. Alternatively, the inhibitory effects seen in experiments performed without cherry tagged Best1 could be due to variability in Ano1 expression. Because transfected cells were identified based on EGFP expression, we cannot be certain that all cells patched were expressing Ano1. While these results are inconclusive, results from Best1 W93C mutant knock-in mice support an indirect mechanism for CaCC regulation by Best1. Whole cell patch clamp recordings demonstrate that RPE isolated from W93C mice possess normal CaCCs (Zhang et al. 2010). Furthermore, while some Best1 is expressed on the basolateral membrane of RPE, a significant portion of Best1 is localized intracellularly where it influences  $Ca^{2+}$  uptake into  $Ca^{2+}$  stores (Barro-Soria et al. 2010; Strauss et al. 2012). As an intracellular anion channel, Best1 may serve as a regulator of  $Ca^{2+}$  homeostasis, thereby indirectly affecting the function of plasma membrane CaCCs.

### **The mechanism of BVMD is still unknown**

Evidence suggests that the LP deficit is secondary to the hBest1 Cl<sup>-</sup> channel defect, but the mechanism of BVMD is still unknown. It is clear that there are other genetic or environmental factors involved in the progression of BVMD that have yet to be identified. First, patients harboring the same mutations can have varying degrees of vision loss (23). In addition, vision loss is rarely symmetric, and there are no predictive criteria for the loss of visual acuity (Deutman 1969). With few exceptions, the vast majority of Best patients exhibit a reduced LP. Therefore, conclusively identifying the protein responsible for generating the LP will be critical for understanding the progression of BVMD. While our results are preliminary, this study indicates that Ano1 may be involved in mediating RPE CaCCs.

Best1 mutations could potentially result in a diminished LP by regulating Ano1 function via an indirect mechanism. One possible scenario is that Best1 alters Ano1 currents by regulating Ca<sup>2+</sup> signaling. The observation that voltage-dependent Ca<sup>2+</sup> channels (VDCCs) are required to generate the LP (L. Y. Marmorstein et al. 2006), and that Best1 can modulate voltage gated Ca<sup>2+</sup> channels raises the possibility that Best1 affects the LP via its action on VDCCs (Yu et al. 2008). However, it is still unclear how VDCCs are activated in RPE, and if they are responsible for activating basolateral CaCCs. Another way in which Best1 could alter Ca<sup>2+</sup> signaling is by modulating Ca<sup>2+</sup> recruitment from intracellular stores. RPE from Best1 deficient mice do in fact exhibit higher levels of resting [Ca<sup>2+</sup>]<sub>i</sub> than wild-type mice. In addition, ATP stimulated [Ca<sup>2+</sup>]<sub>i</sub> increases rose faster and decayed slower in RPE from Best1 deficient mice. Best1 is expressed in the ER of airway epithelia where it is important for ER Ca<sup>2+</sup> handling (Barro-Soria et al. 2010). In cultured mouse RPE cells, Best1 deficient mice display higher levels of resting Ca<sup>2+</sup> than WT mice (Neussert et al. 2010). Therefore, Best1 may function as an ER protein

which serves as a counterion channel for  $\text{Ca}^{2+}$  release and reuptake. In this manner, Best1 could affect the activation and regulation of Ano1 currents.

Once we have determined the efficiency of Ano1 knockdown in our inducible conditional knockout model, future studies will be aimed at examining LP deficits in knockout mice and morphological analysis of RPE from wild-type versus Ano1 knockout mice. Although there may be species specific differences in the function of Best1 in mouse RPE versus human RPE, the Best1 W93C knock-in mice indicate that there is some functional overlap in the mechanisms contributing to BVMD. Therefore, studies using the Ano1 inducible conditional knockout model will likely provide important information regarding the function of Ano1 in RPE, and the role of CaCCs in the pathology of BVMD.

## **Materials and Methods**

**Cell culture and transfection.** HEK293 cells were cultured in DMEM supplemented with 10% fetal bovine serum and 0.5% penicillin-streptomycin at 37°C. hRPE cells grown on Transwell filters were provided by Alan Marmorstein. hiPS derived RPE cells grown on fibroblast feeder cells were provided by Stephen Tsang. Both hRPE and hiPS derived RPE were maintained in specially formulated MEM as previously described (Miller 2006). For electrophysiology, low-passage HEK293 cells were transfected using Fugene 6 with 1  $\mu\text{g}$  of green fluorescent protein (GFP)-tagged Ano1 or Ano2 constructs. For co-transfection of Ano1 with Best1 mutant constructs, 0.6  $\mu\text{g}$  of each construct were used. Transfected cells were then plated at low density and used for electrophysiology 24–48 hrs after transfection. Cells expressing fluorescent proteins were patched. For hiPS RPE electrophysiology experiments, cells were treated with TrypLE for 4-5 minutes

and plated on coverslips coated with Matrigel at a 1:10 dilution. Cells were used for electrophysiology between 1-36hrs after plating.

**Electrophysiology.** Recordings were performed using the whole cell patch clamp configuration. Patch pipettes were fire polished to final resistances of 2–4 M $\Omega$ . Data were acquired by an Axopatch 200A amplifier controlled by Clampex 8.2 via a Digidata 1322A data acquisition system (Molecular Devices). Voltage ramps of 200 ms from –100 to +100 mV were applied at 10-s intervals, followed by a voltage-step protocol from –100 to +100 mV in 20-mV intervals applied every 10 s. Data were analyzed using ClampFit 8.2 software (Molecular Devices).

#### **Solutions for electrophysiology.**

The high Ca<sup>2+</sup> (24  $\mu$ M free Ca<sup>2+</sup>) intracellular pipette solution contained (in mM) 146 CsCl, 2 MgCl<sub>2</sub>, 5 Ca-EGTA, 10 sucrose, and 8 HEPES, pH 7.3 with NMDG. A final [Ca<sup>2+</sup>] of 1  $\mu$ M free Ca<sup>2+</sup> was made by mixing the high Ca<sup>2+</sup> solution with a Ca<sup>2+</sup>-free solution containing 5 mM EGTA in a 9:1 ratio, as described previously (Kuruma and Hartzell 2000). The extracellular solution contained (in mM) 140 NaCl, 5 KCl, 2 CaCl<sub>2</sub>, 1 MgCl<sub>2</sub>, 15 glucose, and 10 HEPES, pH 7.4 with NaOH. Osmolarity was adjusted with sucrose to 303 mOsm for all solutions.

#### **RPE Isolation**

Mouse eyes were enucleated and the cornea, lens, and retina were removed. The remaining posterior eyecups were incubated at 37C for 10 min in a solution containing (in mM) 135 NMDG-Cl, 5 KCl, 10 glucose, 3 EDTA, 3 L-cysteine, 10 HEPES, 1 MgCl<sub>2</sub>, 1.8 CaCl<sub>2</sub>, and 4U/mL papain, pH 7.4 w/ HCl. Following enzymatic digest, posterior eye

cups were rinsed with Ringer solution. RPE cells were dissociated by gently pipetting. Large debris was removed, and cells were spun down for 5 min at 3K rpm. Cells were resuspended in RPE media and plated on glass coverslips for recording. Cells were recorded from 30min-1hr after plating.

### **RT-PCR**

Total RNA was purified from isolated mouse RPE cells or human fetal RPE cells using the Purelink Mini Kit system according to the manufacturers protocol (Invitrogen). cDNA synthesis was performed using the Superscript III One-Step RT-PCR kit (Invitrogen). First Strand Synthesis kit (Invitrogen). Primers used are listed in Table 6-1. For quantitative RT-PCR, cDNA synthesis was performed using the Superscript III First Strand Synthesis kit according to the manufacturers protocol (Invitrogen). cDNA samples were diluted 1:10 for qPCR analysis. qPCR was performed using the LightCycler real-time thermocycler (Roche). qPCR of each cDNA sample was performed in triplicate. The primer pair used to detect Anol1 expression is as follows: Forward: 5'-ACAAGACCTGCAGCTACTGGAAGA-3'; Reverse: 5'-AGAAGACGGTGGCAGGGTTATCAA-3'. Optimized amplification conditions were 4mM MgCl<sub>2</sub>, annealing at 55 °C, and extension at 72 °C. Relative arbitrary fluorescent units were determined from standard curves.

### **Immunoblot**

Tissues or cells were homogenized in lysis buffer containing 1% Triton X-100, 1 mM EDTA, 50 mM Tris·HCl (pH 7.4), and protease inhibitor cocktail III (Calbiochem) plus 10 μM phenylmethylsulfonyl chloride. Samples were diluted in SDS Laemmli buffer, and aliquots were run on 7.5% reducing SDS-PAGE and transferred to nitrocellulose. ANO1

antibody was used at a 1:1,000 dilution and detected by enhanced chemiluminescence (Super Signal, Thermo Scientific).

### **Doxycycline treatment of Ano1 inducible conditional knockout mice**

Inducible RPE specific cre mice (Le et al. 2008) were graciously provided by Joseph Besharse. These mice were crossed with Ano1 floxed mice, which were provided by Jason Rock. Best1 driven rtTA-cre pregnant mothers were given doxycycline in drinking water *ad libitum* at developmental day E17 until the birth of pups. The doxycycline solution contained 1mg/mL doxycycline (Sigma-Aldrich) and 5% sucrose.

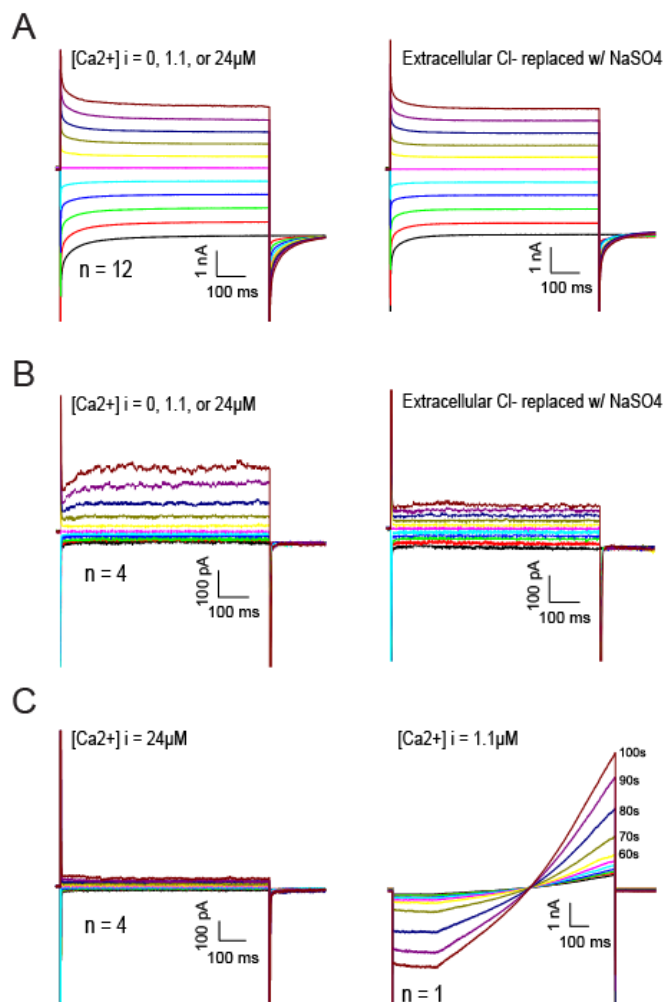


**Figure 5-1.** Representative whole cell recordings from hiPS RPE cells. **A)** 12 out of 21 cells expressed a Ca<sup>2+</sup>-independent current that was not carried by Cl<sup>-</sup>, as evidenced by replacement of extracellular NaCl<sup>-</sup> with NaSO<sub>4</sub>. **B)** Some cells expressed an outwardly rectifying Ca<sup>2+</sup>-independent current that was inhibited by replacing extracellular Cl<sup>-</sup> with NaSO<sub>4</sub>, while others **C)** expressed no currents. One cell expressed an outwardly rectifying current that activated gradually over the course of 2 minutes. All current traces were acquired using a voltage step protocol from -100mV to +100mV, with the exception of the outwardly rectifying current shown in C, which was acquired using a ramp protocol from -100mV to 100mV applied every 10 seconds.

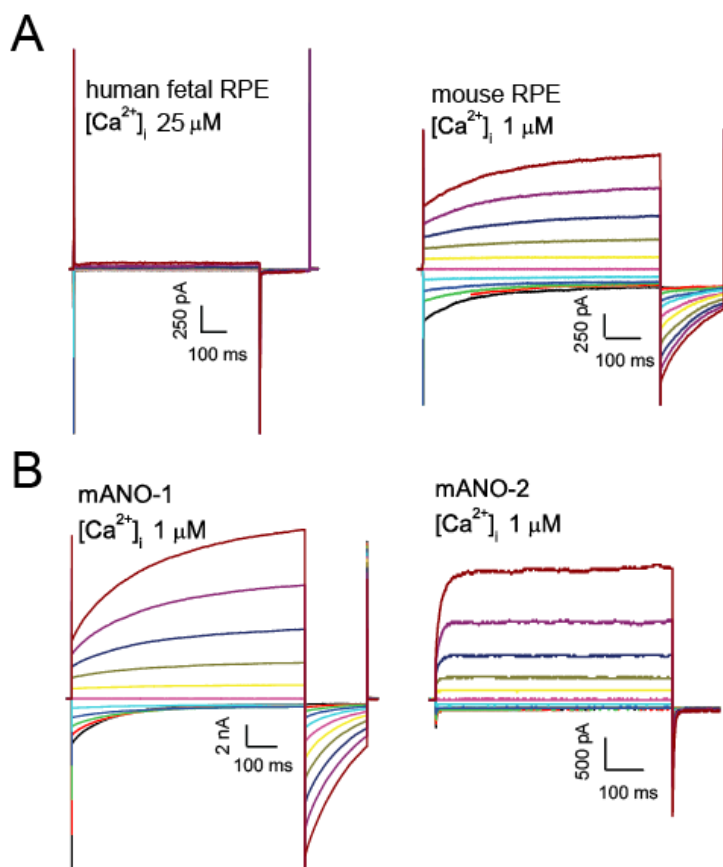


**Figure 5-2:** Representative whole cell patch clamp recordings of CaCCs in response to voltage steps from  $-100mV$  to  $+100mV$ . **A)** Human fetal RPE cells do not generate CaCCs in response to  $25\mu M$   $[Ca^{2+}]_i$ , ( $n=7$ ) while isolated mouse RPE cells display an outwardly rectifying CaCC in response to  $1\mu M$   $[Ca^{2+}]_i$ . **B)** Current traces of mAno1 or mAno2 expressed in HEK293 cells in response to  $1\mu M$   $[Ca^{2+}]_i$ .

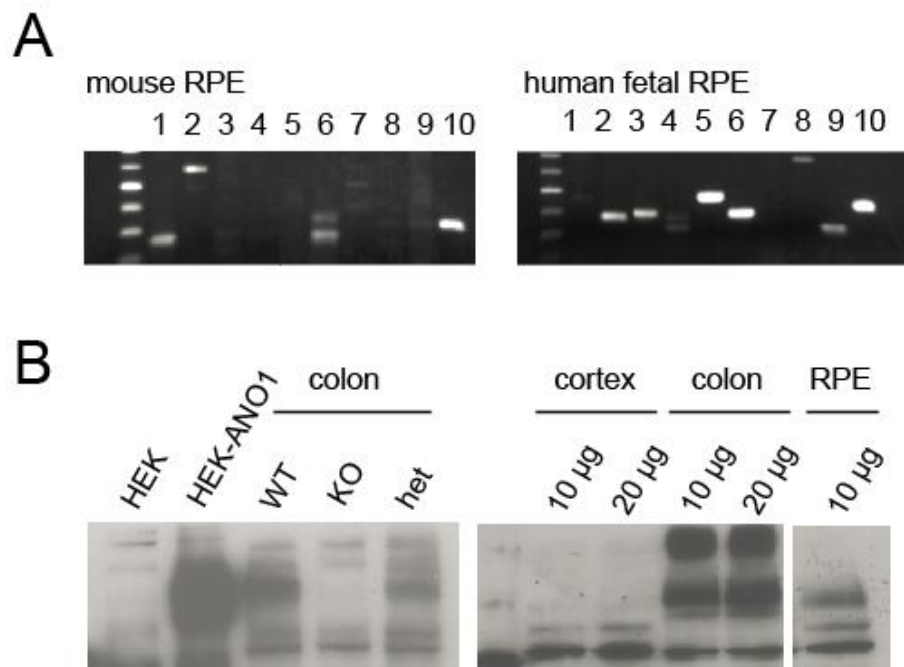


**Figure 5-3:** Expression of anoctamins in RPE. **A)** Expression of anoctamins in mouse and human fetal RPE cells as determined by RT-PCR. **B)** Immunoblot demonstrating the specificity of the Ano1 antibody, and detection of Ano1 protein in mouse RPE.

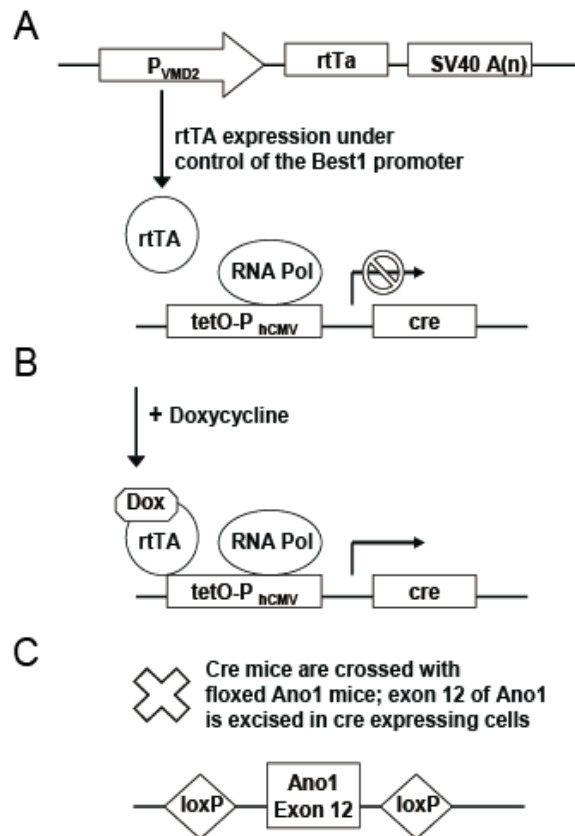


**Figure 5-4:** Tetracycline-inducible knockout of Ano1 in RPE (Le et al. 2008). **A)** Tet-dependent transactivator (rtTA) expression is under the control of the VMD2 (Best1) promoter. In the absence of tetracycline, rtTA does not bind the tetO operator. **B)** In the presence of doxycycline (a tetracycline derivative), rtTA binds the tetO operator, thus promoting cre expression. **C)** RPE specific tet-inducible cre mice are crossed with mice harboring loxP sites flanking exon 12 of Ano1. Administration of doxycycline results in RPE specific knockdown of Ano1.

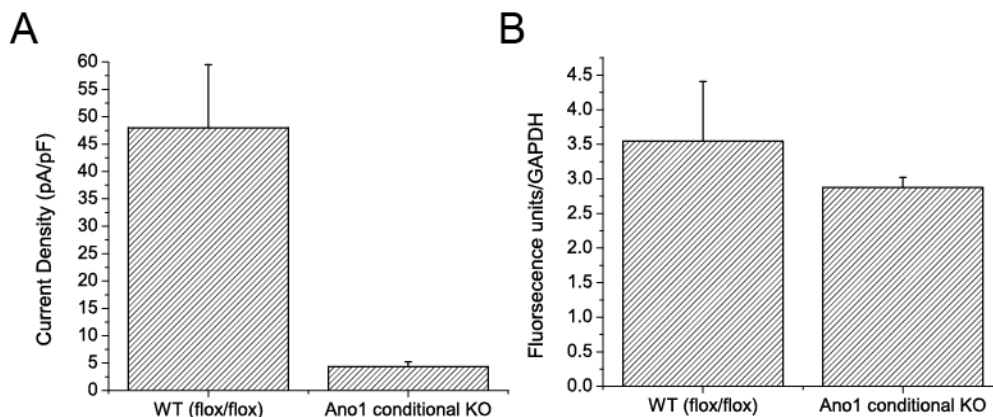


**Figure 5-5:** Ano1 expression in RPE from wild-type mice versus Ano1 conditional knockout mice. **A)** Maximum current amplitude at +100mV of CaCCs recorded from wild-type (n = 12) or Ano1 knockout mice (n = 6) in response to  $1\mu\text{M}$   $[\text{Ca}^{2+}]_i$ . **B)** Quantitative RT-PCR showing expression of Ano1 in RPE from wild-type or Ano1 knockout mice mouse. Fluorescence units are arbitrary, and normalized to GAPDH expression. qRT-PCR was performed on RPE cells isolated from 3 mice for each condition, and run in triplicate for each sample. Data is presented as mean  $\pm$  SEM.

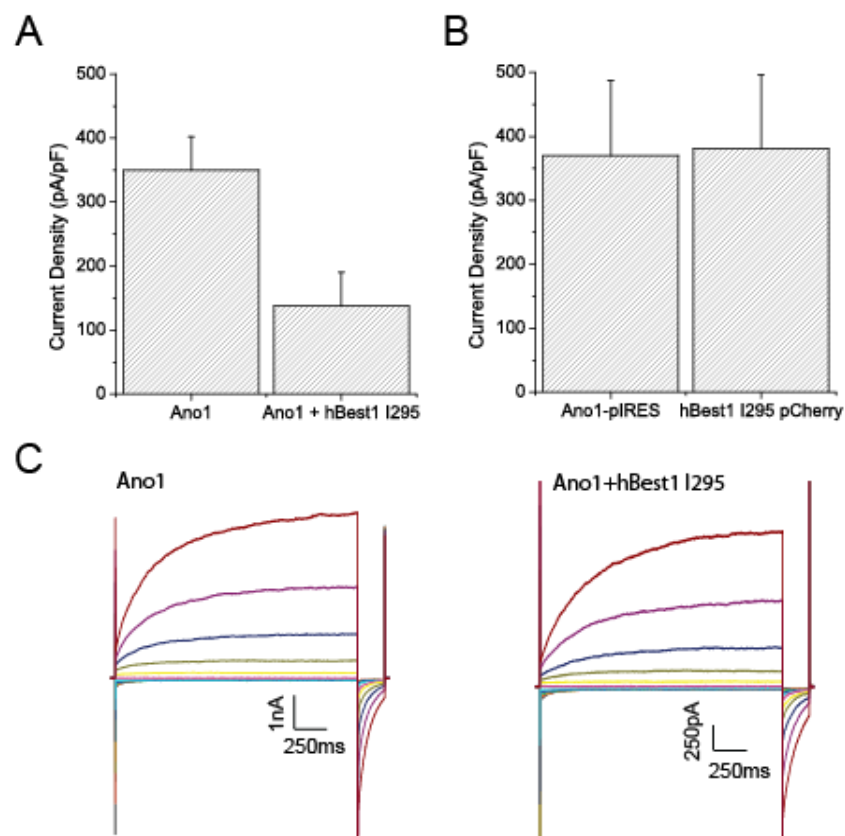


**Figure 5-6:** Co-expression of Ano1 with Best1  $\Delta$ I295. **A)** Average current density of CaCC currents recorded from HEK293 cells transfected with Ano1 alone or Ano1 co-expressed with the  $\Delta$ I295 Best1 mutant. **B)** Average current density of CaCC currents recorded from HEK293 cells transfected with an Ano1 construct with reduced expression, or co-expressed with Best1  $\Delta$ I295-cherry. Error bars represent  $\pm$  SEM. **C)** Representative current traces from HEK293 cells expressing Ano1 only, or both Ano1 and Best1  $\Delta$ I295.

Mouse Primer Pairs	
ANO1	ATGAGGGTCCCCGAGAA; TTGTAGTCCCCTCCTGGCCG
ANO2	CCACTACCGGAAACGAGG; GTTGTTGGCTCGAGAACAG
ANO3	ATGGTCCACCACTCAGGCT; GAGTCCTTTCTACTCTCCTCCG
ANO4	ATGGGTTTTCTTCTCGACTGG; GGGATTGTTGAAGAAAGTGTCT
ANO5	ATGGTGGAGCAGGAAGGC; TCTGCCTTCAGCTCTCCATC
ANO6	ATGCAGATGATGACTAGGAAGG; GTCCCTTTCTTATTGTTCTCCTTT
ANO7	GGGGGCAAGCGCGAGAAGAA; TGCAGCGGCCTCATCCTGGA
ANO8	CGGCGCCTGCGTCTGGAGTACTGGA; TTCCGGCCTTGCGCAGACCCA
ANO9	CACCTTTGAGGACCTGGTG; CCTCTTCCTCATCCCATTC
ANO10	ATGAGAGTGACTTTATCAACGCTG; AAGTTGTGGCGTGTTCATAG
Human Primer Pairs	
ANO1	GCGTCCACATCATCAACATC; ATCCTCGTGGTAGTCCATCG
ANO2	TGCCTACCACTACCGGAAAC; ACTTCTTTGCAATGCTGCCT
ANO3	AAACCTGAACCACATCAGCC; TCTTCCCAAAAAGAAAGCGA
ANO4	CATGGGAAGTCCTTGGGAAGA; GCCATTGGTAAGCAAACGAT
ANO5	ACACTTCACCAGAATTGGGC; GAAGCTGCTGTTCTCT
ANO6	CAGTTTGGGTTTCGTCACCTT; AGTACGGGTTTCCCTTGCTT
ANO7	CTACTCCTGCCGTTTCAGAG; GTTCCTGCGTGGGTATGTCT
ANO8	ACTTCGCTCTGCTCCTCAAG; CTCATGACGTTGTTGGGTG
ANO9	TGGAGATCAGCACCTGTGAG; CGAAGTTCACGATTCGGATT
ANO10	GAGGTGCCCAGTTGTTGTTT; CCGAGTGTACCAGGTGTCCT

**Table 5-1:** RT-PCR primer pairs for mouse and human anoctamins

**CHAPTER 6**

**CONCLUSIONS AND IMPLICATIONS**

## Overview

Although the vital roles of CaCCs in various physiological processes are well documented, the controversy surrounding the molecular identity of “classical” CaCCs has for many years plagued the field of CaCC research. When I began my thesis work, bestrophins represented the most promising molecular candidates for mediating the “classical” CaCCs observed in epithelial tissues. In August of 2008, however, it was reported that Ano1 more closely resembled these endogenous CaCCs, and that its expression was required for CaCCs in salivary gland epithelial cells (Caputo et al. 2008; Schroeder et al. 2008; Y. D. Yang et al. 2008). This discovery necessitated reassessment of the relative contribution of bestrophins and anoctamins to native CaCC currents. The work presented here furthers our understanding of CaCC physiology by using multi-disciplinary approaches to examine anoctamin structure, function, and localization; in addition, this work highlights the discrete, but important roles of anoctamins and bestrophins in physiology, and regulatory mechanisms governing endogenous CaCC function. The primary findings of this work are as follows:

- 1) Anos 1& 2 function as plasma membrane CaCCs, while Anos 3-7 likely have intracellular roles
- 2) Residues within the sixth transmembrane domain of Ano1 are indispensable for its channel function
- 3) Endogenous *Drosophila* CaCCs are regulated via a CaMKII dependent mechanism
- 4) Ano1 may play a role in the pathophysiology of BVMD as a mediator of the light peak

In this chapter I will summarize the findings of this dissertation and discuss their significance for understanding of anoctamin function and CaCC physiology. I will then

discuss the implications of these results for outstanding questions regarding CaCC function and physiology, potential caveats to these results, and future directions.

### **Summary and Significance**

Data presented in Chapter 2 demonstrate that heterologous expression of An<sub>o1/2</sub> generates Ca<sup>2+</sup>-dependent Cl<sup>-</sup> currents, while expression of An<sub>os</sub> 3-7 does not. Using a combination of patch clamp electrophysiology and confocal microscopy, I show for the first time that An<sub>os</sub> 3-7 do not generate current because they are not trafficked to the plasma membrane. Various chimeras between An<sub>o1</sub> and An<sub>o5/7</sub> also do not traffic to the plasma membrane, indicating that An<sub>o5/7</sub> may have significant structural or functional differences from An<sub>o1</sub>. Using immunohistochemistry I demonstrate that endogenously expressed An<sub>o7</sub> is localized intracellularly, which further supports an intracellular role for anoctamins.

The work in Chapter 3 furthers our understanding of the mechanisms underlying An<sub>o1</sub> channel function by identifying regions critical for its channel activity. Notably, this work identifies residues adjacent to the sixth transmembrane domain, E702 and E705, which are required for Ca<sup>2+</sup> sensitivity of An<sub>o1</sub>. Epitope tag insertion accessibility demonstrates that these residues are localized intracellularly, indicating that they may directly participate in Ca<sup>2+</sup> binding. A nearby mutation within the sixth transmembrane domain, T714V, was found to affect the voltage dependent gating of An<sub>o1</sub>. Because the residues examined here are highly conserved across the anoctamin family, these studies lay the groundwork for future experiments examining the channel function of other anoctamin family members.

In Chapter 4 I explore the regulatory mechanisms governing the function of endogenous *Drosophila* Best1 (dBest1) in S2 cells. In this study I demonstrate that

dBest1 activation by intracellular  $\text{Ca}^{2+}$  is regulated by phosphorylation via a CaMKII dependent mechanism. dBest1 current activation is more rapid in the presence of intracellular ATP, and treatment with CaMKII specific kinase inhibitors significantly reduces dBest1 current amplitude. The majority of studies on Best1 channel function have been conducted in heterologous over-expression systems. Because Best1 function has been shown to differ depending on the expression system, studying its regulation in endogenous systems is critical to understanding its physiological roles in retinal diseases. The results of this study provide evidence for a regulatory mechanism for endogenous Best1 involving CaMKII and protein phosphorylation.

In Chapter 5, I evaluate the usefulness of various models for studying CaCC function in the retinal pigment epithelium. I demonstrate that a conditional inducible knockout mouse model is a suitable model for examining RPE electrophysiology. Preliminary studies with these mice indicate that Ano1 may be the molecular correlate of the CaCC current observed in isolated mouse RPE, as knockout mice exhibit a deficit in CaCCs. Because bestrophinopathies usually present with deficits in the light peak, identifying the channel responsible for generating the light peak will be instrumental to understanding these macular dystrophies. Here I have developed a promising method to identify the molecular correlate of the endogenous RPE CaCC.

### **What is the function and subcellular localization of Anos 3-10?**

While significant progress has been made over the past several years in understanding the function of Ano1 and Ano2, there is relatively little known regarding the function of other anoctamin family members. Four years after the discovery of the anoctamin family, with the exception of Ano6, it is still unknown if Anos 3-10 definitively function as channels. There are conflicting reports on their plasma membrane

localization and channel function of anoctamins expressed in heterologous expression systems (Duran et al. 2012; Tian et al. 2012); it could be that membrane trafficking of anoctamins is dependent on the system in which they are expressed. Currently, the endogenous localization of anoctamins is only known for Ano1, 2, 5, and 7. Anos 1 and 2 are clearly plasma membrane proteins (Mercer et al. 2011; Y. D. Yang et al. 2008). A small portion of Ano5 co-fractionates with plasma membrane markers, but it appears to be predominantly intracellular (Mizuta et al. 2007). Here I examined the endogenous localization of Ano7 in human prostate using confocal microscopy (Duran et al. 2012). Ano7 was primarily intracellular, but the specific subcellular compartments in which it was localized were not determined. Having demonstrated the specificity of the Ano7 antibody for immunoblot, future experiments involving subcellular fractionation of human prostate tissue to more closely examine the subcellular localization of Ano7 are possible. Identifying the subcellular compartments in which other anoctamins reside will be vital to understanding their physiological roles, but will have to await the development of suitable antibodies.

Anoctamins that are exclusively intracellular will be more difficult to study using electrophysiological methods. Although some intracellular transporters will traffic to the plasma membrane when overexpressed in a heterologous system (Picollo and Pusch 2005; Scheel et al. 2005), I have shown that this is not true for Anos 3-7 expressed in various cell lines including HEK293, CHO, COS-7, and HeLa. Furthermore, using a chimeric approach to identify regions critical for plasma membrane expression of anoctamins is not feasible. There are alternative methods, albeit technically demanding ones, which may be useful for studying intracellular anoctamin function. First, reconstitution of purified protein into lipid bilayers has traditionally been used to examine the channel function of intracellular membrane proteins (Lai et al. 1988;

Tomlins and Williams 1986). Purification of membrane proteins presents its own unique set of challenges, but a recently developed method for purifying FLAG-tagged Ano1 may be applicable to other anoctamins (Perez-Cornejo et al. 2012). Another recently described method that could potentially be used to examine the channel function of intracellular anoctamins is patch clamp recording from plant cell central vacuoles (Costa et al. 2012). This novel method was successfully used to study the function of ClC-7, an intracellular Cl<sup>-</sup> transporter. Transient transfection of mesophyll protoplasts resulted in the incorporation of functional ClC-7 into the vacuolar membrane. Due to the large size and ease of isolation of the central vacuole, this system is ideal for patch clamp studies and could potentially be utilized for studying intracellular anoctamins.

### **What are the determinants of anion:cation selectivity in anoctamins?**

In contrast to Ano1 and Ano2, Ano6 may be a non-selective cation channel, although there are conflicting reports (Martins et al. 2011; Tian et al. 2012; H. Yang et al. 2011). Although this discrepancy remains to be resolved, these results raise the possibility that other anoctamins function as cation channels. Of the anoctamins, Ano6 is phylogenetically most closely related to Ano5. It is particularly interesting that Ano6 null mice exhibit musculoskeletal deficits (Ehlen et al. 2012) reminiscent of those found in human disorders caused by mutations in Ano5 (Tsutsumi et al. 2004), implying that Ano5 may also function as a cation channel. Because the anoctamin family is comprised of both anion and cation channels, the opportunity exists to examine the molecular and structural determinants of ion selectivity and permeability via direct comparison across family members. Recent work on Ano6 reveals that the E702/705Q mutations, which I report in this dissertation drastically reduce the Ca<sup>2+</sup> sensitivity of Ano1, also reduce the

Ca<sup>2+</sup> sensitivity of Ano6 (Yang et al. 2012). These findings suggest that the mechanisms underlying channel gating are similar for Ano1 and Ano6, thus supporting the feasibility of comparing family members to study other aspects of channel function such as selectivity.

We were unable to dramatically alter the anion:cation permeability ratio of Ano1 via site directed mutations (Yu et al. 2012). It is likely that significantly altering selectivity will require multiple mutations. This was indeed the case for members of the ligand gated ion channel (LGIC) superfamily (Keramidas et al. 2004). The LGIC superfamily, which is comprised of both anion and cation channels, share considerable structural homology. By comparing residues within the nicotinic acetylcholine receptor implicated in ion permeation with the corresponding residues of the glycine receptor, it was possible to identify residues critical for glycine receptor anion selectivity (Keramidas et al. 2000). Now that Ano6 has been identified as a cation channel, it may be possible to take a similar approach for studying anoctamin selectivity. However, identifying residues which line the pore via site directed mutagenesis may be more difficult for anoctamins. Unlike LGICs, which are pentameric proteins with a pore comprised of homologous regions within each subunit, Ano1 exists as a homodimer and may be more structurally similar to ClCs (Fallah et al. 2011). The ClC pore is formed by a single subunit with several non-homologous regions; thus, using mutagenesis to identify the pore was difficult, because mutations in several different regions of the protein affected pore properties. Furthermore, for ClC channels and bestrophins alike, pore mutations appear to only have modest effects on selectivity (Fahlke 2001; Qu and Hartzell 2004). Until a crystal structure is solved for Ano1, sequence comparison of cation vs anion selective anoctamins may be the best approach for understanding determinants of anoctamin anion/cation selectivity.

### **What are the mechanisms underlying Ca<sup>2+</sup> regulation of Ano1?**

Determining how Ano1 is regulated by Ca<sup>2+</sup> will be necessary for understanding how Ano1 channel activity is involved in various signaling pathways. Ano1 may be activated by direct Ca<sup>2+</sup> binding to a site within Ano1. Alternatively, Ano1 may be indirectly regulated via Ca<sup>2+</sup> binding proteins or other processes such as phosphorylation. In Chapter 3 we have identified residues that are indispensable for Ca<sup>2+</sup> sensitivity of Ano1, E702 and E705, but this alone is not definitive evidence for a Ca<sup>2+</sup> binding site. When using site directed mutagenesis to study ligand gated ion channels, it is difficult to distinguish effects on ligand binding from effects on channel gating in response to ligand binding. Because of this caveat, identifying the Ca<sup>2+</sup> binding site will require Ca<sup>2+</sup> binding assays to demonstrate direct binding of Ca<sup>2+</sup> to specific regions of Ano1, or the crystallization of Ano1 in the presence of Ca<sup>2+</sup>.

The E702/705Q mutations may alter Ca<sup>2+</sup> sensitivity by either directly disrupting a Ca<sup>2+</sup> binding site within Ano1, altering Ca<sup>2+</sup> dependent gating of the channel, or affecting the interaction of Ano1 with regulatory subunits critical for Ca<sup>2+</sup> sensitivity. Ano1 does not possess any canonical Ca<sup>2+</sup> binding sites, suggesting that the Ca<sup>2+</sup> binding site may lie within an accessory subunit. Calmodulin (CaM) is reportedly required for Ano1 activation by Ca<sup>2+</sup> (Tian et al. 2011); however, a recent study shows that CaM is not present in the Ano1 interactome (Perez-Cornejo et al. 2012). This discrepancy could be explained by the fact that the Ano1 splice variant used for the proteomics study lacks a segment that partially overlaps with the putative CaM binding site. Although CaM was not present in the Ano1 interactome, several other proteins that bind Ca<sup>2+</sup> or are regulated by Ca<sup>2+</sup> were present including annexin1 (ANXA1), phospholipid scramblase (PLSCR1), and calmodulin-activated serine kinase (CASK) (Perez-Cornejo et al. 2012). In addition, recent experiments from our lab show that the abundance of several Ca<sup>2+</sup>

sensitive proteins identified in the Ano1 interactome is significantly reduced in the interactome of Ano1 harboring the E702/705Q mutations (unpublished data). Thus, the E702/705Q mutations could possibly alter Ca<sup>2+</sup> activation of Ano1 by affecting the interaction of Ano1 with a Ca<sup>2+</sup> sensing regulatory subunit. Although the physiological significance of the interactions between Ano1 these Ca<sup>2+</sup> sensitive proteins need to be verified, these results serve as a basis for future experiments examining the mechanisms underlying Ca<sup>2+</sup> regulation of Ano1.

### **Best1 and Ano1: CaCCs with distinct roles in physiology**

It is clear that both Ano1 and Best1 can function as plasma membrane CaCCs, but their function and localization are dependent on the system in which they are expressed. This heterogeneity has certainly contributed to the confusion surrounding the role of CaCCs in diseases such as BVMD. When heterologous expression of Best1 was first shown to generate CaCCs, its endogenous CaCC function was uncertain because Best1 null mice did not display CaCC deficits in RPE (L. Y. Marmorstein et al. 2006), and they had biophysical properties that differed from “classical” CaCCs (H. C. Hartzell et al. 2008). We now know that Ano1 is the mediator of the classical outwardly rectifying CaCC observed in various epithelia, but this does not discredit the important roles that Best1 CaCC function may have in other cell types. It is now apparent that Ano1 and Best1, while both CaCCs, have discrete roles in physiology. This is represented in dorsal root ganglion (DRG) neurons, where both Ano1 and Best1 function as CaCCs, but in distinct neuronal subpopulations where they are implicated in nociception and neuronal regeneration respectively (Boudes et al. 2009; Cho et al. 2012). This is also demonstrated by results presented in Chapter 4 using *Drosophila* S2 cells as a model system; although *Drosophila* Ano1 and Best1 can function as CaCCs when heterologously

overexpressed in HEK293 cells (Figure 4-1C), endogenous S2 cell CaCCs/VRACs are mediated primarily by Best1 (Chien et al. 2006).

Further complicating the study of CaCCs is that heterogeneity is due not only to an underlying molecular diversity, but also cell-type specific differences in the regulatory mechanisms of CaCCs. In various cell types CaCCs can display differences in their mechanism of activation, the source of  $\text{Ca}^{2+}$  required for activation, and their localization. As such, it is important to recognize this limitation when drawing conclusions from studies performed in heterologous expression systems. Most studies on Ano1 and Best1 function have been performed in heterologous expression systems where  $\text{Ca}^{2+}$  has been artificially elevated. While heterologous expression systems may be useful for examining CaCC structure/function, they present notable limitations with regard to understanding the physiological function and regulation of CaCCs. As an example, Ano1 mediates CaCCs in salivary epithelia, colonic epithelia, and coronary arterial smooth muscle (Ousingsawat et al. 2009; Y. D. Yang et al. 2008). However, colonic secretory cells are activated by CaMKII, (Arreola et al. 1998; Worrell and Frizzell 1991) parotid cell CaCCs are not regulated by CaMKII, (Arreola et al. 1998) and CaMKII is a negative regulator of coronary arterial smooth muscle CaCCs (M. Wang et al. 2012).

The pitfalls of heterologous expression systems are illustrated by the controversy surrounding the role of Best1 in BVMD. Because the characteristic feature of BVMD is a reduction in the LP of the EOG, it was originally thought that Best1 is the CaCC that mediates the LP. Even though heterologous expression of Best1 generates plasma membrane CaCCs in HEK293 cells (Tsunenari et al. 2003), Best1 is not required for RPE CaCCs because Best1 knockout mice have normal CaCC currents (L. Y. Marmorstein et al. 2006). Furthermore, some patients reportedly exhibit a progressive light peak deficit, indicating that Best1 only indirectly regulates the light peak (Wabbels et al. 2006).

Although Best1 is expressed in the basolateral membrane of RPE, the majority of endogenous Best1 may function intracellularly where it might regulate  $\text{Ca}^{2+}$  homeostasis (Neussert et al. 2010). In order to understand the pathophysiology of BVMD, it will be critical to determine the intracellular roles of Best1, and to identify the channel that mediates the LP.

In this dissertation I have described a mouse model that may be useful for examining the molecular identity of the LP. As discussed above, the foremost concern regarding model systems for CaCCs is that CaCC properties can differ depending on the system. It is possible that there are species specific differences in Best1 function between human and mouse. Notably, Best1 knockout mice do not phenocopy autosomal recessive bestrophinopathy (ARB), which represents the Best1 null phenotype in humans (Burgess et al. 2008). Also, the LP of the mouse EOG is significantly smaller than that of human, suggesting there may be different ionic mechanisms underlying the LP. Despite the limitations of this mouse model, it is still a useful model for studying CaCC physiology in RPE, as the majority of mouse RPE cells express CaCC currents. In this dissertation, I demonstrate that the biophysical properties of mouse RPE CaCCs more closely resemble those of Ano1 mediated currents. This evidence, coupled with preliminary data from Ano1 RPE specific knockout mice, suggests that Ano1 is the mediator of RPE CaCCs in mice. Once the efficiency of Ano1 knockdown is verified, future questions that this model will help address are: 1) Is Ano1 responsible for mediating the LP of the mouse EOG? 2) Does knockdown of Ano1 result in RPE pathology? and 3) Does knockdown of Ano1 produce visual deficits in mice?

## Concluding Remarks

CaCCs are a diverse group of channels with critical roles in physiology. Since the discovery of anoctamins as CaCCs, our understanding of CaCC physiology has been greatly augmented. Even before this discovery, the importance of anoctamins in various disease states had been recognized. As the number of gene families known to encode CaCCs expands, so does the need to determine which putative CaCC genes correlate with currents observed in various cell types, and the subcellular compartments in which they function. The work presented here has contributed to this process by characterizing the localization and chloride channel function of Anos 1-7, thus revealing which anoctamins are the most likely contributors to plasma membrane CaCCs. Although the channel function of intracellular anoctamins is currently unknown, the findings presented in this dissertation provide a basis for future work examining the channel function of other anoctamin family members by identifying highly conserved residues within Ano1 critical for its channel function and Ca<sup>2+</sup> sensitivity. This work also sheds light on the context dependent function of CaCCs and the discrete physiological roles of Ano1 and Best1 by examining endogenous CaCCs in *Drosophila* S2 cells and mouse RPE. Taken together, this work provides a foundation for future work studying the functions of anoctamins and their roles in physiology and disease.

## REFERENCES

- Ablonczy, Z., et al. (2011), 'Human retinal pigment epithelium cells as functional models for the RPE in vivo', *Invest Ophthalmol Vis Sci*, 52 (12), 8614-20.
- Accardi, A. and Picollo, A. (2010), 'CLC channels and transporters: proteins with borderline personalities', *Biochim Biophys Acta*, 1798 (8), 1457-64.
- Almaca, J., et al. (2009), 'TMEM16 proteins produce volume-regulated chloride currents that are reduced in mice lacking TMEM16A', *J Biol Chem*, 284 (42), 28571-8.
- Amanchy, R., et al. (2007), 'A curated compendium of phosphorylation motifs', *Nat Biotechnol*, 25 (3), 285-6.
- Andre, S., et al. (2003), 'Axotomy-induced expression of calcium-activated chloride current in subpopulations of mouse dorsal root ganglion neurons', *J Neurophysiol*, 90 (6), 3764-73.
- Arreola, J., Melvin, J. E., and Begenisich, T. (1997), 'CaM kinase II regulation of calcium-activated chloride channels in epithelial cells.', *Biophysical Journal*, 72 (2), Thp96-Thp96.
- (1998), 'Differences in regulation of Ca(2+)-activated Cl- channels in colonic and parotid secretory cells', *Am J Physiol*, 274 (1 Pt 1), C161-6.
- Ayoub, C., et al. (2010), 'ANO1 amplification and expression in HNSCC with a high propensity for future distant metastasis and its functions in HNSCC cell lines', *Br J Cancer*, 103 (5), 715-26.
- Bader, C. R., Bertrand, D., and Schwartz, E. A. (1982), 'Voltage-activated and calcium-activated currents studied in solitary rod inner segments from the salamander retina', *J Physiol*, 331, 253-84.
- Bao, L., et al. (2002), 'Elimination of the BK(Ca) channel's high-affinity Ca(2+) sensitivity', *J Gen Physiol*, 120 (2), 173-89.
- Bao, L., et al. (2004), 'Mapping the BKCa channel's "Ca2+ bowl": side-chains essential for Ca2+ sensing', *J Gen Physiol*, 123 (5), 475-89.
- Barish, M. E. (1983), 'A transient calcium-dependent chloride current in the immature *Xenopus* oocyte', *J Physiol*, 342, 309-25.
- Barrett, K. E. and Keely, S. J. (2000), 'Chloride secretion by the intestinal epithelium: molecular basis and regulatory aspects', *Annu Rev Physiol*, 62, 535-72.
- Barro-Soria, R., et al. (2010), 'ER-localized bestrophin 1 activates Ca2+-dependent ion channels TMEM16A and SK4 possibly by acting as a counterion channel', *Pflugers Arch*, 459 (3), 485-97.

- Barry, P. H. (2006), 'The reliability of relative anion-cation permeabilities deduced from reversal (dilution) potential measurements in ion channel studies', *Cell Biochem Biophys*, 46 (2), 143-54.
- Ben-Ari, Y., et al. (2007), 'GABA: a pioneer transmitter that excites immature neurons and generates primitive oscillations', *Physiol Rev*, 87 (4), 1215-84.
- Bera, T. K., et al. (2004), 'NGEP, a gene encoding a membrane protein detected only in prostate cancer and normal prostate', *Proc Natl Acad Sci U S A*, 101 (9), 3059-64.
- Bian, S., Favre, I., and Moczydlowski, E. (2001), 'Ca<sup>2+</sup>-binding activity of a COOH-terminal fragment of the Drosophila BK channel involved in Ca<sup>2+</sup>-dependent activation', *Proc Natl Acad Sci U S A*, 98 (8), 4776-81.
- Billig, G. M., et al. (2011), 'Ca<sup>2+</sup>-activated Cl<sup>-</sup> currents are dispensable for olfaction', *Nature Neuroscience*, 14 (6), 763-9.
- Blodi, C. F. and Stone, E. M. (1990), 'Best's vitelliform dystrophy', *Ophthalmic Paediatr Genet*, 11 (1), 49-59.
- Bolduc, V., et al. (2010), 'Recessive mutations in the putative calcium-activated chloride channel Anoctamin 5 cause proximal LGMD2L and distal MMD3 muscular dystrophies', *Am J Hum Genet*, 86 (2), 213-21.
- Boudes, M. and Scamps, F. (2012), 'Calcium-activated chloride current expression in axotomized sensory neurons: what for?', *Front Mol Neurosci*, 5, 35.
- Boudes, M., et al. (2009), 'Best1 is a gene regulated by nerve injury and required for Ca<sup>2+</sup>-activated Cl<sup>-</sup> current expression in axotomized sensory neurons', *J Neurosci*, 29 (32), 10063-71.
- Brambillasca, S., et al. (2006), 'Unassisted translocation of large polypeptide domains across phospholipid bilayers', *J Cell Biol*, 175 (5), 767-77.
- Burgess, R., et al. (2008), 'Biallelic mutation of BEST1 causes a distinct retinopathy in humans', *Am J Hum Genet*, 82 (1), 19-31.
- Caputo, A., et al. (2008), 'TMEM16A, a membrane protein associated with calcium-dependent chloride channel activity', *Science*, 322 (5901), 590-4.
- Carles, A., et al. (2006), 'Head and neck squamous cell carcinoma transcriptome analysis by comprehensive validated differential display', *Oncogene*, 25 (12), 1821-31.
- Cenedese, V., et al. (2012), 'The voltage dependence of the TMEM16B/noctamin2 calcium-activated chloride channel is modified by mutations in the first putative intracellular loop', *J Gen Physiol*, 139 (4), 285-94.

- Cereda, V., et al. (2010), 'New gene expressed in prostate: a potential target for T cell-mediated prostate cancer immunotherapy', *Cancer Immunol Immunother*, 59 (1), 63-71.
- Chao, S. H., et al. (1984), 'Activation of calmodulin by various metal cations as a function of ionic radius', *Mol Pharmacol*, 26 (1), 75-82.
- Chien, L. T. and Hartzell, H. C. (2007), 'Drosophila bestrophin-1 chloride current is dually regulated by calcium and cell volume', *Journal of General Physiology*, 130 (5), 513-24.
- (2008), 'Rescue of volume-regulated anion current by bestrophin mutants with altered charge selectivity', *J Gen Physiol*, 132 (5), 537-46.
- Chien, L. T., Zhang, Z. R., and Hartzell, H. C. (2006), 'Single Cl<sup>-</sup> channels activated by Ca<sup>2+</sup> in Drosophila S2 cells are mediated by bestrophins', *J Gen Physiol*, 128 (3), 247-59.
- Cho, H., et al. (2012), 'The calcium-activated chloride channel anoctamin 1 acts as a heat sensor in nociceptive neurons', *Nature Neuroscience*, 15 (7), 1015-21.
- Collier, M. L., et al. (1996), 'Unitary Cl<sup>-</sup> channels activated by cytoplasmic Ca<sup>2+</sup> in canine ventricular myocytes', *Circ Res*, 78 (5), 936-44.
- Colquhoun, D. (1998), 'Binding, gating, affinity and efficacy: the interpretation of structure-activity relationships for agonists and of the effects of mutating receptors', *Br J Pharmacol*, 125 (5), 924-47.
- Cooper, P. R., et al. (1997), 'A sequence-ready high-resolution physical map of the best macular dystrophy gene region in 11q12-q13', *Genomics*, 41 (2), 185-92.
- Costa, A., et al. (2012), 'The Arabidopsis central vacuole as an expression system for intracellular transporters: functional characterization of the Cl<sup>-</sup>/H<sup>+</sup> exchanger CLC-7', *J Physiol*, 590 (Pt 15), 3421-30.
- Cross, H. E. and Bard, L. (1974), 'Electro-oculography in Best's macular dystrophy', *Am J Ophthalmol*, 77 (1), 46-50.
- d'Anglemont de Tassigny, A., et al. (2003), 'Structure and pharmacology of swelling-sensitive chloride channels, I(Cl<sub>swell</sub>)', *Fundam Clin Pharmacol*, 17 (5), 539-53.
- Das, S., et al. (2007), 'NGEP, a prostate-specific plasma membrane protein that promotes the association of LNCaP cells', *Cancer Res*, 67 (4), 1594-601.
- Das, S., et al. (2008), 'Topology of NGEP, a prostate-specific cell:cell junction protein widely expressed in many cancers of different grade level', *Cancer Res*, 68 (15), 6306-12.

- Davis, A. J., et al. (2010), 'Expression profile and protein translation of TMEM16A in murine smooth muscle', *Am J Physiol Cell Physiol*, 299 (5), C948-59.
- de Roos, A. D., van Zoelen, E. J., and Theuvenet, A. P. (1996), 'Determination of gap junctional intercellular communication by capacitance measurements', *Pflugers Arch*, 431 (4), 556-63.
- Deutman, A. F. (1969), 'Electro-oculography in families with vitelliform dystrophy of the fovea. Detection of the carrier state', *Arch Ophthalmol*, 81 (3), 305-16.
- Devor, D. C., et al. (1999), 'Bicarbonate and chloride secretion in Calu-3 human airway epithelial cells', *J Gen Physiol*, 113 (5), 743-60.
- Dorwart, M. R., et al. (2008), 'The solute carrier 26 family of proteins in epithelial ion transport', *Physiology (Bethesda)*, 23, 104-14.
- Duran, C. and Hartzell, H. C. (2011), 'Physiological roles and diseases of Tmem16/Anoctamin proteins: are they all chloride channels?', *Acta Pharmacol Sin*, 32 (6), 685-92.
- Duran, C., et al. (2010), 'Chloride channels: often enigmatic, rarely predictable', *Annu Rev Physiol*, 72, 95-121.
- Duran, C., et al. (2012), 'ANOs 3-7 in the anoctamin/Tmem16 Cl<sup>-</sup> channel family are intracellular proteins', *Am J Physiol Cell Physiol*, 302 (3), C482-93.
- Dutta, A. K., et al. (2011), 'Identification and functional characterization of TMEM16A, a Ca<sup>2+</sup>-activated Cl<sup>-</sup> channel activated by extracellular nucleotides, in biliary epithelium', *J Biol Chem*, 286 (1), 766-76.
- Dutzler, R., et al. (2002), 'X-ray structure of a ClC chloride channel at 3.0 Å reveals the molecular basis of anion selectivity', *Nature*, 415 (6869), 287-94.
- Duvvuri, U., et al. (2012), 'TMEM16A Induces MAPK and Contributes Directly to Tumorigenesis and Cancer Progression', *Cancer Res*, 72 (13), 3270-81.
- Eggermont, J. (2004), 'Calcium-activated chloride channels: (un)known, (un)loved?', *Proc Am Thorac Soc*, 1 (1), 22-7.
- Eggermont, J., et al. (2001), 'Cellular function and control of volume-regulated anion channels', *Cell Biochem Biophys*, 35 (3), 263-74.
- Ehlen, H. W., et al. (2012), 'Inactivation of Anoctamin-6/Tmem16f, a regulator of phosphatidylserine scrambling in osteoblasts, leads to decreased mineral deposition in skeletal tissues', *Journal of Bone and Mineral Research*.
- Fahlke, C. (2001), 'Ion permeation and selectivity in ClC-type chloride channels', *Am J Physiol Renal Physiol*, 280 (5), F748-57.

- Fallah, G., et al. (2011), 'TMEM16A(a)/anoctamin-1 shares a homodimeric architecture with CLC chloride channels', *Mol Cell Proteomics*, 10 (2), M110 004697.
- Faundez, V. and Hartzell, H. C. (2004), 'Intracellular chloride channels: determinants of function in the endosomal pathway', *Sci STKE*, 2004 (233), re8.
- Fein, A. and Terasaki, M. (2005), 'Rapid increase in plasma membrane chloride permeability during wound resealing in starfish oocytes', *J Gen Physiol*, 126 (2), 151-9.
- Ferrera, L., et al. (2009), 'Regulation of TMEM16A chloride channel properties by alternative splicing', *J Biol Chem*, 284 (48), 33360-8.
- Frizzell, R. A., et al. (1986), 'Chloride channel regulation in secretory epithelia', *Fed Proc*, 45 (12), 2727-31.
- Fujii, S., et al. (1992), 'Direct evidence for a basolateral membrane Cl<sup>-</sup> conductance in toad retinal pigment epithelium', *Am J Physiol*, 262 (2 Pt 1), C374-83.
- Fuller, C. M., et al. (1994), 'Phosphorylation and activation of a bovine tracheal anion channel by Ca<sup>2+</sup>/calmodulin-dependent protein kinase II', *J Biol Chem*, 269 (43), 26642-50.
- Gajewski, C., et al. (2011), 'Biogenesis of the pore architecture of a voltage-gated potassium channel', *Proc Natl Acad Sci U S A*, 108 (8), 3240-5.
- Gallemore, R. P. and Steinberg, R. H. (1993), 'Light-evoked modulation of basolateral membrane Cl<sup>-</sup> conductance in chick retinal pigment epithelium: the light peak and fast oscillation', *J Neurophysiol*, 70 (4), 1669-80.
- GomezHernandez, J. M., Stuhmer, W., and Parekh, A. B. (1997), 'Calcium dependence and distribution of calcium-activated chloride channels in *Xenopus* oocytes', *Journal of Physiology-London*, 502 (3), 569-74.
- Gribkoff, V. K., et al. (1996), 'Effects of channel modulators on cloned large-conductance calcium-activated potassium channels', *Mol Pharmacol*, 50 (1), 206-17.
- Griff, E. R. and Steinberg, R. H. (1982), 'Origin of the light peak: in vitro study of *Gekko gekko*', *J Physiol*, 331, 637-52.
- Hahn, Y., et al. (2009), 'Anoctamin and transmembrane channel-like proteins are evolutionarily related', *Int J Mol Med*, 24 (1), 51-5.
- Hamill, O. P., et al. (1981), 'Improved patch-clamp techniques for high-resolution current recording from cells and cell-free membrane patches', *Pflugers Arch*, 391 (2), 85-100.
- Hartzell, C., Putzier, I., and Arreola, J. (2005), 'Calcium-activated chloride channels', *Annu Rev Physiol*, 67, 719-58.

- Hartzell, H. C. and Qu, Z. (2003), 'Chloride currents in acutely isolated *Xenopus* retinal pigment epithelial cells', *J Physiol*, 549 (Pt 2), 453-69.
- Hartzell, H. C., et al. (2008), 'Molecular physiology of bestrophins: multifunctional membrane proteins linked to best disease and other retinopathies', *Physiol Rev*, 88 (2), 639-72.
- Hartzell, H. C., et al. (2009), 'Anoctamin/TMEM16 family members are Ca<sup>2+</sup>-activated Cl<sup>-</sup> channels', *J Physiol*, 587 (Pt 10), 2127-39.
- Hengl, T., et al. (2010), 'Molecular components of signal amplification in olfactory sensory cilia', *Proc Natl Acad Sci U S A*, 107 (13), 6052-7.
- Hicks, D., et al. (2011), 'A founder mutation in Anoctamin 5 is a major cause of limb-girdle muscular dystrophy', *Brain*, 134 (Pt 1), 171-82.
- Hodgkin, A. L. and Huxley, A. F. (1952a), 'Currents carried by sodium and potassium ions through the membrane of the giant axon of *Loligo*', *J Physiol*, 116 (4), 449-72.
- (1952b), 'A quantitative description of membrane current and its application to conduction and excitation in nerve', *J Physiol*, 117 (4), 500-44.
- Hodgkin, A. L. and Keynes, R. D. (1955), 'The potassium permeability of a giant nerve fibre', *J Physiol*, 128 (1), 61-88.
- Hoffmann, E. K. and Simonsen, L. O. (1989), 'Membrane mechanisms in volume and pH regulation in vertebrate cells', *Physiol Rev*, 69 (2), 315-82.
- Holevinsky, K. O., Jow, F., and Nelson, D. J. (1994), 'Elevation in intracellular calcium activates both chloride and proton currents in human macrophages', *J Membr Biol*, 140 (1), 13-30.
- Horton, R. M., et al. (1989), 'Engineering hybrid genes without the use of restriction enzymes: gene splicing by overlap extension', *Gene*, 77 (1), 61-8.
- Huang, F., et al. (2009), 'Studies on expression and function of the TMEM16A calcium-activated chloride channel', *Proc Natl Acad Sci U S A*, 106 (50), 21413-8.
- Huang, F., et al. (2012a), 'Calcium-activated chloride channel TMEM16A modulates mucin secretion and airway smooth muscle contraction', *Proc Natl Acad Sci U S A*.
- Huang, W. C., et al. (2012b), 'Calcium-activated chloride channels (CaCCs) regulate action potential and synaptic response in hippocampal neurons', *Neuron*, 74 (1), 179-92.
- Huang, X., et al. (2002), 'High-resolution mapping of the 11q13 amplicon and identification of a gene, TAOS1, that is amplified and overexpressed in oral cancer cells', *Proc Natl Acad Sci U S A*, 99 (17), 11369-74.

- Huang, X., et al. (2006), 'Comprehensive genome and transcriptome analysis of the 11q13 amplicon in human oral cancer and syteny to the 7F5 amplicon in murine oral carcinoma', *Genes Chromosomes Cancer*, 45 (11), 1058-69.
- Hussy, N. (1992), 'Calcium-activated chloride channels in cultured embryonic *Xenopus* spinal neurons', *J Neurophysiol*, 68 (6), 2042-50.
- Hwang, S. J., et al. (2009), 'Expression of anoctamin 1/TMEM16A by interstitial cells of Cajal is fundamental for slow wave activity in gastrointestinal muscles', *J Physiol*, 587 (Pt 20), 4887-904.
- Hwang, T. C. and Sheppard, D. N. (2009), 'Gating of the CFTR Cl<sup>-</sup> channel by ATP-driven nucleotide-binding domain dimerisation', *J Physiol*, 587 (Pt 10), 2151-61.
- Jentsch, T. J., et al. (2002), 'Molecular structure and physiological function of chloride channels', *Physiol Rev*, 82 (2), 503-68.
- Kaneko, H., Mohrlen, F., and Frings, S. (2006), 'Calmodulin contributes to gating control in olfactory calcium-activated chloride channels', *J Gen Physiol*, 127 (6), 737-48.
- Keramidas, A., et al. (2004), 'Ligand-gated ion channels: mechanisms underlying ion selectivity', *Prog Biophys Mol Biol*, 86 (2), 161-204.
- Keramidas, A., et al. (2000), 'M2 pore mutations convert the glycine receptor channel from being anion- to cation-selective', *Biophysical Journal*, 79 (1), 247-59.
- Keramidas, A., et al. (2002), 'Cation-selective mutations in the M2 domain of the inhibitory glycine receptor channel reveal determinants of ion-charge selectivity', *J Gen Physiol*, 119 (5), 393-410.
- Kiessling, A., et al. (2005), 'D-TMPP: a novel androgen-regulated gene preferentially expressed in prostate and prostate cancer that is the first characterized member of an eukaryotic gene family', *Prostate*, 64 (4), 387-400.
- Klockner, U. (1993), 'Intracellular Calcium-Ions Activate a Low-Conductance Chloride Channel in Smooth-Muscle Cells Isolated from Human Mesenteric-Artery', *Pflugers Archiv-European Journal of Physiology*, 424 (3-4), 231-37.
- Koumi, S., Sato, R., and Aramaki, T. (1994), 'Characterization of the calcium-activated chloride channel in isolated guinea-pig hepatocytes', *J Gen Physiol*, 104 (2), 357-73.
- Kramer, F., Stohr, H., and Weber, B. H. (2004), 'Cloning and characterization of the murine Vmd2 RFP-TM gene family', *Cytogenet Genome Res*, 105 (1), 107-14.
- Kramer, F., et al. (2000), 'Mutations in the VMD2 gene are associated with juvenile-onset vitelliform macular dystrophy (Best disease) and adult vitelliform macular

- dystrophy but not age-related macular degeneration', *Eur J Hum Genet*, 8 (4), 286-92.
- Kramer, J. and Hawley, R. S. (2003), 'The spindle-associated transmembrane protein Axs identifies a membranous structure ensheathing the meiotic spindle', *Nat Cell Biol*, 5 (3), 261-3.
- Kranjc, A., et al. (2009), 'Regulation of bestrophins by Ca<sup>2+</sup>: a theoretical and experimental study', *PLoS One*, 4 (3), e4672.
- Kuntz, C. A., et al. (1994), 'Modification by cyclic adenosine monophosphate of basolateral membrane chloride conductance in chick retinal pigment epithelium', *Invest Ophthalmol Vis Sci*, 35 (2), 422-33.
- Kunzelmann, K. (2005), 'Ion channels and cancer', *J Membr Biol*, 205 (3), 159-73.
- Kuruma, A. and Hartzell, H. C. (2000), 'Bimodal control of a Ca<sup>2+</sup>-activated Cl<sup>-</sup> channel by different Ca<sup>2+</sup> signals', *Journal of General Physiology*, 115 (1), 59-80.
- Lai, F. A., et al. (1988), 'Purification and reconstitution of the calcium release channel from skeletal muscle', *Nature*, 331 (6154), 315-9.
- Lang, F., et al. (1998), 'Functional significance of cell volume regulatory mechanisms', *Physiol Rev*, 78 (1), 247-306.
- Le, Y. Z., et al. (2008), 'Inducible expression of cre recombinase in the retinal pigmented epithelium', *Invest Ophthalmol Vis Sci*, 49 (3), 1248-53.
- Lee, S., et al. (2010), 'Channel-mediated tonic GABA release from glia', *Science*, 330 (6005), 790-6.
- Li, Y., et al. (2012), 'Long-term safety and efficacy of human induced pluripotent stem cell (iPS) grafts in a preclinical model of retinitis pigmentosa', *Mol Med*.
- Lindemann, B. (2001), 'Predicted profiles of ion concentrations in olfactory cilia in the steady state', *Biophysical Journal*, 80 (4), 1712-21.
- Ling, B. N., Seal, E. E., and Eaton, D. C. (1993), 'Regulation of mesangial cell ion channels by insulin and angiotensin II. Possible role in diabetic glomerular hyperfiltration', *J Clin Invest*, 92 (5), 2141-51.
- Liu, B., et al. (2010), 'The acute nociceptive signals induced by bradykinin in rat sensory neurons are mediated by inhibition of M-type K<sup>+</sup> channels and activation of Ca<sup>2+</sup>-activated Cl<sup>-</sup> channels', *J Clin Invest*, 120 (4), 1240-52.
- MacLeish, P. R. and Nurse, C. A. (2007), 'Ion channel compartments in photoreceptors: evidence from salamander rods with intact and ablated terminals', *J Neurophysiol*, 98 (1), 86-95.

- Maduke, M., Pheasant, D. J., and Miller, C. (1999), 'High-level expression, functional reconstitution, and quaternary structure of a prokaryotic ClC-type chloride channel', *J Gen Physiol*, 114 (5), 713-22.
- Mahjneh, I., et al. (2010), 'A new distal myopathy with mutation in anoctamin 5', *Neuromuscul Disord*, 20 (12), 791-5.
- Maminishkis, A., et al. (2006), 'Confluent monolayers of cultured human fetal retinal pigment epithelium exhibit morphology and physiology of native tissue', *Invest Ophthalmol Vis Sci*, 47 (8), 3612-24.
- Manoury, B., Tamuleviciute, A., and Tamaro, P. (2010), 'TMEM16A/anoctamin 1 protein mediates calcium-activated chloride currents in pulmonary arterial smooth muscle cells', *J Physiol*, 588 (Pt 13), 2305-14.
- Marmorstein, A. D., Cross, H. E., and Peachey, N. S. (2009), 'Functional roles of bestrophins in ocular epithelia', *Prog Retin Eye Res*, 28 (3), 206-26.
- Marmorstein, A. D., et al. (2000), 'Bestrophin, the product of the Best vitelliform macular dystrophy gene (VMD2), localizes to the basolateral plasma membrane of the retinal pigment epithelium', *Proc Natl Acad Sci U S A*, 97 (23), 12758-63.
- Marmorstein, L. Y., et al. (2002), 'Bestrophin interacts physically and functionally with protein phosphatase 2A', *J Biol Chem*, 277 (34), 30591-7.
- Marmorstein, L. Y., et al. (2006), 'The light peak of the electroretinogram is dependent on voltage-gated calcium channels and antagonized by bestrophin (best-1)', *J Gen Physiol*, 127 (5), 577-89.
- Marquardt, A., et al. (1998), 'Mutations in a novel gene, VMD2, encoding a protein of unknown properties cause juvenile-onset vitelliform macular dystrophy (Best's disease)', *Hum Mol Genet*, 7 (9), 1517-25.
- Martin, D. K. (1993), 'Small Conductance Chloride Channels in Acinar-Cells from the Rat Mandibular Salivary-Gland Are Directly Controlled by a G-Protein', *Biochem Biophys Res Commun*, 192 (3), 1266-73.
- Martins, J. R., et al. (2011), 'Anoctamin 6 is an essential component of the outwardly rectifying chloride channel', *Proc Natl Acad Sci U S A*, 108 (44), 18168-72.
- Matsuda, K., et al. (2010), 'Cbln1 is a ligand for an orphan glutamate receptor delta2, a bidirectional synapse organizer', *Science*, 328 (5976), 363-8.
- Mazzone, A., et al. (2011), 'Altered expression of Ano1 variants in human diabetic gastroparesis', *J Biol Chem*, 286 (15), 13393-403.
- Melvin, J. E. (1999), 'Chloride channels and salivary gland function', *Crit Rev Oral Biol Med*, 10 (2), 199-209.

- Mercer, A. J., et al. (2011), 'Location of release sites and calcium-activated chloride channels relative to calcium channels at the photoreceptor ribbon synapse', *J Neurophysiol*, 105 (1), 321-35.
- Miledi, R. (1982), 'A calcium-dependent transient outward current in *Xenopus laevis* oocytes', *Proc R Soc Lond B Biol Sci*, 215 (1201), 491-7.
- Milenkovic, V. M., et al. (2009), 'Functional assembly and purinergic activation of bestrophins', *Pflugers Arch*, 458 (2), 431-41.
- Milenkovic, V. M., et al. (2010), 'Evolution and functional divergence of the anoctamin family of membrane proteins', *BMC Evol Biol*, 10, 319.
- Mizuta, K., et al. (2007), 'Molecular characterization of GDD1/TMEM16E, the gene product responsible for autosomal dominant gnathodiaphyseal dysplasia', *Biochem Biophys Res Commun*, 357 (1), 126-32.
- Mobasheri, A., et al. (2001), 'Isoforms of Na<sup>+</sup>, K<sup>+</sup>-ATPase in human prostate; specificity of expression and apical membrane polarization', *Histol Histopathol*, 16 (1), 141-54.
- Mobasheri, A., et al. (2003), 'Expression and cellular localization of Na,K-ATPase isoforms in the rat ventral prostate', *BJU Int*, 92 (7), 793-802.
- Mohammad-Panah, R., et al. (2009), 'An essential role for ClC-4 in transferrin receptor function revealed in studies of fibroblasts derived from Clcn4-null mice', *J Cell Sci*, 122 (Pt 8), 1229-37.
- Mohler, C. W. and Fine, S. L. (1981), 'Long-term evaluation of patients with Best's vitelliform dystrophy', *Ophthalmology*, 88 (7), 688-92.
- Monera, O. D., et al. (1995), 'Relationship of sidechain hydrophobicity and alpha-helical propensity on the stability of the single-stranded amphipathic alpha-helix', *J Pept Sci*, 1 (5), 319-29.
- Moroni, M., et al. (2011), 'Chloride ions in the pore of glycine and GABA channels shape the time course and voltage dependence of agonist currents', *J Neurosci*, 31 (40), 14095-106.
- Morris, A. P. and Frizzell, R. A. (1993), 'Ca<sup>2+</sup>-dependent Cl<sup>-</sup> channels in undifferentiated human colonic cells (HT-29). II. Regulation and rundown', *Am J Physiol*, 264 (4 Pt 1), C977-85.
- Mullins, R. F., et al. (2007), 'Differential macular and peripheral expression of bestrophin in human eyes and its implication for best disease', *Invest Ophthalmol Vis Sci*, 48 (7), 3372-80.
- Munro, S. and Pelham, H. R. (1987), 'A C-terminal signal prevents secretion of luminal ER proteins', *Cell*, 48 (5), 899-907.

- Nakahari, T. and Marunaka, Y. (1995), 'ADH-evoked  $[Cl^-]_i$ -dependent transient in whole cell current of distal nephron cell line A6', *Am J Physiol*, 268 (1 Pt 2), F64-72.
- Namkung, W., Phuan, P. W., and Verkman, A. S. (2011), 'TMEM16A inhibitors reveal TMEM16A as a minor component of calcium-activated chloride channel conductance in airway and intestinal epithelial cells', *J Biol Chem*, 286 (3), 2365-74.
- Neher, E. and Sakmann, B. (1976), 'Single-channel currents recorded from membrane of denervated frog muscle fibres', *Nature*, 260 (5554), 799-802.
- Neussert, R., et al. (2010), 'The presence of bestrophin-1 modulates the  $Ca^{2+}$  recruitment from  $Ca^{2+}$  stores in the ER', *Pflugers Arch*, 460 (1), 163-75.
- Nilius, B. and Droogmans, G. (2003), 'Amazing chloride channels: an overview', *Acta Physiol Scand*, 177 (2), 119-47.
- Nilius, B., et al. (1997), 'Properties of volume-regulated anion channels in mammalian cells', *Prog Biophys Mol Biol*, 68 (1), 69-119.
- Nilius, B., et al. (1997c), 'Calcium-activated chloride channels in bovine pulmonary artery endothelial cells', *J Physiol*, 498 ( Pt 2), 381-96.
- Nishimoto, I., et al. (1991), 'Regulation of  $Cl^-$  channels by multifunctional CaM kinase', *Neuron*, 6 (4), 547-55.
- Nordstrom, S. and Barkman, Y. (1977), 'Hereditary macular degeneration (HMD) in 246 cases traced to one gene-source in central Sweden', *Hereditas*, 84 (2), 163-76.
- Ousingsawat, J., et al. (2009), 'Loss of TMEM16A causes a defect in epithelial  $Ca^{2+}$ -dependent chloride transport', *J Biol Chem*, 284 (42), 28698-703.
- Ousingsawat, J., et al. (2011), 'Rotavirus toxin NSP4 induces diarrhea by activation of TMEM16A and inhibition of  $Na^+$  absorption', *Pflugers Arch*, 461 (5), 579-89.
- Papazian, D. M., et al. (1991), 'Alteration of voltage-dependence of Shaker potassium channel by mutations in the S4 sequence', *Nature*, 349 (6307), 305-10.
- Park, H., et al. (2009), 'Bestrophin-1 encodes for the  $Ca^{2+}$ -activated anion channel in hippocampal astrocytes', *J Neurosci*, 29 (41), 13063-73.
- Perez-Cornejo, P., et al. (2012), 'Anoctamin 1 (Tmem16A)  $Ca^{2+}$ -activated chloride channel stoichiometrically interacts with an ezrin-radixin-moesin network', *Proc Natl Acad Sci U S A*, 109 (26), 10376-81.
- Pestov, N. B., et al. (2002), 'Nongastric H-K-ATPase in rodent prostate: lobe-specific expression and apical localization', *Am J Physiol Cell Physiol*, 282 (4), C907-16.

- Petrukhin, K., et al. (1998), 'Identification of the gene responsible for Best macular dystrophy', *Nat Genet*, 19 (3), 241-7.
- Piccolo, A. and Pusch, M. (2005), 'Chloride/proton antiporter activity of mammalian CLC proteins ClC-4 and ClC-5', *Nature*, 436 (7049), 420-3.
- Pifferi, S., Dibattista, M., and Menini, A. (2009a), 'TMEM16B induces chloride currents activated by calcium in mammalian cells', *Pflugers Arch*, 458 (6), 1023-38.
- Pifferi, S., et al. (2006), 'Bestrophin-2 is a candidate calcium-activated chloride channel involved in olfactory transduction', *Proc Natl Acad Sci U S A*, 103 (34), 12929-34.
- Pifferi, S., et al. (2009b), 'Calcium-activated chloride currents in olfactory sensory neurons from mice lacking bestrophin-2', *J Physiol*, 587 (Pt 17), 4265-79.
- Piper, A. S. and Large, W. A. (2003), 'Multiple conductance states of single Ca<sup>2+</sup>-activated Cl<sup>-</sup> channels in rabbit pulmonary artery smooth muscle cells', *J Physiol*, 547 (Pt 1), 181-96.
- Piwon, N., et al. (2000), 'ClC-5 Cl<sup>-</sup>-channel disruption impairs endocytosis in a mouse model for Dent's disease', *Nature*, 408 (6810), 369-73.
- Planells-Cases, R. and Jentsch, T. J. (2009), 'Chloride channelopathies', *Biochim Biophys Acta*, 1792 (3), 173-89.
- Pusch, M., et al. (1995a), 'Gating of the voltage-dependent chloride channel ClC-0 by the permeant anion', *Nature*, 373 (6514), 527-31.
- Pusch, M., et al. (1995b), 'Mutations in dominant human myotonia congenita drastically alter the voltage dependence of the ClC-1 chloride channel', *Neuron*, 15 (6), 1455-63.
- Qu, Z. and Hartzell, C. (2004), 'Determinants of anion permeation in the second transmembrane domain of the mouse bestrophin-2 chloride channel', *J Gen Physiol*, 124 (4), 371-82.
- Qu, Z., Fischmeister, R., and Hartzell, C. (2004), 'Mouse bestrophin-2 is a bona fide Cl<sup>-</sup> channel: identification of a residue important in anion binding and conduction', *J Gen Physiol*, 123 (4), 327-40.
- Qu, Z., et al. (2003), 'Two bestrophins cloned from *Xenopus laevis* oocytes express Ca<sup>2+</sup>-activated Cl<sup>-</sup> currents', *J Biol Chem*, 278 (49), 49563-72.
- Qu, Z., et al. (2006), 'The anion-selective pore of the bestrophins, a family of chloride channels associated with retinal degeneration', *J Neurosci*, 26 (20), 5411-9.
- Quinn, R. H. and Miller, S. S. (1992), 'Ion transport mechanisms in native human retinal pigment epithelium', *Invest Ophthalmol Vis Sci*, 33 (13), 3513-27.

- Quinn, R. H., Quong, J. N., and Miller, S. S. (2001), 'Adrenergic receptor activated ion transport in human fetal retinal pigment epithelium', *Invest Ophthalmol Vis Sci*, 42 (1), 255-64.
- Quinton, P. M. (1999), 'Physiological basis of cystic fibrosis: a historical perspective', *Physiol Rev*, 79 (1 Suppl), S3-S22.
- Rak, D. J., et al. (2006), 'Ca<sup>++</sup>-switch induction of RPE differentiation', *Exp Eye Res*, 82 (4), 648-56.
- Rasche, S., et al. (2010), 'Tmem16b is specifically expressed in the cilia of olfactory sensory neurons', *Chem Senses*, 35 (3), 239-45.
- Reisert, J., et al. (2003), 'The Ca-activated Cl channel and its control in rat olfactory receptor neurons', *J Gen Physiol*, 122 (3), 349-63.
- Rock, J. R., Futtner, C. R., and Harfe, B. D. (2008), 'The transmembrane protein TMEM16A is required for normal development of the murine trachea', *Dev Biol*, 321 (1), 141-9.
- Rock, J. R., et al. (2009), 'Transmembrane protein 16A (TMEM16A) is a Ca<sup>2+</sup>-regulated Cl<sup>-</sup> secretory channel in mouse airways', *J Biol Chem*, 284 (22), 14875-80.
- Romanenko, V. G., et al. (2010), 'Tmem16A encodes the Ca<sup>2+</sup>-activated Cl<sup>-</sup> channel in mouse submandibular salivary gland acinar cells', *J Biol Chem*, 285 (17), 12990-3001.
- Ronchi, P., et al. (2008), 'Transmembrane domain-dependent partitioning of membrane proteins within the endoplasmic reticulum', *J Cell Biol*, 181 (1), 105-18.
- Rosenthal, R., et al. (2006), 'Expression of bestrophin-1, the product of the VMD2 gene, modulates voltage-dependent Ca<sup>2+</sup> channels in retinal pigment epithelial cells', *Faseb Journal*, 20 (1), 178-80.
- Saggheddu, C., et al. (2010), 'Calcium concentration jumps reveal dynamic ion selectivity of calcium-activated chloride currents in mouse olfactory sensory neurons and TMEM16b-transfected HEK 293T cells', *J Physiol*, 588 (Pt 21), 4189-204.
- Scheel, O., et al. (2005), 'Voltage-dependent electrogenic chloride/proton exchange by endosomal CLC proteins', *Nature*, 436 (7049), 424-7.
- Schenck, S., et al. (2009), 'A chloride conductance in VGLUT1 underlies maximal glutamate loading into synaptic vesicles', *Nature Neuroscience*, 12 (2), 156-62.
- Schlenker, T. and Fitz, J. G. (1996), 'Ca<sup>(2+)</sup>-activated Cl<sup>-</sup> channels in a human biliary cell line: regulation by Ca<sup>2+</sup>/calmodulin-dependent protein kinase', *Am J Physiol*, 271 (2 Pt 1), G304-10.

- Schredelseker, J., et al. (2010), 'Non-Ca<sup>2+</sup>-conducting Ca<sup>2+</sup> channels in fish skeletal muscle excitation-contraction coupling', *Proc Natl Acad Sci U S A*, 107 (12), 5658-63.
- Schreiber, M. and Salkoff, L. (1997), 'A novel calcium-sensing domain in the BK channel', *Biophysical Journal*, 73 (3), 1355-63.
- Schreiber, R., et al. (2010), 'Expression and function of epithelial anoctamins', *J Biol Chem*, 285 (10), 7838-45.
- Schroeder, B. C., et al. (2008), 'Expression cloning of TMEM16A as a calcium-activated chloride channel subunit', *Cell*, 134 (6), 1019-29.
- Shen, H. and Chou, J. J. (2008), 'MemBrain: improving the accuracy of predicting transmembrane helices', *PLoS One*, 3 (6), e2399.
- Sicinski, P., et al. (1989), 'The molecular basis of muscular dystrophy in the mdx mouse: a point mutation', *Science*, 244 (4912), 1578-80.
- Stephan, A. B., et al. (2009), 'ANO2 is the ciliary calcium-activated chloride channel that may mediate olfactory amplification', *Proc Natl Acad Sci U S A*, 106 (28), 11776-81.
- Stobrawa, S. M., et al. (2001), 'Disruption of ClC-3, a chloride channel expressed on synaptic vesicles, leads to a loss of the hippocampus', *Neuron*, 29 (1), 185-96.
- Stohr, H., et al. (1998), 'A gene map of the Best's vitelliform macular dystrophy region in chromosome 11q12-q13.1', *Genome Res*, 8 (1), 48-56.
- Stohr, H., et al. (2009), 'TMEM16B, a novel protein with calcium-dependent chloride channel activity, associates with a presynaptic protein complex in photoreceptor terminals', *J Neurosci*, 29 (21), 6809-18.
- Stotz, S., Keating, M., and Clapham, D. (2012), 'Drosophila Bestrophin 1 is a Swell Activated Chloride Channel', *Biophysical Journal* (doi:10.1016/j.bpj.2011.11.2999 edn., 102), 550a.
- Strauss, O., et al. (2012), 'A potential cytosolic function of bestrophin-1', *Adv Exp Med Biol*, 723, 603-10.
- Sumi, M., et al. (1991), 'The newly synthesized selective Ca<sup>2+</sup>/calmodulin dependent protein kinase II inhibitor KN-93 reduces dopamine contents in PC12h cells', *Biochem Biophys Res Commun*, 181 (3), 968-75.
- Sun, H., et al. (2002), 'The vitelliform macular dystrophy protein defines a new family of chloride channels', *Proc Natl Acad Sci U S A*, 99 (6), 4008-13.
- Suzuki, J., et al. (2010), 'Calcium-dependent phospholipid scrambling by TMEM16F', *Nature*, 468 (7325), 834-8.

- Suzuki, M., Morita, T., and Iwamoto, T. (2006), 'Diversity of Cl(-) channels', *Cell Mol Life Sci*, 63 (1), 12-24.
- Takahashi, T., Neher, E., and Sakmann, B. (1987), 'Rat brain serotonin receptors in *Xenopus* oocytes are coupled by intracellular calcium to endogenous channels', *Proc Natl Acad Sci U S A*, 84 (14), 5063-7.
- Taleb, O., et al. (1988), 'Small-conductance chloride channels activated by calcium on cultured endocrine cells from mammalian pars intermedia', *Pflugers Arch*, 412 (6), 641-6.
- Thevenod, F. (2002), 'Ion channels in secretory granules of the pancreas and their role in exocytosis and release of secretory proteins', *Am J Physiol Cell Physiol*, 283 (3), C651-72.
- Thorburn, W. and Nordstrom, S. (1978), 'EOG in a large family with hereditary macular degeneration. (Best's vitelliform macular dystrophy) identification of gene carriers', *Acta Ophthalmol (Copenh)*, 56 (3), 455-64.
- Tian, Y., Schreiber, R., and Kunzelmann, K. (2012), 'Anoctamins are a family of Ca<sup>2+</sup> activated Cl<sup>-</sup> channels', *J Cell Sci*.
- Tian, Y., et al. (2011), 'Calmodulin-dependent activation of the epithelial calcium-dependent chloride channel TMEM16A', *Faseb Journal*, 25 (3), 1058-68.
- Tokumitsu, H., et al. (1990), 'KN-62, 1-[N,O-bis(5-isoquinolinesulfonyl)-N-methyl-L-tyrosyl]-4-phenylpiperazine, a specific inhibitor of Ca<sup>2+</sup>/calmodulin-dependent protein kinase II', *J Biol Chem*, 265 (8), 4315-20.
- Tomlins, B. and Williams, A. J. (1986), 'Solubilisation and reconstitution of the rabbit skeletal muscle sarcoplasmic reticulum K<sup>+</sup> channel into liposomes suitable for patch clamp studies', *Pflugers Arch*, 407 (3), 341-7.
- Tsunenari, T., et al. (2003), 'Structure-function analysis of the bestrophin family of anion channels', *J Biol Chem*, 278 (42), 41114-25.
- Tsutsumi, S., et al. (2004), 'The novel gene encoding a putative transmembrane protein is mutated in gnathodiaphyseal dysplasia (GDD)', *Am J Hum Genet*, 74 (6), 1255-61.
- Vandenberg, R. J., Huang, S. W., and Ryan, R. M. (2008), 'Slips, leaks and channels in glutamate transporters', *Channels*, 2 (1), 51-58.
- Vermeer, S., et al. (2010), 'Targeted next-generation sequencing of a 12.5 Mb homozygous region reveals ANO10 mutations in patients with autosomal-recessive cerebellar ataxia', *Am J Hum Genet*, 87 (6), 813-9.

- Vogalis, F., Hegg, C. C., and Lucero, M. T. (2005), 'Ionic conductances in sustentacular cells of the mouse olfactory epithelium', *J Physiol*, 562 (Pt 3), 785-99.
- Wabbels, B., et al. (2006), 'Genotype-phenotype correlation and longitudinal course in ten families with Best vitelliform macular dystrophy', *Graefes Arch Clin Exp Ophthalmol*, 244 (11), 1453-66.
- Wagner, J. A., et al. (1991), 'Activation of chloride channels in normal and cystic fibrosis airway epithelial cells by multifunctional calcium/calmodulin-dependent protein kinase', *Nature*, 349 (6312), 793-6.
- Wajima, R., et al. (1993), 'Correlating visual acuity and electrooculogram recordings in Best's disease', *Ophthalmologica*, 207 (4), 174-81.
- Wang, M., et al. (2012), 'Downregulation of TMEM16A calcium-activated chloride channel contributes to cerebrovascular remodeling during hypertension by promoting basilar smooth muscle cell proliferation', *Circulation*, 125 (5), 697-707.
- Wang, S. S., et al. (2000), 'Mice lacking renal chloride channel, CLC-5, are a model for Dent's disease, a nephrolithiasis disorder associated with defective receptor-mediated endocytosis', *Hum Mol Genet*, 9 (20), 2937-45.
- Watanabe, M., Yumoto, K., and Ochi, R. (1994), 'Indirect activation by internal calcium of chloride channels in endothelial cells', *Jpn J Physiol*, 44 Suppl 2, S233-6.
- Weber, B. H., et al. (1994), 'Best's vitelliform dystrophy (VMD2) maps between D11S903 and PYGM: no evidence for locus heterogeneity', *Genomics*, 20 (2), 267-74.
- West, R. B., et al. (2004), 'The novel marker, DOG1, is expressed ubiquitously in gastrointestinal stromal tumors irrespective of KIT or PDGFRA mutation status', *Am J Pathol*, 165 (1), 107-13.
- Williams, R. M. and Naz, R. K. (2010), 'Novel biomarkers and therapeutic targets for prostate cancer', *Front Biosci (Schol Ed)*, 2, 677-84.
- Worrell, R. T. and Frizzell, R. A. (1991), 'CaMKII mediates stimulation of chloride conductance by calcium in T84 cells', *Am J Physiol*, 260 (4 Pt 1), C877-82.
- Xiao, Q., et al. (2009), 'Dysregulation of human bestrophin-1 by ceramide-induced dephosphorylation', *J Physiol*, 587 (Pt 18), 4379-91.
- Xiao, Q., et al. (2008), 'Regulation of bestrophin Cl channels by calcium: role of the C terminus', *J Gen Physiol*, 132 (6), 681-92.
- Xiao, Q., et al. (2011), 'Voltage- and calcium-dependent gating of TMEM16A/Ano1 chloride channels are physically coupled by the first intracellular loop', *Proc Natl Acad Sci U S A*, 108 (21), 8891-6.

- Yang, H., et al. (2011), 'Scan: A Novel Small-Conductance Ca<sup>2+</sup>-Activated Non-Selective Cation Channel Encoded by TMEM16F', *Biophysical Journal* (100), 259a.
- Yang, H., et al. (2012), 'TMEM16F Forms a Ca(2+)-Activated Cation Channel Required for Lipid Scrambling in Platelets during Blood Coagulation', *Cell*, 151 (1), 111-22.
- Yang, Y. D., et al. (2008), 'TMEM16A confers receptor-activated calcium-dependent chloride conductance', *Nature*, 455 (7217), 1210-5.
- Yoshikawa, M., et al. (2002), 'CLC-3 deficiency leads to phenotypes similar to human neuronal ceroid lipofuscinosis', *Genes Cells*, 7 (6), 597-605.
- Yu, K., Cui, Y., and Hartzell, H. C. (2006), 'The bestrophin mutation A243V, linked to adult-onset vitelliform macular dystrophy, impairs its chloride channel function', *Invest Ophthalmol Vis Sci*, 47 (11), 4956-61.
- Yu, K., et al. (2007), 'Chloride channel activity of bestrophin mutants associated with mild or late-onset macular degeneration', *Invest Ophthalmol Vis Sci*, 48 (10), 4694-705.
- Yu, K., et al. (2008), 'The best disease-linked Cl<sup>-</sup> channel hBest1 regulates Ca V 1 (L-type) Ca<sup>2+</sup> channels via src-homology-binding domains', *J Neurosci*, 28 (22), 5660-70.
- Yu, K., et al. (2012), 'Explaining calcium-dependent gating of anoctamin-1 chloride channels requires a revised topology', *Circ Res*, 110 (7), 990-9.
- Zhang, Y., et al. (2010), 'Suppression of Ca<sup>2+</sup> signaling in a mouse model of Best disease', *Hum Mol Genet*, 19 (6), 1108-18.
- Zhu, M. H., et al. (2009), 'A Ca(2+)-activated Cl(-) conductance in interstitial cells of Cajal linked to slow wave currents and pacemaker activity', *J Physiol*, 587 (Pt 20), 4905-18.
- Zitron, A. E. and Hawley, R. S. (1989), 'The genetic analysis of distributive segregation in *Drosophila melanogaster*. I. Isolation and characterization of Aberrant X segregation (Axs), a mutation defective in chromosome partner choice', *Genetics*, 122 (4), 801-21.